TAMPEREEN TEKNILLINEN YLIOPISTO
TAMPERE UNIVERSITY OF TECHNOLOGY

RIIKKA MIKKONEN

EVALUATION OF COMMERCIALLY AVAILABLE SILVER INKS SCREEN PRINTED ON A PPE BASED SUBSTRATE

Master of Science Thesis

Examiner: Assoc. prof. Matti Mäntysalo

Examiner and topic approved by the Vice Dean of the Faculty of Computing and Electrical Engineering on 1st March 2017

ABSTRACT

RIIKKA MIKKONEN: Evaluation of commercially available silver inks screen printed on a PPE based substrate
Tampere University of technology
Master of Science Thesis, 76 pages, 5 appendix pages
April 2017
Master's Degree Programme in Electrical Engineering
Major: Electronics Device Design
Examiner: Associate Professor Matti Mäntysalo

Keywords: Printed electronics, screen printing, PPE, silver ink, surface modification, sheet resistance, adhesion, reliability

Printed electronics enable fabrication of environmentally friendly wireless applications on novel substrates. Development of multidimensional substrates enables fabrication of creative applications and new communication networks between devices and users may be formed. These applications can be utilized in various industry fields, such as automotive industry or aviation, where integration of electrical devices into machine structures can provide significant benefits, as devices do not require additional space and wireless sensing and monitoring are enabled.

In this study, performance of silver inks screen printed on PPE polymer compound was evaluated. Advantages of this substrate material include low dissipation factor and relative permittivity, making it thus an attractive substrate for high frequency applications. In addition, substrate fabrication by injection-molding allows usage of innovative substrate structures. However, low surface energy and resulted hydrophobic nature of this substrate make printing of high quality lines with proper electrical and mechanical performance difficult. To modify substrate surface, and thus to enhance performance, suitable surface treatments were selected for this survey. Effect of different surface treatments was inspected, and performance of printed structures was evaluated by sheet resistance measurements and crosscut adhesion tests. Effects of aging were simulated with accelerated environmental reliability tests.

Results of this study indicate that material parameters have a great impact on performance of the printed structures. By the modification of surface properties, substrate can be made hydrophilic and rougher surface profile can be achieved. Furthermore, by the modification of the surface properties, better mechanical performance of printed structures can be obtained. In addition, it was observed that formed substrate-ink interface has a significant effect on the aging properties of the printed structures. On the other hand, ink selection has great impact on aging of printed structures. Therefore, protective layers are needed to shield devices from environmental stress. Sheet resistance values between 12 mΩ/□ and 25 mΩ/□ could be obtained, indicating excellent electrical performance of printed conductors.

TIIVISTELMÄ

RIIKKA MIKKONEN: Kaupallisten hopeamusteiden arviointi silkkipainettuna PPE-pohjaiselle alustalle
Tampereen teknillinen yliopisto
Diplomityö, 76 sivua, 5 liitesivua
Huhtikuu 2017
Sähkötekniikan diplomi-insinöörin tutkinto-ohjelma
Pääaine: Elektroniikan laitesuunnittelu
Tarkastaja: Associate Professor Matti Mäntysalo

Avainsanat: Painettava elektroniikka, silkkipaino, PPE, hopeamuste, pintaenergia, pintakäsittely, neliöresistanssi, adheesio, luotettavuus

Painettavan elektroniikan avulla voidaan valmistaa ympäristöystävällisiä langattomia sovelluksia, jotka mahdollistavat uusien alustamateriaalien käytön. Moniulotteisten alustojen kehittäminen voi luoda täysin uudenlaisia sovelluksia, jotka mahdollistavat sekä laitteiden välisen kommunikoinnin, että laitteiden ja käyttäjän välisen kommunikoinnin uudella tavalla. Näitä sovelluksia voidaan hyödyntää monilla teollisuudenaloilla, kuten autoteollisuudessa ja ilmailussa. Näillä aloilla elektroniikan sulauttaminen lopputuotteiden runkoihin tarjoaa monia etuja, koska tällöin elektroniikka ei vie ylimääräistä tilaa, ja mahdollistaa samalla toimintojen langattoman valvonnan ja mittauksen.

Tässä työssä arvioitiin silkkipainettavien hopeamusteiden ominaisuuksia PPE-pohjaisella polymeerialustalla. Tämän alustan etuja ovat alhainen häviökerroin sekä matala suhteellinen permittiivisyys, jotka tekevät tästä materiaalista houkuttelevan alustavaihtoehdon suurtaajuussovelluksissa. Lisäksi alustoiden valmistukseen käytettävä ruiskuvalutekniikka mahdollistaa monipuolisten alustarakenteiden valmistuksen. Toisaalta tämän alustan pintaenergia on matala, minkä vuoksi alusta on erittäin huonosti vettyvä. Huono vettyvyys vaikeuttaa hyvälaatuisten johtimien painamista ja saattaa heikentää niiden suorituskykyä. Tässä työssä alustaa muokattiin erilaisilla pintakäsittelyillä ominaisuuksien parantamiseksi. Käsittelyjen vaikutus alustan ominaisuuksiin selvitettiin. Lisäksi johtimien suorituskykyä arvioitiin neliöresistanssin mittauksilla ja tartuntatesteillä.

Tulosten perusteella materiaalien ominaisuuksilla on merkittävä vaikutus painettujen rakenteiden suorituskykyyn. Käsittelyjen avulla alustan vettyvyyttä voidaan parantaa ja pinnasta saadaan karheampi. Tartuntatestien perusteella voidaan todeta, että alustojen ominaisuuksia muokkaamalla on mahdollista saavuttaa parempi mekaaninen suorituskyky. Lisäksi alustan ominaisuudet vaikuttivat painettujen rakenteiden ikääntymiseen. Toisaalta myös mustevalinnalla on merkittävä vaikutus luotettavuuteen. Ikääntymistestien perusteella rakenteisiin tulisi lisätä suojaava päällyste, jotta laitteista saadaan luotettavia. Mitatut neliöresistanssien arvot olivat varsin matalia, vaihdellen 12 mΩ/□ ja 25 mΩ/□ välillä, joten painettujen johtimien sähköiset ominaisuudet ovat erittäin hyviä.

PREFACE

This Master's thesis was written at Department of Electronics and Communications Engineering at Tampere University of Technology.

I would like to thank my thesis instructor and examiner, Assoc. Prof. Matti Mäntysalo for guidance and support. In addition, I would like to thank TUT Foundation for funding of this thesis. I would like to thank Antti Helminen from Premix for providing test substrates for this work. In addition, I would like to thank everyone at TUT Laboratory for Future Electronics for support.

Finally, I would like to thank my family and friends for support during this work and over the years.

Tampere, 19.04.2017

Riikka Mikkonen

CONTENTS

LIST OF FIGURES

LIST OF TABLES

SYMBOLS AND ABBREVIATIONS

3D	Three Dimensional
4PP	Four-Point Probe
AD	Anderson-Darling value
CL	Confidence Level
CNT	Carbon Nanotube
DF	Dissipation Factor
DI	Deionized
ESD	Electrostatic Discharge
GPS	Global Positioning System
HF	High Frequency
IC	Integrated Circuit
KOH	Potassium Hydroxide
MID	Molded Interconnect Devices
NaCl	Sodium Chloride
PDMS	Polydimethylsiloxane
P	Probability value
PE	Printed Electronics
PEN	Polyethylene Naphthalene
PET	Polyethylene Terephthalate
PI	Polyimide
PP	Polypropylene
PPE	Polyphenylene Ether
PPO	Polyphenylene Oxide
PTFE	Polytetrafluoroethylene
PVC	Polyvinyl Chloride
RFID	Radio Frequency Identification Technology
RMS	Root-Mean-Square
SEM	Scanning Electron Microscopy
UHF	Ultra High Frequency
UX	Super High Modulus Polyester Monofilament

θ	Contact angle
ε_r	Relative permittivity
γ_{LV}	Liquid surface tension
γ_{SL}	Solid-liquid surface tension
γ_{SV}	Solid surface energy
A	Cross-sectional area
l	length
R_q	Root-mean-square surface roughness
R_p	Highest peak on surface
R_s	Sheet resistance
R_t	Difference between highest peak and lowest valley of the surface
R_v	Lowest valley on the surface
t	thickness
w	width

1. INTRODUCTION

Printed electronics (PE) have gained popularity in electronics manufacturing. This is due to the multiple benefits that PE can provide over traditional methods, such as etching or lithography. One of the most significant benefits of printing is additivity, as conductive structures are manufactured by adding material layers, whereas traditional methods are bases on material subtraction. Subtraction of unnecessary material layers increases produced waste amount, leading to environmental issues. Thus, additive processes are more environmental friendly. In addition, printing will also reduce process steps needed on electronics production line, thus being less complicated and significantly faster method than traditional methods. As a large variety of traditional printing techniques, such as inkjet printing, screen printing and gravure printing may be utilized to fabricate functional structures, range of possible applications is expanded. [1]

On the other hand, fabrication of functional layers by printing enables usage of thin and flexible substrates. Therefore, printed structures may be integrated to novel substrates, such as clothing, and even onto skin. These applications can provide significant benefits for example in healthcare, since body monitoring is made simpler and more efficient, when less devices and wiring is needed [1].

In addition, significant benefits may be achieved in for example logistics and other such industry fields, where tracking applications are necessary. For example, printed RFID (Radio frequency identification technology) tags and printed sensors may be utilized [1]. In addition, printed energy harvesters enable novel, wireless energy production and storage applications, which can be applied everywhere [2]. Therefore, the very concept of electrical device may change dramatically in the future, as electronics integration into everyday environment reduces need of devices.

At the moment, the most significant drawbacks of PE are related to the limited availability of suitable materials. Traditionally, enabling functionality of printing inks requires thermal curing at high temperatures, which limits the usage of temperature-sensitive materials, such as polymers. However, continuous research and development of both printing techniques and materials has already enabled significant increased availability of both substrate and ink materials. In addition, new curing methods are available.

Polymers are popular substrate materials in PE manufacturing due to their flexibility and mechanical strength. In addition, polymers are inexpensive to fabricate and thin structures may be achieved. In the future, additive printing techniques may even enable usage of paper or wood substrates, and other such highly environmentally friendly materials. [1]

In this thesis, performance of commercial conductive silver inks on a PPE (Polyphenylene ether) based polymer substrate is evaluated. The material parameters of this substrate material, including low DF (Dissipation Factor) and low relative permittivity, make this material compound an attractive substrate for HF (High Frequency) applications. In addition, these substrates are fabricated by injection-molding technology, which enables fabrication of creative 3D (Three Dimensional) substrate structures.

When this fabrication method is combined with PE, it is possible to manufacture truly revolutionizing products in the field of wireless HF applications. A few examples of such products are included in Figure 1. As demonstrated in this Figure, printing of functional layers on 3D substrates can offer benefits for multiple industry fields, from health care to aviation. With these IoT (Internet of Things) devices, more data is available than ever, and wireless communication systems enable innovative connections between devices. In the future, development of these applications will pave the way for IoE (Internet of Everything), where users are linked to this communication network as well.

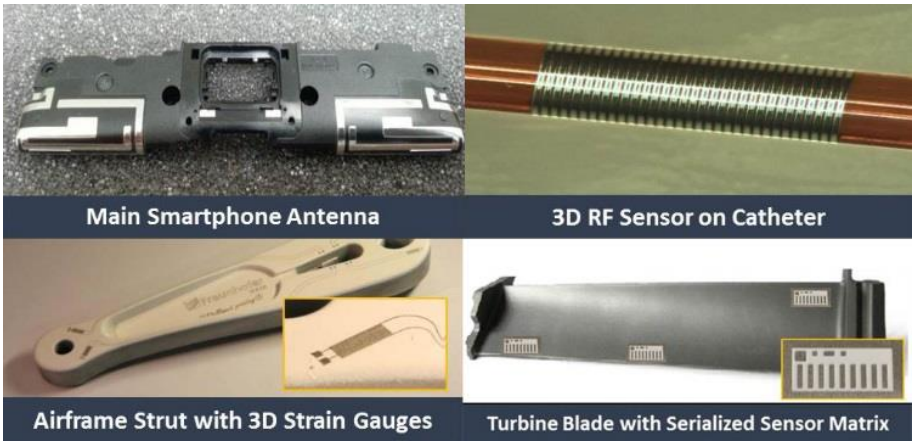

Figure 1. *PE applications on 3D substrates. Adapted from [3].*

Despite the many advantages of this substrate material, the surface energy of the substrate material is rather low, and thus material is hydrophobic. Therefore, surface modification may be required to enable reliable, high quality prints. In this thesis, both chemical and physical surface treatments are used to enhance performance of screen printed conductive structures. Initial performance of these structures is evaluated, and environmental reliability are used to see the effects of aging. Objective of this thesis was to find such substrate-ink combinations, which could be used to fabricate reliable, high performance HF applications.

This thesis is structured as follows. Chapter 2 discusses briefly the basics of screen printing technology, including material characteristics, printing process and methods typically used to evaluate printed structures. In Chapter 3, selected materials are presented and selection is motivated. Chapter 4 represents used substrate modification methods, as well

as the used printing process and environmental reliability tests. In Chapter 5, methods for both substrate surface characterization and performance characterization of printed structures are presented. Results are presented and discussed in Chapter 6. Thesis outcome is summarized and proposals for future work are given in Chapter 7.

2. PRINTING TECHNOLOGY

As already discussed, PE is an important manufacturing method for future electronics applications, and may revolutionize the very idea of an electrical device. PE applications may be manufactured by multiple techniques, and suitable printing technique is often dependent on the end-application requirements. Most of these techniques are traditional, widely known printing techniques, such as gravure, offset, flexography, inkjet and screen printing.

Screen printing was chosen as a printing technique in this thesis, and it will be discussed in further detail. Key features of this technique include high aspect ratio. Line thickness values of approximately 10-60 µm may be obtained, whereas line thickness of e.g. inkjet printed patterns are usually less than 5 µm, even below 1 µm [4]. Line thickness is closely related to the electrical performance of the printed conductors, since thicker lines enable better conductivity. This relation is covered in further detail in Subchapter 2.4.1. In addition, screen printing is an old and well matured technology [5]. Therefore, there are plenty of suitable materials available for this technique.

However, few disadvantages are related to this technique. The width of the screen printed lines is limited to approximately 50 µm, which leads to relatively small resolution compared to other techniques [4]. Therefore, screen printing is best suited for large scale manufacturing, where high resolution is not necessary. Typical applications of screen printed electronics include for example display manufacturing, where this technique may be utilized in especially backplane wiring fabrication [4]. Other attractive applications of this technique are stretchable applications, such as wearable electronics in health care, which have been demonstrated in for example [6] and [7]. Since screen printing enables both more accurate single-sheet printing and high-speed rotary printing, it is therefore attractive printing technique for mass production lines, and for more accurate small-scale production.

The output of the screen printing process is dependent on many factors. The most important factors include material characteristics, as both the substrate properties and ink composition affect material interactions during printing, and have thus a significant effect on the performance of the finished structures. Material characteristics and their influence in printing process are covered in Subchapter 2.1. Material modification techniques and their quality enhancing abilities are covered in Subchapter 2.2. In addition, there are several other parameters related to the printing process, such as selection of screen and adjustment of printer parameters. On the other hand, to enable functionality of the printed patterns, they have to be cured. These parameters are discussed further in Subchapter 2.3.

Typical characterization methods used to evaluate both electrical and mechanical performance of the printed structures are covered in Subchapter 2.4. In addition, methods used to simulate product aging are discussed.

2.1 Material characteristics

In PE applications, it is necessary to determine surface parameters of materials present in the printing process, since they have a great impact on the final process output. Important parameters related to ink composition are viscosity and surface tension, which affect wet interface behavior, and therefore, their impact on print quality is significant. If functional inks are used, material components, such as functional material and solvent type should be considered.

In addition to ink parameters, substrate properties affect print quality and performance. Important substrate parameters include surface energy, which determines substrate wettability. Furthermore, substrate surface parameters are closely related to the adhesion bonds formed in the material interface. In addition to surface energy, surface roughness should be considered.

2.1.1 Ink

Large variety of different coatings may be printed on substrate surface, but since focus of this thesis is on functional inks, they will be discussed in further detail. These inks typically consist of various components to enable proper interactions in both wet and dry material interface. These components include functional material, such as conductor or dielectric. In addition, functional inks include solvent component, which affects both viscosity and surface tension of the ink composition. Other components may be included, such as a polymer binder used in nanoparticle inks, whereas flake inks used in screen printing typically include only functional and solvent components. [4]

Viscosity is a critical parameter related to printing ink selection. It describes fluid's ability to resist flow, and is dependent on molecule composition in the fluid [8]. In general, fluids can be classified into either Newtonian or non-Newtonian fluids. If ink is Newtonian, its viscosity remains constant, whereas viscosity of a non-Newtonian fluid may vary, depending on shear stress applied to the fluid. Non-Newtonian fluids, also known as shear-thinning inks, are preferred as printing inks due to their decreasing viscosity over increased shear. This property is desirable, because viscosity remains high without additional pressure, but inks spread easily when pressure is applied [8].

Typical viscosities of screen printable inks are rather high compared to for example inkjet or flexo printing inks. Suitable ink viscosities for different techniques are listed in Table

1. Lower viscosity enables ink to spread freely, which is desirable in inkjet printing, whereas in screen printing, high ink viscosity is essential to enable controlled ink spreading on the screen, thus ensuring good print quality [9]. Low viscosity, on the other hand, leads to undesirable drying of the ink, thus clogging screen. Another drawback of low viscosity is the risk of ink flowing through screen mesh prior to printing [8]. If necessary, ink viscosity may be modified by changing either volume or composition of the solvent component. [10]

Table 1. *Typical ink viscosities for different printing techniques [4].*

Printing technique	**Ink viscosity (cP)**
Inkjet	10-20
Gravure	100-1000
Screen	500-5000
Flexo	50-500
Offset	100-10000

Another parameter influencing ink spreading abilities is surface tension, which is determined by the molecule bonding strength in the fluid. Molecular bonds inside the fluid are steady, whereas molecular bonds close to the fluid surface are instable. Therefore, cohesion energy on the surface is only half of the energy inside. To reduce this instability, fluid molecules are organized so that their surface area is minimized. The remaining energy loss per surface area is determined as surface tension γ_{LV} [11]. Surface tension values of a few common liquids are listed in Table 2. As shown in Table 2, surface tension of organic cleaning solvents, such as acetone of ethanol, is rather low compared to water surface tension. Thus, organic solvents tend to spread more freely than water.

Table 2. *Surface tensions of liquids at 25°C [10; 12].*

Liquid	Surface tension (mN/m)
Acetone (2-propanone)	23.0
Benzaldehyde	38.3
Ethanol (ethyl alcohol)	22.0
Methanoic acid (formic acid)	37.7
Toluene	27.9
Water	72.7

2.1.2 Substrate

To be able to choose suitable substrate material for PE applications, surface energy and surface roughness of substrate should be considered. Surface energy of a solid material is related to molecule bond strength in material compound. In solids, molecular bonds can be either strong ionic or metallic bonds, or weak bonds, such as Wan der Waals forces. Therefore, solid surface energies γ_{SV} vary greatly, depending on the material composition. Polymer surface energies are typically rather low, below 100 mN/m. This is due to weak bonds present in polymer compounds, whereas surface energies of metals and inorganic materials may be as high as 5000 mN/m. [13]

At the moment, polymers are the most common substrate materials in PE applications due to their suitability for flexible and stretchable applications. In addition, rather thin polymer foils may be used, which enables for example fabrication of thin and flexible display backplanes with low cost. Surface energies of common polymers used in PE applications and in other industries are listed in Table 3. It may be observed, that polymer surface energy may be higher, as in the case of Nylon 6 or Nylon 12 (67 mN/m), or rather low, as that of PDMS (Polydimethylsiloxane), only 20.4 mN/m. PDMS has gained popularity in flexible sensor and implant applications for its stretching abilities [14]. PET (Polyethylene terephthalate) and PI (Polyimide) are common substrate materials in printed electronics applications [15].

On the other hand, surface roughness of substrate material has an affects the interactions between substrate surface and applied coating. Changing surface roughness of the substrate may improve interface behavior or have an opposite effect, depending on original wettability of substrate material. This relationship is covered in further detail in Subchapter 2.2.

Table 3. *Common polymers and their surface energies [16].*

Polymer	Surface energy (mN/m)
Nylon 6,12	67.0
Polydimethylsiloxane (PDMS)	20.4
Polyethylene terephthalate (PET)	44.0
Polyimide (PI)	43.8
Polypropylene (PP)	30.2
Polyvinyl chloride (PVC)	40.1

In addition to polymer foils, alternative substrate materials, such as wood and paper have been searched for printed electronics applications to enable truly environmentally friendly manufacturing [17]. In addition, direct printing on textiles has been studied as well [18]. However, these substrate materials are rather sensitive to both moisture and temperature fluctuation, and are extremely porous materials. Therefore, several challenges remain before they may be utilized to PE applications.

2.1.3 Substrate-ink interface

When ink is pressed on the substrate, a substrate-ink interface is formed. Behavior of this interface is highly dependent on material parameters of both substrate and ink. The surface tension of the liquid, as well as the surface energy of the substrate should be considered, when aiming at the optimal interface behavior. The main parameters related to interface behavior are wetting and adhesion. Wetting is related to the interactions of a wet interface, whereas adhesion is a property of a cured structure.

As discussed earlier, wetting describes the fluid spreading abilities on a certain surface. Level of wetting is determined by contact angle θ: the higher the contact angle in the material interface, the worse the wetting. This relationship may be presented by Young's equation:

$$\cos\theta = \frac{\gamma_{SV}-\gamma_{SL}}{\gamma_{LV}}, \quad (1)$$

where γ_{SV}, γ_{SL} and γ_{LV} describe solid-gas surface tension, solid-liquid surface tension and liquid-gas surface tension, respectively [13; 19]. This relationship is demonstrated in Figure 2.

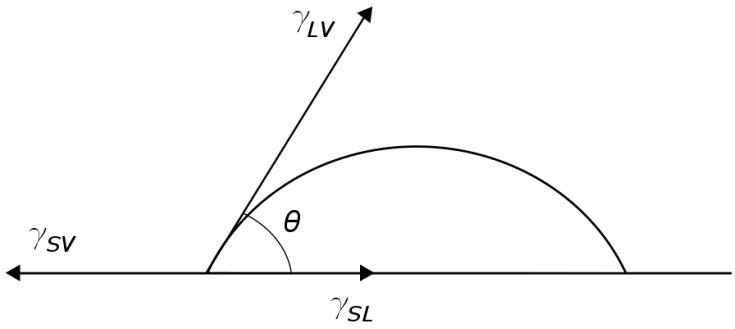

Figure 2. *Contact angle by Young's equation.*

It should be considered, that three material variables exist in this interface: substrate, coating and the gas in the atmosphere. Therefore, different behavior may be expected for example in vacuum and air. Figure 3 illustrates the impact of contact angle on interface wetting.

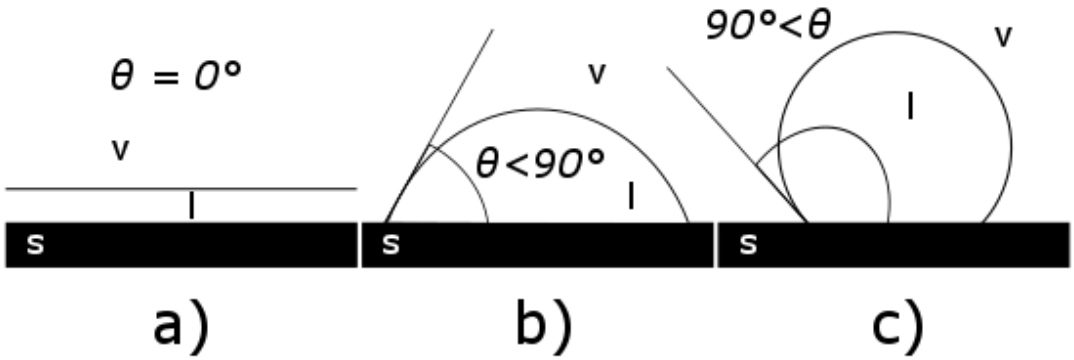

Figure 3. *Contact angle and wetting in the interface of liquid (l), vapor (v) and solid (s). a) Complete wetting, b) partial wetting and c) poor wetting. Adapted from [20].*

As shown in Figure 3, when contact angle is close to 0°, interface is wetted completely, whereas increasing the contact angle leads to reduced interface wetting. On the contrary, at a contact angle over 90°, interface cannot be wet. Typically, a contact angle of 30-40° is desirable. However, a sufficient contact angle is highly application-dependent and both too low and too high contact angle are likely to cause issues in the printing process. Too low contact angle may lead to excessive wetting, thus causing bulging of printed lines, and too high contact angle may prevent uniform pattern formation.

To be able to control wetting, one must know the surface energy of the used substrate as well as the surface tension of the used liquid. Such a critical surface energy of the substrate γ_{SV} may be found that liquid surface tension $\gamma_{LV} < \gamma_{SV}$, and thus the solid surface is wetted properly. On the contrary, if $\gamma > \gamma_{SV}$, substrate is wetted only partially [20]. In other

words, if solid surface energy is lower than water surface tension, substrate is hydrophobic, whereas in opposite situation substrate is hydrophilic [21]. For example, comparison of Tables 2 and 3 values indicates that PDMS surface energy is only 20 mN/m,which is significantly lower than water surface tension (7.7 mN/m), and PDMS is thus an extremely hydrophobic material. On the other hand, most of the organic solvents listed in Table 2 would wet polymer surfaces listed in Table 3.

Adhesion describes bonds between substrate and coating in a dry interface [22]. Strength and type of these bonds is dependent on the interacting materials, and they are divided from molecular level to microscopic level [23]. Therefore, many factors affect adhesion strength between these materials. Wetting may affect adhesion strength, since wetting level determines the likelihood of two materials forming a uniform physical interface. If wetting is poor, materials will not be in contact, and thus no adhesive bonds can be generated.

However, especially in printed electronics, where dry material interface is generated between substrate and cured functional ink, adhesion is dependent on many parameters other than wetting. Since the ink solvent component is removed by curing, interface bonds are dependent on substrate and the annealed functional material. Proper wetting may enhance adhesion by enabling formation of uniform conductive material layer on substrate surface. Nonetheless, there are plenty of other significant bonds to be considered in this interface.

If an adhesive bond is generated, it may be mechanical. Thus, coating material is anchored to the substrate due to rough substrate surface by interlocking [23]. Therefore, increased surface roughness may increase likelihood of these bonds. This phenomenon is discussed further in next subchapter.

Another type of adhesive bonds is created by electrostatic forces [23], and is based on the charge difference between interacting materials. This bond is likely to be found in an interface between a dielectric and a conductor. Therefore, electrostatic forces may enhance adhesion between polymer (dielectric) and metal coating (conductor).

In addition to other bonds, bonding may be chemical. Stronger chemical bonds include hydrogen, ion and covalent bonds, whereas dispersive bonds, such as the Van der Waals forces, are the weakest [23]. Stronger chemical bonds require stable and mutual functional groups in each interacting material. If these groups are not present in the interface, only weak, instable bonds are generated.

2.2 Surface modification

To achieve desired wetting level and to promote adhesion, it might be necessary to modify properties of used materials. In printed electronics applications, either substrate or ink

parameters may be modified. In this thesis, focus will be on the substrate surface treatments.

Two main reasons for substrate surface modification are to change either wettability or surface roughness. Figure 4 demonstrates relationship between surface energy and surface roughness. If substrate is originally hydrophilic and wetting is partial (Figure 4a)), it is possible to enhance wetting by increased surface roughness of the substrate (Figure 4b))). On the other hand, if substrate is hydrophobic, roughening of the substrate surface can make it even more hydrophobic, as in Figures 4c) and 4d). Therefore, suitable method for surface modification has to be chosen carefully.

There are many methods available for surface modification. Methods for surface energy elevation include for example corona and plasma treatment, as well as different chemical coating treatments [24]. Depending on the substrate material and treatment parameters, these methods may also be used to modify substrate surface roughness. On the other hand, it might be necessary to reduce surface energy in some applications, to achieve for example high resolution patterns. This may be achieved by adding a chemical coating with low surface energy, which has been done in [25]. Surface treatments used in this thesis are discussed further in Chapter 4.

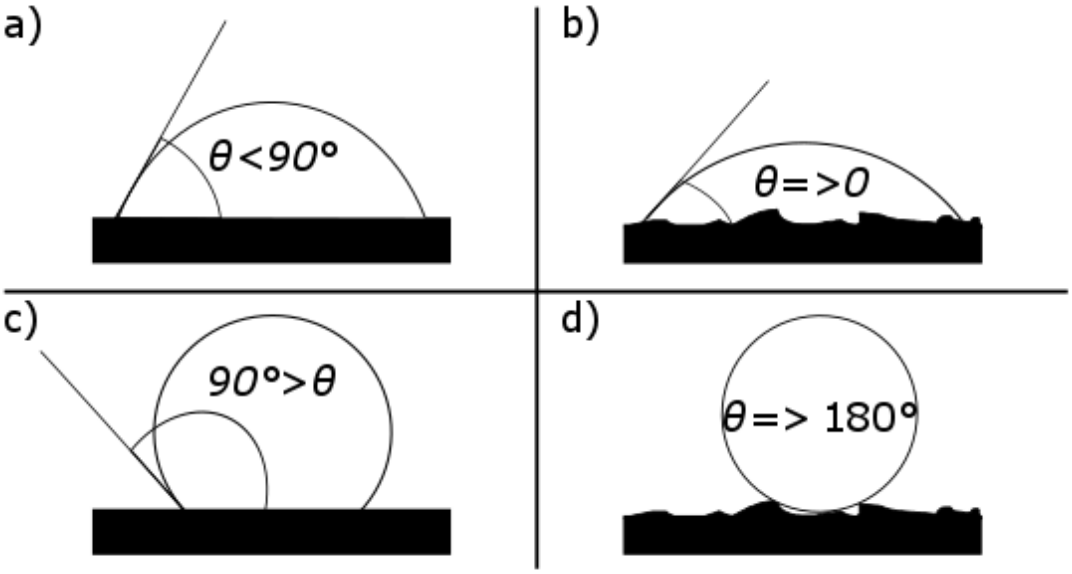

Figure 4. *a) Hydrophilic, smooth surface b) hydrophilic, rough surface c) hydrophobic, smooth surface and b) hydrophobic, rough surface. Adapted from [21].*

2.3 Screen printing process

When material parameters have been adjusted, test patterns may be printed. The principle of screen printing process is illustrated in Figure 5. As shown in this Figure, screen, in

tension on the frame, is placed above substrate. A little gap should be left between the screen and substrate to ensure high resolution print. In addition, physical contact between screen and substrate causes unnecessary stress to the screen mesh. After screen placement, a squeegee is used to apply ink to the substrate through screen. A sufficient pressure should be used to bend the squeegee at desired angle, which depends on the used ink and screen mesh. In addition to the squeegee parameters, ink spreading may be controlled by adjusting printing speed [4].

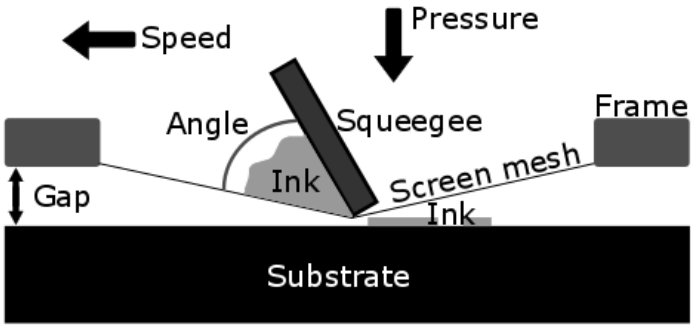

Figure 5. *The principle of screen printing process. Adapted from [4].*

In addition, screen parameters have a great impact on the process output. A mesh, consisting of crossed threads, is tightened to the screen frame with a defined thread angle, depending on the application resolution. Typical thread materials include polyester or stainless steel [5]. A stencil, typically consisting of a photosensitive emulsion, is applied to the mesh for image formation. When the squeegee is pressed against the screen, ink will flow through mesh openings not covered with emulsion [4; 5].

Furthermore, other screen parameters, such as thread count per centimeter or per inch, are highly related to print quality. Higher thread count enables both better print quality and finer details. Thus, finer threads should be used when aiming at small prints with high resolution. Another considerable parameter is particle size of the used ink. As a rule of thumb, mesh openings should be at least three times larger than ink particle size, or three times higher than thread diameter, to prevent screen from clogging [5; 26]. Line thickness also increases proportional to thread diameter and screen thickness [26].

After printing, formed patterns must be cured to remove the solvent component and to enable functionality of the lines [8]. Popular curing methods include traditional thermal treatment, which is based on solvent evaporation by heat [27; 28]. It is a mature and rather simple curing method. On the other hand, high temperature limits the availability of suitable substrate materials and thermal curing is often time-consuming. Therefore, novel curing methods have been developed. These alternative curing methods include for ex-

ample plasma sintering, photonic sintering and laser sintering. The benefits of these techniques include shorter sintering times and are more environmentally friendly. In addition, more substrate materials may be used, when high temperatures are not needed to cure printed structures. However, process optimization remains a challenge and more development is required [17; 29].

2.4 Evaluation of printed structures

When printed patterns have been cured, formed structures should be inspected and measured to be able to evaluate, whether material selection and printing process have been successful or not. One of the most essential measures is print quality. Line thickness, variations in line width and print porosity affect electrical performance of printed patterns. The relationship between line dimensions and electrical performance is covered in Subchapter 2.4.1. In addition, methods for conductivity measurement of printed structures are discussed.

Another important factor is mechanical performance. As the mechanical performance of the printed structures is dependent on adhesion bonds formed in the ink-substrate interface, it is necessary to evaluate the initial bonding strength. Adhesion failure mechanisms and causes are discussed further in Subchapter 2.4.2. Furthermore, methods for adhesion evaluation are covered.

In addition, both electrical and mechanical performance are highly related to product lifetime. Therefore, effects of aging should be inspected. Subchapter 2.4.3. presents failure mechanisms caused by aging. In addition, common methods used for aging effect inspection are discussed.

2.4.1 Electrical performance

Conductivity is the basic measure of electrical performance evaluation, and is inversely proportional to resistance, which is determined as the tendency of the conductor to oppose current flow. Therefore, low resistance enables good conductivity and vice versa. In general, Ohm's law may be used to define resistance *R* of a conductor. According to this law, resistance is proportional to potential difference *V*, which is formed by current *I* supplied to the conductor [30]:

$$R = \frac{V}{I}. \tag{2}$$

To be able to measure resistance of a conductive line, a four-point probe (4PP) measurement may be used. The principle of this measurement is demonstrated in Figure 6.

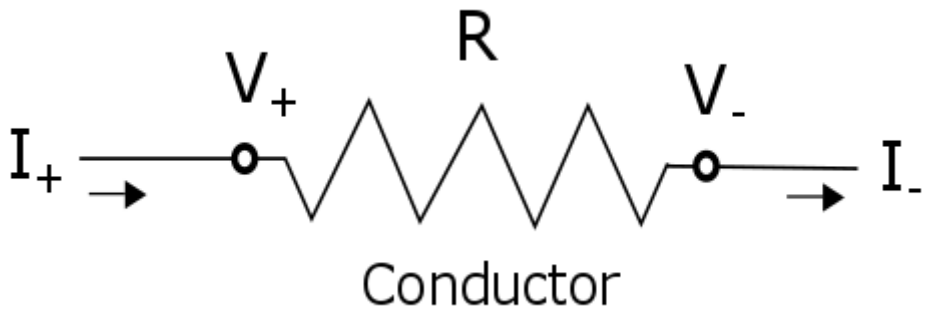

Figure 6. *Principle of 4PP-measurement.*

As shown in Figure 6, source current I_+ is fed to one end of the conductor, and conductor series resistance results to lower current I_- on the other end of the conductor. Resulting voltage difference between voltages V+ and V- can be read from multimeter display when measurement probes have been placed to both ends of the conductor.

Furthermore, resistance is a property of a printed line, whereas resistivity ρ is material property. When resistivity of a conductive material is known, and the dimensions of a conductive line have been measured, resistance may be conducted from:

$$R = \frac{\rho l}{A} = \frac{\rho l}{wt}, \tag{3}$$

where A is the cross-sectional area of the conductor, formed as a product of width w and thickness t, and l is conductor length. When the dimensions of the conductive line are known, a 4PP measurement system may be implemented to measure sheet resistance R_s [31]. The principle of sheet resistance is illustrated in Figure 7. Conductor surface may be divided in squares, where one side of the square equals to conductor width w. Thus, sheet resistance may be conducted:

$$R_S = \frac{\rho}{t}. \tag{4}$$

Sheet resistance is thus highly dependent on both material resistivity and printed line thickness [31]. Therefore, it is possible to use less conductive materials, if line thickness is increased. On the other hand, by using highly conductive materials, thinner lines may be printed. The relationship between sheet resistance and total resistance may be conducted from (3) and (4):

$$R = \frac{\rho l}{wt} = \frac{R_S l}{w}. \tag{5}$$

Furthermore, using Ohm's law (2) may be conducted:

$$\frac{V}{I} = \frac{R_S l}{w}. \quad (5)$$

and thus sheet resistance may be written:

$$R_S = \frac{Vw}{Il}. \quad (6)$$

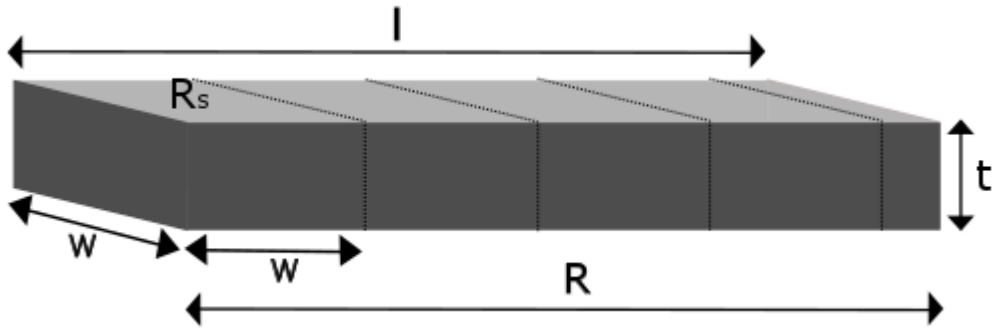

Figure 7. *Conductor dimensions.*

As shown in (6), sheet resistance is also dependent on width and length of a conductive structure. The ratio of these two dimensions can be determined so that the measured resistance between probes is as low as possible. In theory, increasing line length over line width will reduce sheet resistance, and thus enable better conductivity. However, extremely narrow lines are more sensitive to faults in line structure, and amount of conductive material may be decreased, thus leading to poor conductivity. In addition, long conductor lines are more sensitive to interference.

Resistivity values of a few widely used functional materials are listed in Table 4. It can be observed that metals, especially silver, copper and gold are very good conductors due to their low resistivity. On the contrary, glass is a good insulator, whereas silicon is a semiconductor. In PE applications, silver is the most popular conductive material. In addition to low resistivity, silver is a noble metal and therefore resistant to oxidation. Furthermore, even silver oxide is highly conductive, which gives it an advantage over plenty of other materials, since corrosion will not affect conductivity of silver traces as rapidly. In addition, silver is more cost-effective conductor material than gold. [9]

However, as silver still is expensive material, alternatives have been researched. Copper is one the most attractive alternatives at the moment due to its high conductivity. The most significant defect of copper is its rapid oxidation in air, which limits usage in normal

room conditions. Still, promising results have been obtained with copper inks in for example [31] and [32]. Other alternative conductor materials are organic conductors, such as carbon nanotubes (CNT) and graphene [34].

Table 4. *Resistivities of common functional materials* [35].

Material	Resistivity (Ωm)
Silver	$1{,}59 * 10^{-8}$
Copper	$1{,}70 * 10^{-8}$
Gold	$2{,}44 * 10^{-8}$
Platinum	$1{,}10 * 10^{-7}$
Carbon	$3{,}50 * 10^{-5}$
Silicon	$2{,}30 * 10^{3}$
Glass	$1{,}00 * 10^{10}$

2.4.2 Mechanical performance

Mechanical performance of a substrate-ink interface is highly related to adhesion strength of the interface. Initial adhesion strength is related to the freshly printed and cured interfaces, which have not had to endure any stress caused by either user or environment.

There are several methods for interface bonding strength evaluation. For the initial evaluation, standardized adhesion tests, such as crosscut test, exist. If accurate strength measurement is required, the force needed to break interface bonding can be determined fro example by a pull-off test by ISO 4624 standard [37]. In this test, tensile stress is directed to the interface, until either a cohesion failure or adhesion failure occurs. The maximum shear stress, which the system can endure, may be determined by a shear-off test, which is similar to the pull-off test with an additional torque applied [36]. In flexible applications, bending strength and stretching abilities of the interface should be tested.

Since adhesion failure may be caused by for example cutting, pulling, bending or stretching, a PE device has to endure a lot of mechanical stress during its lifetime. In addition, temperature fluctuation or chemicals may affect adhesion strength of material interfaces. Typical failure types and stress mechanisms are illustrated in Figure 8. Two failure types are related to material bond strength. A cohesion failure occurs when the bonds inside either coating or substrate fail. If an adhesion failure occurs, the bonding between two materials has failed. [36]

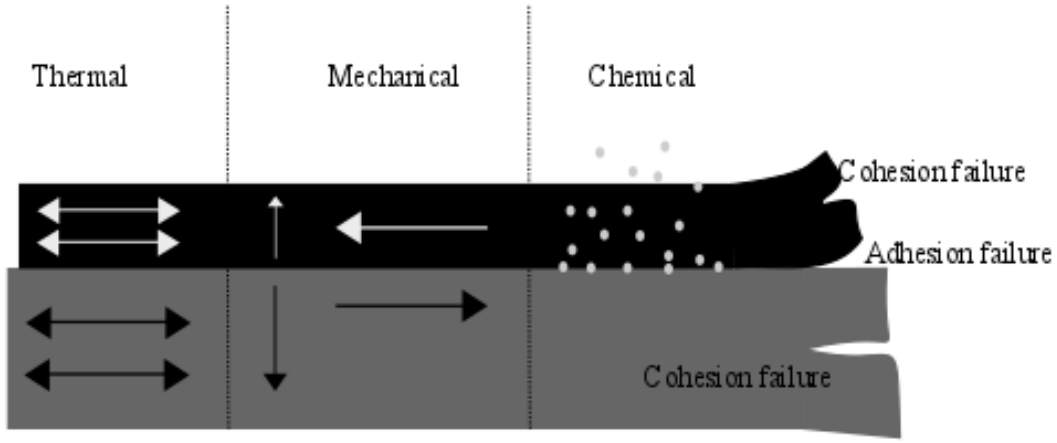

Figure 8. *Adhesion failure mechanisms.*

Thermal stress is typically caused by elevated temperature. Since thermal properties of metals and polymers differ, stress is applied to material interface. In addition, chemicals may penetrate material interface and cause corrosion [36]. Since especially failures caused by thermal and chemical stress are usually caused by the environment-related and occur over time, their effects cannot be measured as easily as effects of mechanical stress. Therefore, reliability tests have been developed to simulate the aging impact caused by environmental stress. Product reliability and related test methods are discussed further in next subchapter.

2.4.3 Reliability

Reliability in electronics can be defined in multiple ways, and there are many aspects that have to be considered when estimating product reliability. In general, reliability describes the likelihood of a product to survive storing and usage. Since failures during product lifetime make products less reliable, failure rate is a useful measure of reliability, determining how well device functionality is maintained over time. The importance of reliability testing is emphasized by the fact that reliability test methods have been developed for a long time, and there are plenty of standards to guide reliability testing. [38]

In Figure 9, different failure types occurring over time are demonstrated by a bathtub curve. As shown in this graph, products are more likely to fail in the beginning of their lifetime, but this likelihood is decreased over time. Failures occurring before the first stabilization point are called early failures. The cause for these failures lies in either negligent manufacturing or defective testing. However, if products are able to survive this phase, failure rate is decreased significantly. From this point, failures will most likely be caused by sudden, high level stresses, and thus, overstress failures occur. Causes behind these failures are often random and unpredictable, such as a single component failure or

ESD (Electrostatic Discharge), leading to the malfunctioning of the whole product [37]. In the end of product lifetime, failure rate starts to increase again due to corrosion or other such unavoidable, long-term aging mechanisms.

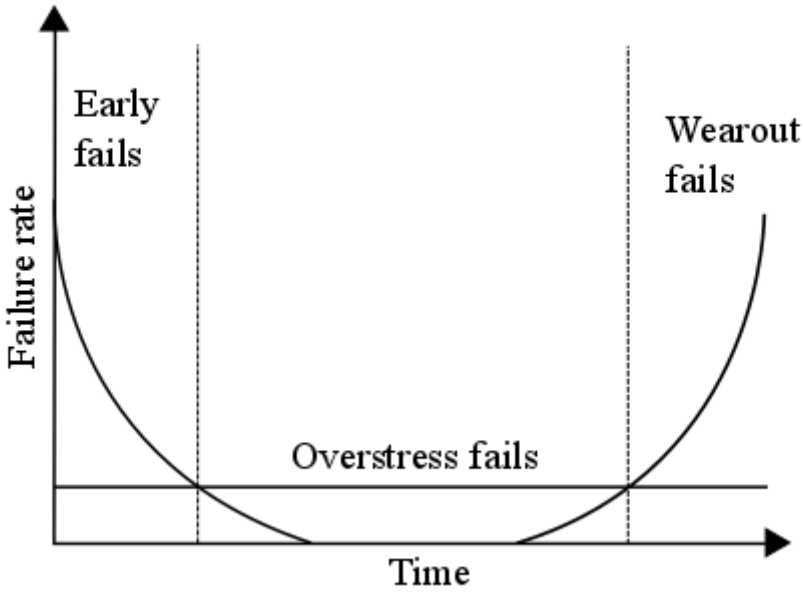

Figure 9. *Failure rate, bathtub curve [38].*

As many failure mechanisms can affect lifetime of a product, it is important to be able to detect possible failure types as early as possible in product development. Accelerated testing methods may be used to simulate failure mechanisms caused by mechanical, environmental and electrical stress. By using elevated testing conditions, failure mechanisms may be detected relatively fast, without need to wait until the device has reached the end of its lifetime.

Environmental tests are used to detect effects of corrosion, and are usually executed with elevated temperature or humidity. One example of reliability test is a so-called 85/85 test, which is used to evaluate lifetime in normal storage conditions. In this test, a constant temperature of 85 °C and relative humidity of 85 % are used as testing conditions. This test is also used in this thesis and will be discussed further in Subchapter 4.3. To inspect the effects of temperature variation only, mechanical durability can be tested by slowly changing temperatures to simulate the effects of mechanical stress over time in normal use, or by rapid changes to see the maximum effect of variating temperatures.

In addition to previously mentioned test methods, effects of dropping and vibration can be inspected. In addition, products may be tested electrically by adding a constant high voltage or ESD. ESD testing is important especially in consumer electronics, since user

is likely to cause a capacitive discharge at some point. When tests have been completed, different microscopes and x-ray can be used to detect failures caused by aging. [38]

3. MATERIALS

The purpose of this thesis was to evaluate suitability of different conductive inks on PPE based test substrates. The properties of this material are suitable for HF devices and is therefore an attractive substrate for printed HF applications. Material parameters of this substrate are discussed further in Subchapter 3.1. PTFE (Polytetrafluoroethylene), also known as Teflon, is another typical substrate for HF applications [38]. The main challenge of these HF applicable materials is that they are usually rather hydrophobic. Therefore, surface treatments may be needed to enhance ink performance on these substrates.

In addition to the used substrate material, five commercially available silver inks were selected for this survey. These inks were selected due to both their manufacturer information and results obtained in literature. The objective was to find screen printing inks, which could be utilized in HF applications printed on the selected PPE substrate. Selected inks are discussed in further detail in Subchapter 3.2.

3.1 Substrate

In this survey, Preperm® L260, a PPE based polymer compound by Premix company was used as a substrate material. This particular substrate material has been designed for especially HF applications. It has a very low DF below 0.001, and low relative permittivity ε_r (2.6) over a wide range of frequencies [40]. Low dissipation factor and relative permittivity enable low-loss signal, because signal is not attenuated by substrate [39; 40]. HF applicability makes this material an excellent substrate for different antenna structures, such as wireless base station applications.

These substrates are fabricated by injection-molding. Injection-molded substrates used in this thesis are 3mm thick, and the dimensions of square-shaped surface area is 100cm^2. By injection molding, melt plastic material is forced to flow into a closed mold [41]. Material is then cooled down, and it forms a solid structure, shaped as the used mold. This process provides many benefits for the manufacturing of wireless PE applications, since various substrate shapes may be achieved by mold selection. Additive PE techniques allow effective fabrication of electrical structures on these 3D substrates and therefore, completely new devices may be manufactured. Such devices are known as MID (Molded Interconnect Devices). MID fabrication by printing electronics on 3D shapes has been researched, and promising results have been obtained [42; 43]. Applications for these devices may be found for example in automotive industry and aviation, where fabrication of MID enables electrical component integration directly to machine structures.

In addition, extruded PPE substrates were used for comparison between different molding techniques. Extruded substrates are fabricated by forcing heated plastic material through an aperture with a defined shape, after which shaped material is cooled rapidly [44]. These substrates are only 1mm thick, thus being thinner and more flexible than the injection-molded substrates.

3.2 Inks

For this survey, five commercial silver inks were selected. Selection was made based on results obtained in literature, and on manufacturer information and recommendations. Selected inks are listed in Table 5, with their most critical technical information, such as solvent type and silver content. In addition, as the used substrate material is sensitive for temperatures over 180 °C [40], required ink curing temperature affected selection.

Table 5. *Selected inks and their technical information provided by manufacturers* [45-49].

Manufacturer/ink						
Type	**Viscosity (cP)**	**Ag-contents (%)**	**Solvent**	**Sheet resistance mΩ/□**	**Line thickness (µm)**	**Curing °C (min)**
SunChemical / CRSN2442						
flake	2000-3000	69-71	Propylene diacetate	10	25	150 (30)
Novecentrix / Metalon HPS-FG32						
flake	8000	75	Butyl carbitol	25	25	140 (10)
Asahi / LS411AW						
flake	20000-30000	75-78	Butyl cellosolve acetate, Isophorone	<40	10	150 (20)
DuPont / 5064H						
flake	10000-20000	63-66	C11-ketone	≤14	25	130 (20)
Novacentrix / Metalon HPS-021LV						
flake	2600	75	Water	11 (25)	25	150 (30)

Resistance information in Table 5 shows that all the inks used in this thesis are highly conductive, which should result to low sheet resistance of printed structures. Importance of conductivity is emphasized especially at high frequencies, where current carrying layer becomes thinner by increasing frequency, and therefore low resistivity is needed [50].

Other inks include organic solvents, excluding aqueous Novacentrix HPS-021LV. Therefore, it is more environmentally friendly than other inks used. In addition, manufacturer recommended this ink for its conductivity abilities. HPS-FG32 ink, from the same manufacturer, was also chosen based on manufacturer recommendation. This ink is recommended to be used in especially those applications, where soldering ability is required, thus enabling attachment of for example IC (Integrated Circuit) chips.

On the other hand, DuPont 5064H should be highly conductive, despite the relatively low silver contents (63-66 %). SunChemical CRSN2442 ink was also recommended due to its conducting abilities, which should be comparable to those of 5064H and HPS-021LV inks. On the contrary, Asahi LS411AW electrical performance seems to be more moderate according to the manufacturer information, but since sheet resistance information has been provided only for relatively thin lines, this ink was selected for conductivity tests as well.

In addition to silver contents and sheet resistance information, it may be observed that there is variation in ink viscosities. Asahi LS411AW viscosity is higher than CRSN2442 and HPS021LV ink viscosities by an order of magnitude. On the other hand, 5064H ink viscosity is approximately 70 % of LS411AW viscosity and HPS-FG32 viscosity is a bit lower than that. These viscosities are suitable for screen printing. However, difference in viscosities is quite significant, and may lead to differences in ink behaviour.

In addition to manufacturer information and recommendations, results obtained in literature were used as other selection criteria. Most of these inks have already been studied in various applications, and they have also been compared to each other. The aqueous HPS-021LV ink has been successfully used earlier in HF applications to produce RFID tags on novel substrates. Examples of this work include brush painting on plywood in [51] and dispensing on textiles in [18]. In [52], this ink's abilities were compared to DuPont 5064H. Inks were used to print electrodes on a microfluidic platform. It was observed, that HPS-021LV sheet resistance was outstanding compared to sheet resistance with 5064H. HPS-021LV also lasted twice as long in adhesion tests as 5064H. However, 5064H oxidation charge performance surpassed HPS-021LV clearly.

In addition, RFID properties of 5064H and CRSN2442 on a cardboard substrate were compared in [53]. Here, CRSN2442 performed slightly better in conductivity, and uniformity of printed lines surpassed those of 5064H. Therefore, CRSN2442 was used for more detailed characterization of printed tags. Promising results were achieved. In an-

other, rather similar study [54], properties of CRSN2442 and 5064H inks were also compared in RFID tag fabrication, printed on paper and cardboard. In that study, more uniform lines were also obtained with CRSN2442. However, significantly better sheet resistances were measured with 5064H. These results indicate that in addition to substrate material and conductor dimensions, properties of printed lines are highly dependent on both process parameters and operators.

In another study, 5064H was compared to LS411AW by sheet resistance and bending reliability on a thin PET substrate [55]. Sheet resistance of both inks was low, compared to another ink used in that survey, but they were not as successful in cyclic bending reliability tests. In [56], promising results for sheet resistance of a moisture sensor printed on a PET substrate were obtained with LS411AW ink by R2R (roll-to-roll) printing and calendaring. On the other hand, in [57], LS411AW was used to print capacitors and inductors on another plastic substrate, and showed promising results in environmental reliability tests.

CRSN2442 was also studied in [58] to see the effects of different surface treatments on PEN (Polyethylene Naphthalene) and PDMS substrates. It was concluded, that this ink had low sheet resistance and good adhesion on the substrates and was also able to endure moderate bending.

Some of the sheet resistances obtained in literature with selected inks are listed in Table 6. It can be observed that rather low sheet resistances have been obtained in different applications. However, obtained sheet resistance is highly dependent on the physical dimensions of the printed lines, as well as on the used substrate material. Paper and cardboard are significantly rougher and more porous substrates than glass or plastic films, which may have influenced results.

Results obtained in literature indicate that especially HPS-021LV is highly conductive, and DuPont 5064H shows promising results. In [54], CRSN2442 sheet resistances are a little more moderate than those obtained with 5064H, and LS411AW conductivity seems to have been dependent on the used line dimensions and fabrication methods. The variation in the results of [56] is caused by the difference in drying conditions and surface roughness of the printed lines. Lower sheet resistance values have been achieved with longer curing times and calendaring of printed lines.

Table 6. *Sheet resistance values obtained in literature with studied inks.*

Reference	Ink	Substrate	Line thickness (µm)	Line width (µm)	Sheet resistance (mΩ/□)
[52]	HPS-021LV	Glass	6	-	15
	5064H	Glass	5	-	28
[54]	CRSN2442	Paper	6-10	3000	<90
		Cardboard			≤92
	5064H	Paper	6-10	3000	<60
		Cardboard			<60
[55]	LS411AW	PET	10-15	1500	31
	5064H	PET	10-15	1500	26
[56]	LS411AW	PET	8-11	500	15-58
[58]	CRSN2442	PEN	10-15	-	50

4. PROCESSES

Since the used PPE based compound is a novel substrate choice for PE applications, literature survey was necessary to determine suitable fabrication and characterization methods for this polymer substrate. Characterization of novel polymer substrates for PE applications has been made earlier in for example [59] and [25]. In [59], a PPO (Polyphenylene Oxide) compound was used as a substrate for electroless copper plating. PPO is a rather similar compound as the one used in this thesis, and was developed to be used in HF applications. In [25], suitability of novel polymer substrates was evaluated in inkjet printed applications.

Selected process flow for this survey is demonstrated in Figure 10. Processes used in this thesis are discussed in further detail in this chapter, and all characterization methods used to analyse fabricated test samples are discussed in Chapter 5. After substrate and ink selection, suitable surface treatments were looked for. As the PPE substrate surface energy was known to be rather low, surface energy increasing treatments were selected to see the effects on print quality and performance. More information of the selected surface treatments is provided in Subchapter 4.1. These treatments were tested on the injection-molded PPE substrate to determine optimal treatment parameters. All surfaces were characterized before and after treatments to see the effects on surface energy and surface profile. Characterization methods used for surface analysis are discussed further in Subchapter 5.1.

After surface characterization and treatment parameter optimization, test substrates were fabricated for printing. Test patterns were screen printed with a self-designed screen pattern, after which both electrical and mechanical performance of printed test samples were characterized. Printing process is discussed further in Subchapter 4.2., whereas methods used to characterize sample performance are discussed in Subchapters 5.3. and 5.4.

Based on initial performance of printed samples, best ink-substrate combinations were selected for accelerated environmental tests to see the effects of environmental stress. Chosen environmental tests and their parameters are presented in Subchapter 4.3. When reliability tests were completed, effects of aging were characterized.

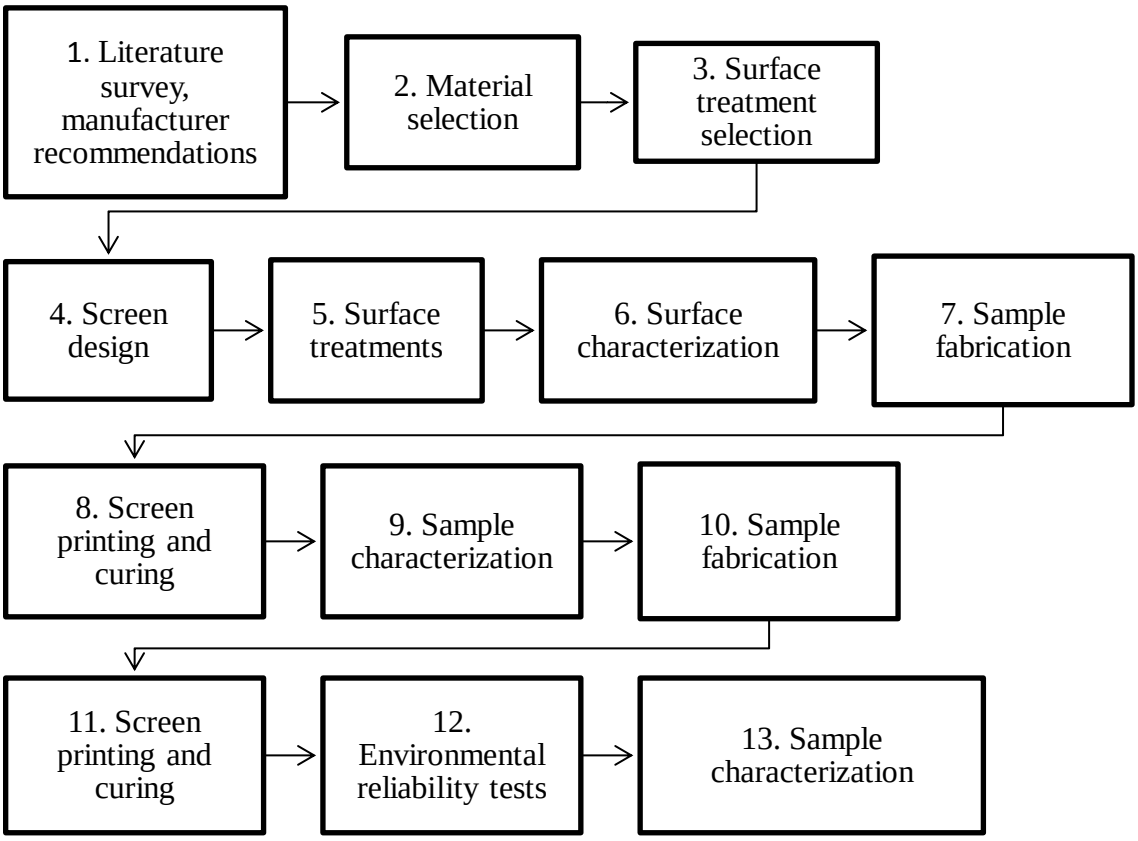

Figure 10. *Survey process flow.*

4.1 Surface treatments

Originally, the surface energy of the PREPERM® L260-substrate is low, which may lead to insufficient level of wetting and cause poor performance of the printed structures, as discussed in Chapter 2. To improve surface wetting and thus to enhance print quality, different surface treatments were selected to improve material interface interactions by increased surface energy. In addition to surface energy modification, such treatments were selected, which could modify surface profile. Thus, the relationship between surface roughness and surface energy could be analyzed. On the other hand, such treatments were selected, which could be utilized on a production line.

Based on literature survey, six treatment methods were selected. These methods include exposure to oxygen plasma, flame-pyrolytic surface silicating, chemical etching with both acid and base, and chemical coating. All surface treatments used in this thesis were applied to the injection-molded substrate and the extruded substrate was used as one of the treatments.

First, initial tests were performed to determine the optimal surface treatment parameters. When these parameters had been optimized, the injection-molded substrates were treated accordingly, and effects were observed prior to printing. Surface treatments used in this thesis are listed in Table 7. Surface treatments are discussed in further detail in next sections.

Table 7. *List of the used surface treatments.*

Surface treatment
Reference (no treatment)
Oxygen plasma
Sulfuric acid, 98 %
KOH, 5-10 %
KOH, 30 %
Flame-pyrolytic silicating
Ethyltriglycol
Ethyltriglycol & sulfuric acid
Extrusion

4.1.1 Plasma

Plasma treatment is a well-known, effective method to for surface energy modification of polymers. In addition, it is possible to modify the functional groups on the surface, and thus adhesion may be promoted with this method, especially when oxygen is used [60-62]. Therefore, exposure to oxygen plasma was chosen as one of the surface modification methods in this thesis. In [63] and [64] it has been concluded, that the effect of the treatment is highly dependent on both substrate compound and selected gas. In addition, longer treatment times lead to effective surface modification. However, as sufficient results may be obtained in only few minutes, this treatment is rather efficient.

The most significant drawback of this method is that the functional groups formed during treatment are often instable, and therefore enhanced surface properties tend to decrease over time. This tendency limits the time period between pretreatment and printing. On the other hand, it was observed that the proportion of new functional groups is saturated above the original level, and therefore this treatment may cause a permanent modification of the surface.

The principle of plasma treatment is illustrated in Figure 11. Substrate is first loaded to a process chamber, and it is cleaned in vacuum atmosphere. Gas flows from the supplement bottle to the chamber, and plasma is created in the chamber by an electrical discharge at a high frequency. Ionized gas then reacts with the substrate molecules, such as carbon, and new functional groups are created on the substrate surface. In addition, some molecules on the surface may be removed entirely by plasma, which leads to significantly altered molecule composition on the surface.

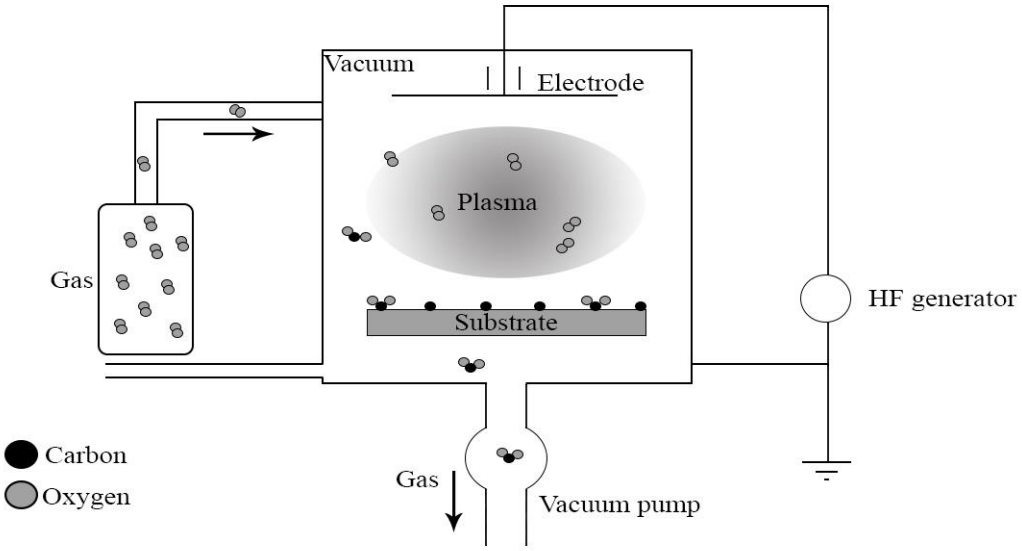

Figure 11. *Principle of oxygen plasma treatment. Adapted from [65].*

In this thesis, an Oxford Plasma Technology RIE System 100 plasma printer was used for plasma surface modification. This device was operated in cleanroom conditions. First, the optimal recipe for plasma treatment was determined with a few test samples. In Table 8 are presented parameters used for initial plasma treatments.

Table 8. *Test parameters for oxygen plasma modifications.*

Treatment	Exposure time	Power	Chamber pressure	Gas (O_2) amount
1.	1 minute	25 W	56.0	30.0
2.	1 minute	50 W	56.0	30.0
3.	1 minute	75 W	56.0	30.0

4.1.2 Flame-pyrolytic silicating

A NanoFlame NF02-device by Polytec, presented in Figure 12, was used to modify the injection-molded substrate surface with both heat and chemical coating. The NanoFlame pistol is filled with a special propane-butane-organosilicon gas [66]. Flame size and the amount of burning-enhancing air can be controlled. With this treatment, a 20-50 nm thick silicon dioxide layer is formed on the substrate surface at high temperature. The purpose of this treatment is to improve both wetting and adhesion of the treated substrate [66]. This treatment has been successfully used earlier as an adhesion promoter for example in [67].

Samples were treated so that the flame was moved back and forth on the substrate surface with rapid movements to avoid burning of substrate material. Samples were then turned 45˚ and treatment was repeated. This was repeated so that sample was turned 360˚ in total during the treatment, to enable as even coating as possible.

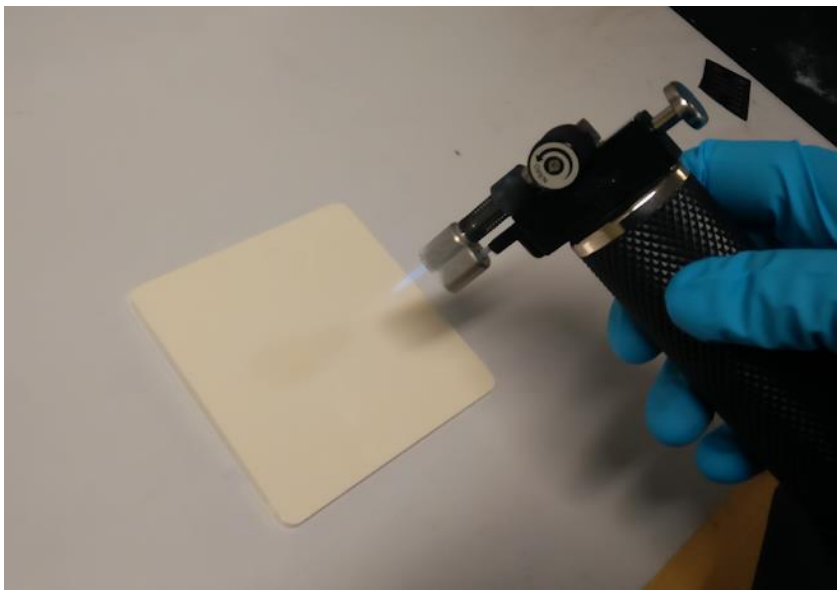

Figure 12. *Sample treatment with a Nanoflame-device.*

4.1.3 Chemical

To modify substrates chemically, they may be dipped, wiped or spray coated. Best technique depends on the used chemical, and the applicability on a production line. For example, organic solvents may be used to spray coat substrates when proper ventilation is

provided, and the most sufficient treatment with strong and hazardous chemicals is dipping, to ensure safety.

In this thesis, three different chemicals were used to modify the surface energy of the substrate. 98 % concentration of sulfuric acid, and 5-10 % and 30 % concentrations of KOH (Potassium Hydroxide) were selected, because promising results have been obtained in literature with for example PPO and PI substrates [59; 68]. In addition, ethyltriglycol was chosen to be used as an ink primer. Conductive ink manufacturer recommended this organic solvent.

First, initial tests were executed to find suitable parameters for chemical treatments. Treatment times of several minutes have been used in literature with sulfuric acid and KOH [59; 68]. In addition to long treatment time, both sulfuric acid and KOH are rather hazardous to inhale and skin contact should be avoided. Thus, dipping seemed to be the most sufficient treatment method for these chemicals. Dipping times of 1 minute, 2 minutes, 5 minutes, 10 minutes and 15 minutes were used. After chemical dipping, samples were dipped in water container and rinsed with DI (Deionized) water to remove the excess chemical from the substrate. Treatment setup is demonstrated in Figure 13 and treatment parameters are presented in Table 9.

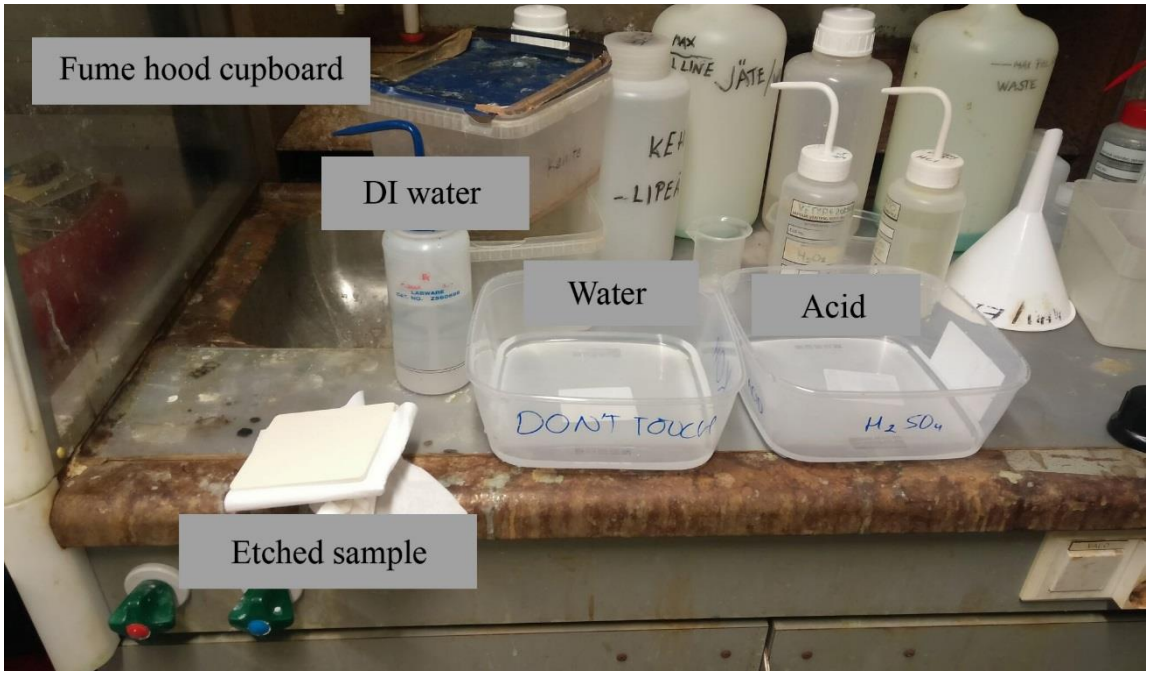

Figure 13. *Etching treatment setup.*

Table 9. *Etching times for the initial base and acid surface treatments.*

Treatment	1.	2.	3.	4.	5.
Sulfuric acid 98 %	1 minute	2 minutes	5 minutes	10 minutes	15 minutes
KOH 5 %	1 minute	2 minutes	5 minutes	10 minutes	15 minutes
KOH 30 %	-	-	5 minutes	10 minutes	-

Ethyltriglycol was sprayed on the substrate with an airbrush device. Spray coating is a well-suited technique for production lines for its simplicity and rapidness, and it was the recommended technique by manufacturer. To better characterize the effect of this primer coating, ethyltriglycol spraying was tried on both untreated substrates and substrates already treated with sulfuric acid. To untreated substrates, three layers of spray-coating was applied. Samples were heated in oven between each layer to cure chemical and to form a permanent coating. To pretreated substrates, only one layer of coating was sprayed, followed by oven-curing. All samples were cured in 100 °C for 10-20 minutes, depending on the thickness and uniformity of the sprayed layers. Spray coating parameters are listed in Table 10. Pressure of the airbrush device and distance from samples was adjusted to optimize coating.

Table 10. *Spray coating parameters used with ethyltriglycol.*

Treatment	Air pressure	Distance	Layer count	Curing conditions
Without acid etching	1.1 bar	15 cm	3	100°C/10-20 min
With acid etching	1.1 bar	15 cm	1	100°C/10-20 min

In Figure 14, test setup used for spray coating is demonstrated. Samples were attached to an aluminum plate to enable coating of multiple samples simultaneously. To prevent chemical spreading to the environment, samples were sprayed inside a sealed plastic box in a fume hood cupboard.

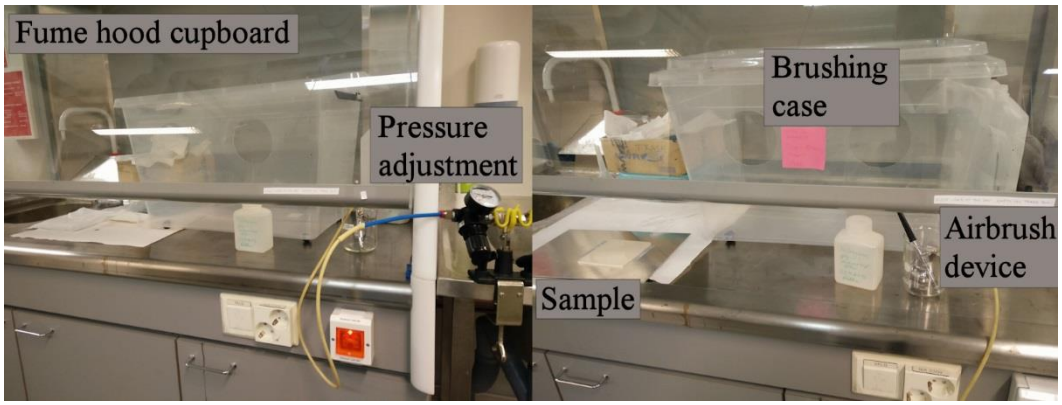

Figure 14. *Primer treatment setup.*

4.2 Printing

After substrate surface preparation, test patterns were screen printed in cleanroom conditions. Used printer is for single-sheet printing only, and it is adjusted manually. In Figure 15 is presented printer, control buttons and squeegee placement above the screen during printing. In this printer, it is possible to adjust squeegee pressure against screen by adjusting the vertical placement of the squeegees. In addition, distance between screen mesh and substrate can be adjusted. A metal squeegee is used to apply ink evenly on the screen, and a rubber squeegee is used to press ink on the substrate. The control buttons are used to move squeegees and to lift frame holder. These printer parameters were adjusted manually for each printing session.

For this survey, a UX79-45 polyester screen with an aluminum frame was used. The specifications for this screen are listed in Table 11. UX stands for "Super High Modulus Polyester Monofilament" [69]. UX-threads of the screen can endure high tensile strength and higher tension level of threads is allowed. Screen was manufactured to best fit the requirements of all the inks used in this thesis. Therefore, it was both solvent- and water-resistant. Threads were placed at 22,5° angle to achieve the best possible print quality.

Two test patterns were used on this screen, both of which were used for different performance tests. These test patterns are presented in Figure 16. Test pattern A was used to print patterns for 4PP conductivity measurements and square patterns (B) were used in adhesion crosscut tests. Patterns were designed so that as many shapes would fit to one sample printed on a 10 cm x 10 cm substrate as possible. In addition, with this design, two substrates could be used simultaneously, thus speeding up the printing process. Two sample sets were printed for both performance tests.

After printing, samples were sintered thermally according to the sintering condition recommendations given on datasheets. Recommended conditions were given for thin PET films, and may therefore not be optimal for rather thick PPE substrates. However, these

conditions were comparable to each other. Used curing conditions are summarised in Table 12.

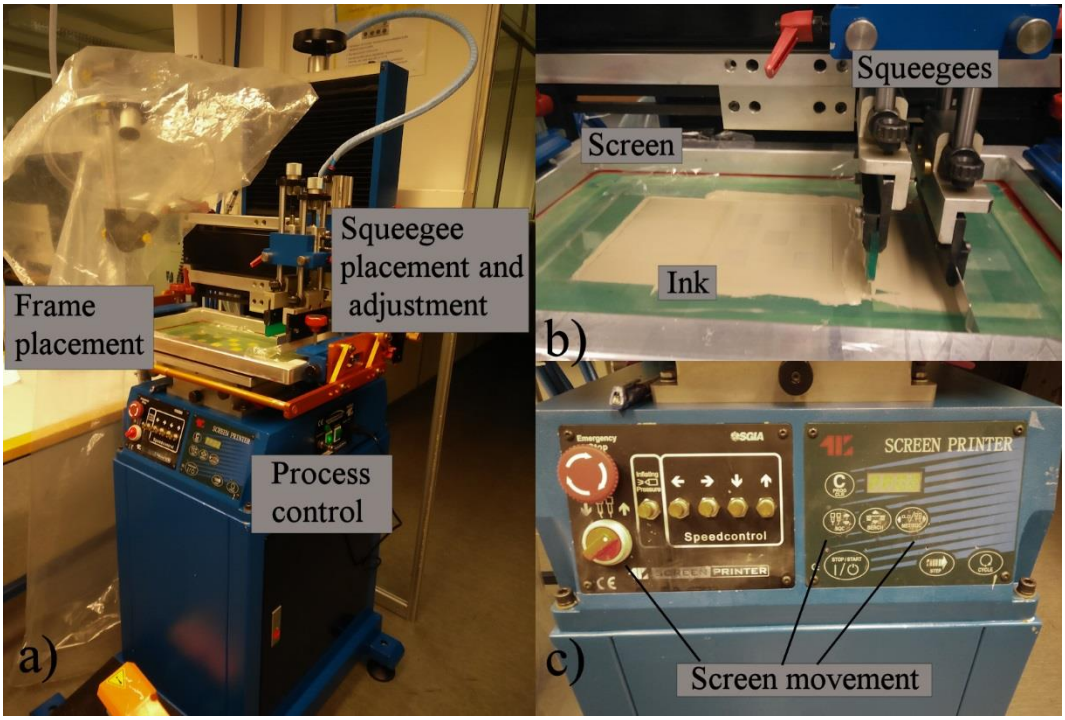

Figure 15. *a) Screen printer. b) Screen and squeegees during printing, c) control buttons.*

Table 11. *UX79-45 screen parameters* [69].

Thread type	Threads/cm	Thread diameter (µm)	Mesh opening (µm)
UX	79	45	81

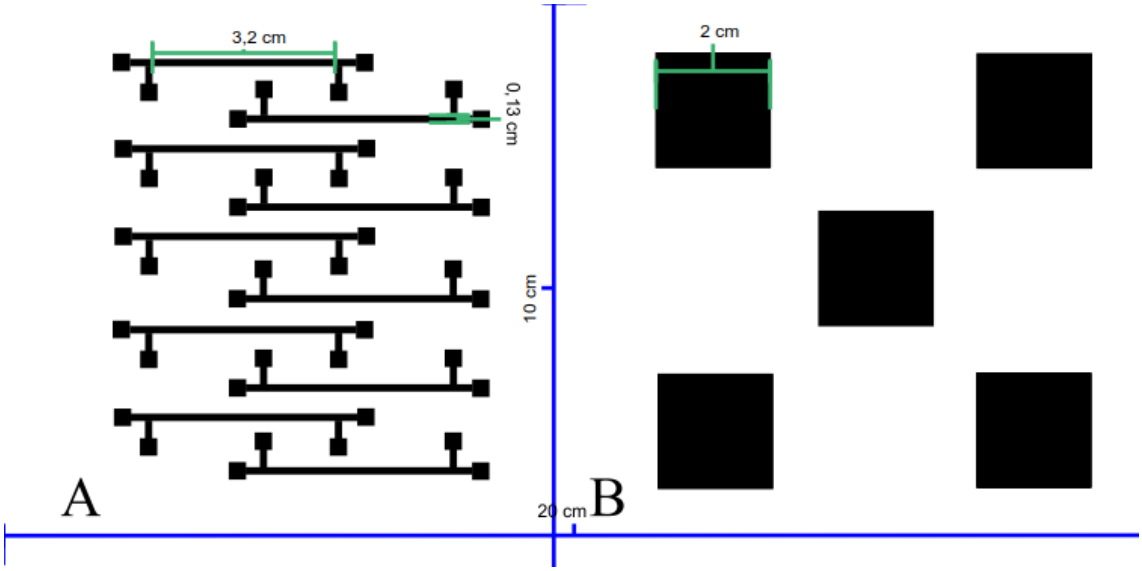

Figure 16. *Designed screen with dimensions.*

Table 12. *Used sintering conditions for each ink.*

Ink	Temperature (°C)	Time (minutes)
SunChemical CRSN2442	150	30
Novacentrix HPS-FG32	140	10
Asahi LS411AW	150	20
DuPont 5064H	130	20
Novacentrix HPS-021LV	150	30

4.3 Environmental reliability tests

Based on the results of the initial conductivity measurements and adhesion classification, best ink-substrate combinations were selected for environmental reliability tests. Four samples were fabricated for each ink-substrate combination with test pattern B, since possible effects were assumed to be more critical to adhesion than conductivity, based on results obtained in for example [70] and [71]. Two reliability tests were used in this thesis. The standardized test conditions for both tests are summarized in Table 13.

Table 13. *Test conditions of the used environmental tests.*

Humidity + temperature	JESD22-A101C, 85/85 test. Constant temperature of 85 °C and constant relative humidity of 85 %. 500 h.
Salt mist	IEC 60068 2-52. NaCl spray at a temperature of 35 °C for 2 h, followed by 7 days in constant temperature of 40 °C and in relative humidity of 93%. 2 Cycles.

First, 85/85-test, according to JEDEC standard JESD22-A101C [72] was used. This test is used to simulate aging caused by heat and moisture simultaneously. Obtained results give a good estimation of the basic environmental durability of the product under normal storing conditions. During test cycle, temperature should be maintained in 85 ± 2 °C and relative humidity should be 85 ± 5 %. In this thesis, one 500-hour cycle was used to detect possible effects on adhesion.

For this test, samples were placed to a self-designed aluminum channel structure to reduce required space in test chamber and to enable more practical placement of the samples. Samples were aligned between aluminum channels so that substrate corners were placed to the diagonally cut slots of the channels. The order of the samples in this test is not significant, since conditions are stable in the whole chamber. Designed holder structure, sample location and placement in Weiss C340 test chamber are demonstrated in Figure 17.

In addition, a cyclic salt mist-test according to the IEC 60068 2-52 standard [73] was used with severity level four. This test is intended for testing of aging effects by frequent changes between salt-laden and dry atmospheres. This test is useful especially for marine applications, where devices are exposed to salty and humid environment. In addition, it is an attractive test method to simulate aging of base station applications, which are often located outdoors.

For this test, samples were placed to an Ascott S450XP chamber, as demonstrated in Figure 18. It may be observed that the used NaCl (Sodium Chloride) concentration is sprayed upwards from the bottom of the chamber. The spray shooting openings are marked with a black circle. Thus, the salt concentration is not sprayed evenly to the chamber. Therefore, to prevent sample placement in chamber from affecting test results, samples were placed to the chamber randomly. Similar aluminum channels were used for sample placement as in 85/85 test. When test was finished, samples were removed from test chamber and rinsed with water to remove excess salt.

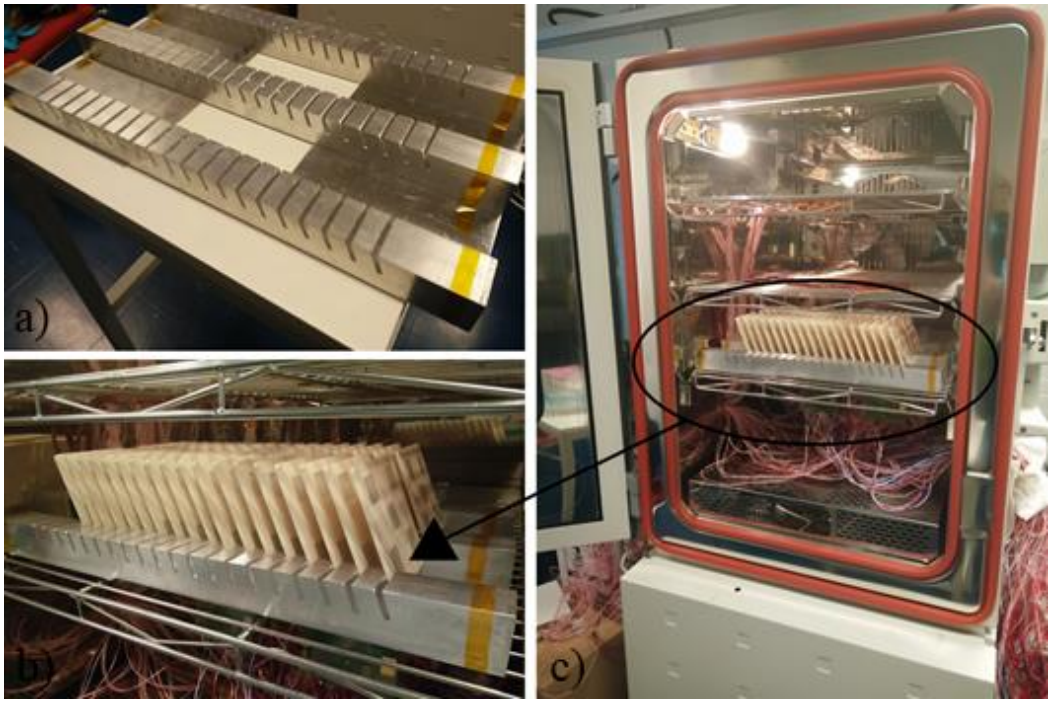

Figure 17. *a) Channel structure designed for the sample placement in 85/85-test, b) sample placement on the holder, c) sample location in the chamber.*

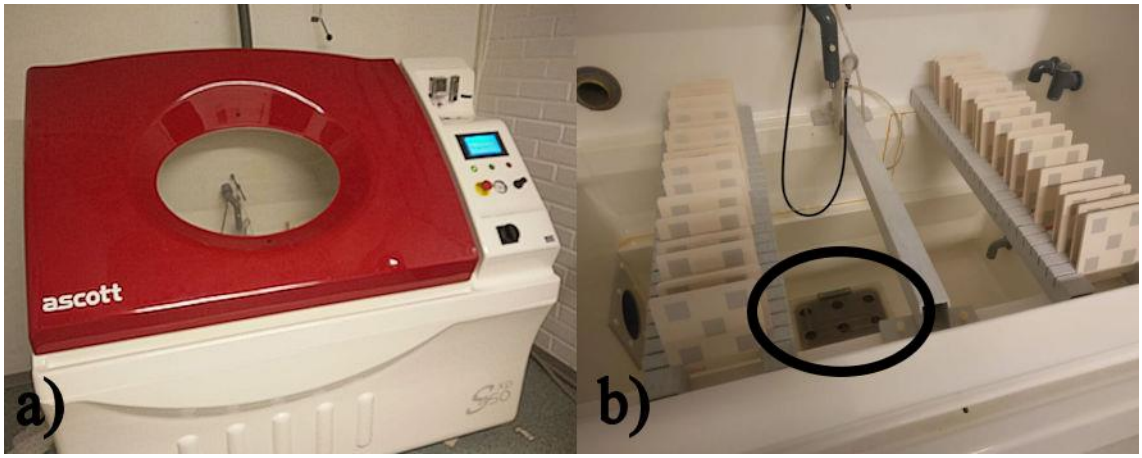

Figure 18. *Salt-mist chamber from a) outside, b) inside.*

5. CHARACTERIZATION

After each fabrication step, samples were characterized according to Figure 10 process chart. Since the objective was to characterize untreated PPE substrates, as well as surface treatment effects on substrates and performance of printed structures, such characterization methods were selected that characterization would be as accurate and effective as possible.

Selected characterization methods are presented in this chapter. First, the surface analysis tools are discussed. Secondly, methods for quality inspection are presented. After that, conductivity measurement setup and adhesion characterization method are discussed respectively.

5.1 Surface analysis

For the characterization of untreated PPE substrates, an optical microscope was used to inspect the main differences between the injection-molded and extruded substrates. In addition, both surface energy and surface roughness of the untreated PPE substrates were measured to be used as a reference for surface treatment characterization. Surface energy was measured with special measurement pens from Dyne-Testing. These pens have been designed to enable rapid and simple measurement of surface energies. Pens contain fluid mixture, concentration of which is varied to produce large scale of surface energies.

With Dyne-pens, surface energy measurement is executed by drawing a line to the substrate surface. If the used fluid remains on the surface for at least three seconds, surface energy has the minimum numeric value of that Dyne-pen. Otherwise, if fluid is drawn back in less than one second, surface energy of the substrate is smaller than the pen surface energy value. Lines are drawn until the best surface energy approximation has been made. A set of 20 Dyne-pens with values 30-60 Dynes/cm (mN/m) were used in this thesis. Surface energies were measured again after surface treatments to compare the measured values.

To be able to analyse the surface profile of samples, substrates were inspected with an optical profilometer Veeco Wyko NT1100 to see the possible effects on surface roughness. With an optical profilometer, several roughness parameters can be obtained. The RMS (Root-Mean-Square) roughness R_q may be calculated:

$$R_q = \sqrt{\frac{1}{n}\sum_{i=1}^{n} y_i^2}, \tag{7}$$

where y is the deviation over the roughness mean, and n is the number of samples [74]. This parameter describes the standard deviation of height distribution on the surface, and it is affected greatly by the deviations from the surface mean line. It is therefore a good measurement parameter for rough substrates with a lot of deviation. In addition to substrate surface characterization, this parameter may be used to evaluate the uniformity of the printed conductors.

Another important parameter used to measure surface roughness is range R_t [74]. It is defined as the difference between the highest peak and lowest valley on the measured surface area and may be written :

$$R_t = R_p - R_v, \tag{8}$$

where R_p is the highest peak of the surface profile and R_v is the lowest valley of the surface profile [74]. This parameter can be used to evaluate surface roughness, as well as thickness of printed conductor lines.

5.2 Print quality inspection

Due to different level of wettability caused by surface treatments, line dimensions may vary in the printed structures. In addition, line thickness and surface porosity of prints may vary due to the different ink compositions and printing parameters. An optical microscope was used for quick print quality check and to measure line widths after sintering, whereas thickness and porosity of cured prints were measured with an optical profilometer. The maximum height difference of the profile R_t was used to determine the maximum line thickness and RMS-roughness R_q was used to analyse the deviations of the line profile. Calculated values were used to analyse print quality obtained with used inks and printing parameters.

SEM (Scanning Electron Microscopy) was used to analyse the silver flake topology of the cured conductors. In addition, SEM images were obtained from ink-substrate cross-sections to see if inks adhere differently on treated surfaces. Results of print quality inspection are presented in Chapter 6.

5.3 Conductivity measurements

To measure sheet resistance of the printed samples, a Keithley 2425 sourcemeter was connected to a 4PP measurement system presented in Figure 19. Two probes were connected to input channels of the sourcemeter, and the other two probes were connected to sensing channels of the sourcemeter. All measurements were executed in 4 wire sense-mode and a source current of 10 mA was used.

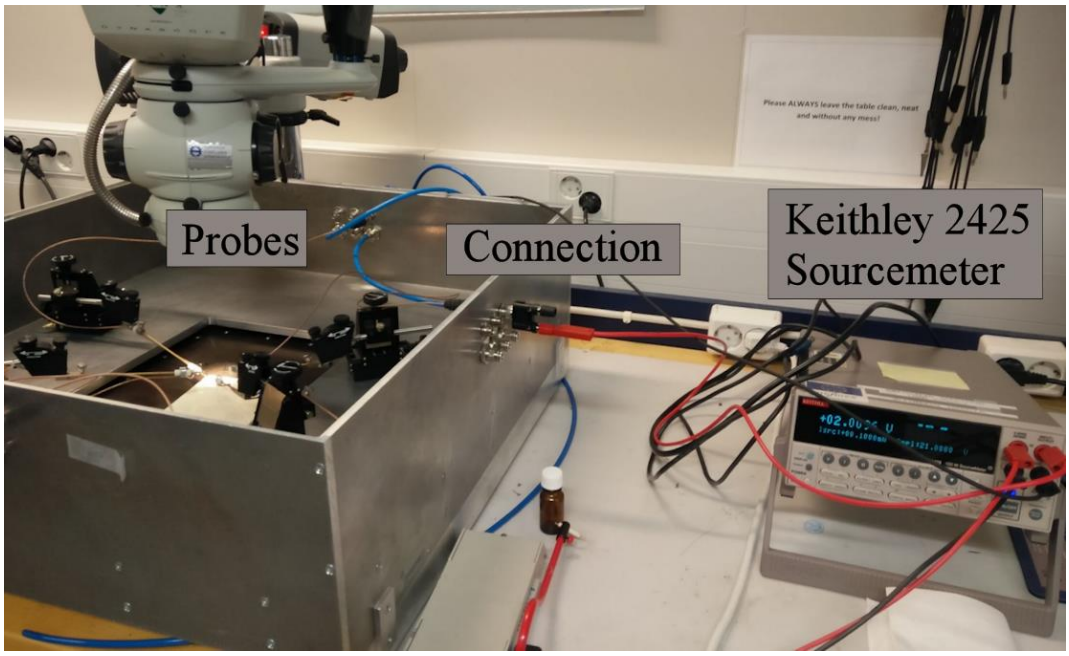

Figure 19. *4PP measurement setup.*

In Figure 20, probe placement on measured conductor pads is demonstrated. The probes on the outer pads feed current to the conductor and the probes on the inner pads are used to measure voltage created between them.

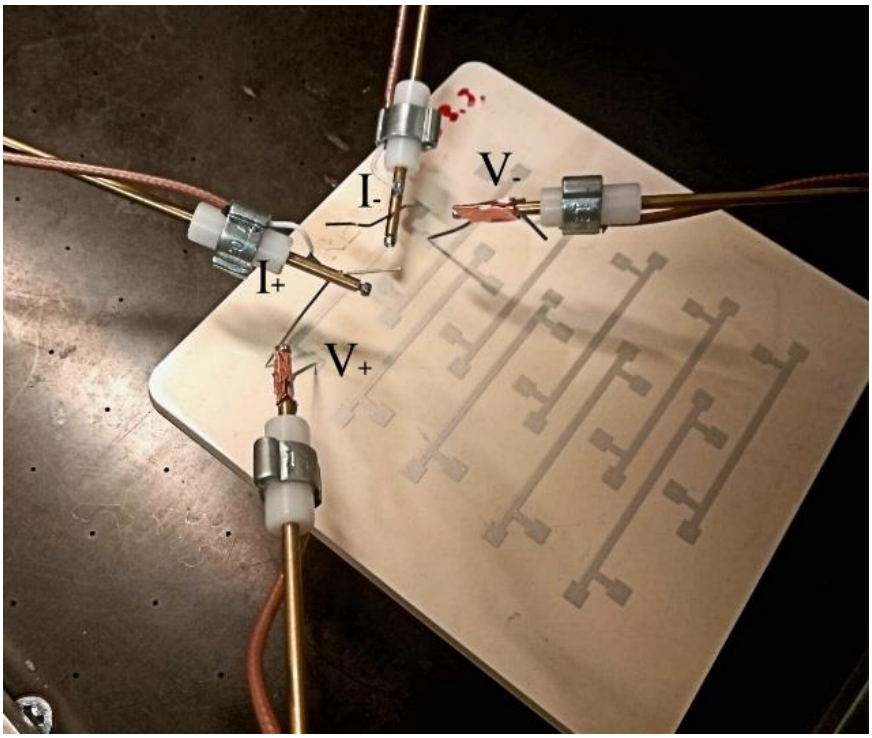

Figure 20. *Probe placement on the conductor pads.*

Conductor sheet resistances were calculated from measured voltage values by equation (6), and calculated values were compared between each ink-substrate combination. Results are discussed in Chapter 6.

5.4 Adhesion classification

Mechanical performance of printed samples was determined by a cross-cut test, as instructed in ASTM D3359 standard [75]. Samples printed with test pattern B were used in this test. As instructed in the standard, first a specific cutting tool was used to cut printed square patterns horizontally so that the printed structure was pierced thoroughly and substrate material was reached. Cuts were inspected with a magnifier lens and when cutting depth was observed to be satisfactory, cutting process was repeated so that new cuts were aligned at 90˚ angle from first cuts. Cutting quality was again inspected and if new cuts were appropriate, next test phase was executed. Otherwise, new cuts were made next to previous cuts, as instructed in the test standard. In Figure 21, a sample before and after cutting phase is demonstrated.

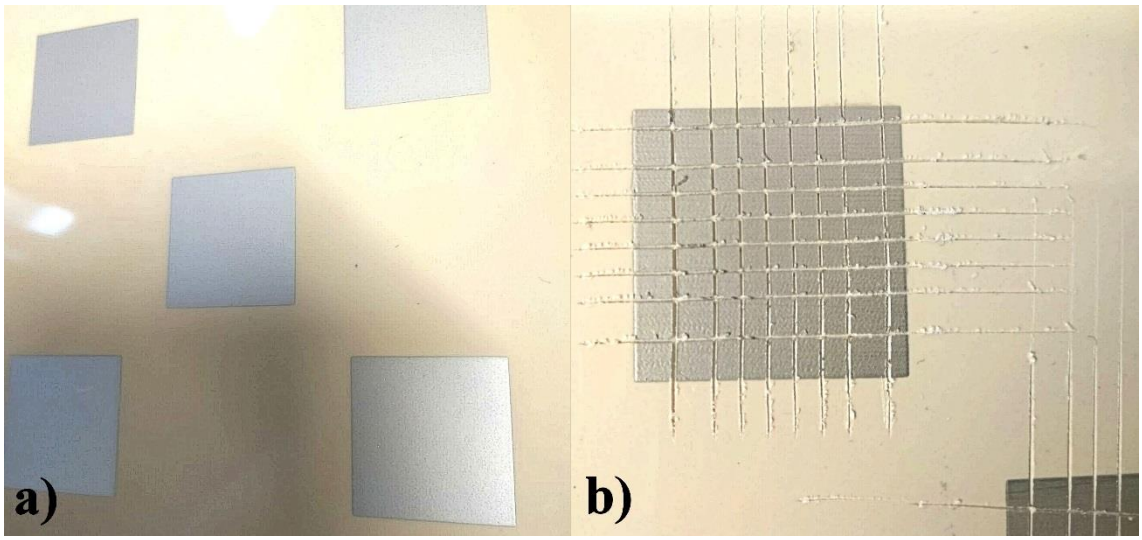

Figure 21. *a) Pattern B after printing, b) Pattern B after crosscut test.*

Next, a standardized adhesion tape was used to determine peel-off adhesion of prints. First, two full rounds of tape were removed from the roll, and approximately 7.5cm-long tape pieces were cut. Tape pieces were then applied onto test patterns so that the cut intersection was aligned in the middle of the tape piece. When tape was applied to the sample, proper adhesion was ensured by rubbing tape surface with finger and eraser. 90 ± 30 s after tape application, it was peeled off from the free end on, pulling it off rapidly at 180˚ angle.

After tape peeling, adhesion was classified from the cut intersection by a standardized classification scale. ASTM-D3359 standard scale used in this thesis is presented in Table 14. The results of this classification are presented in Chapter 6.

Table 14. *Adhesion classification by ASTM-D3359 standard.*

Classification scale	**Area removed, %**
5B	0
4B	<5
3B	5-15
2B	15-35
1B	35-65
0B	>65

6. RESULTS AND DISCUSSION

In this chapter, the main results obtained in this study are presented. In addition to the parameters related to substrate parameters and performance of printed structures, the success of printing process and test method validity are discussed.

First, surface characterization results for each test substrate are presented. Secondly, quality of printed patterns is evaluated. After that, sheet resistance measurement results and adhesion classification results are presented. Finally, aging effects caused by the environmental reliability tests are demonstrated.

6.1 Surface profile

Visual inspection with an optical microscope revealed that surface of the injection-molded Preperm® L260 substrate is rather flat and smooth, despite the faults caused by the molding process. On the contrary, extruded substrates appear to have a rather rough surface profile, but without any visually observed faults. These differences between differently molded substrates are demonstrated in Figure 22.

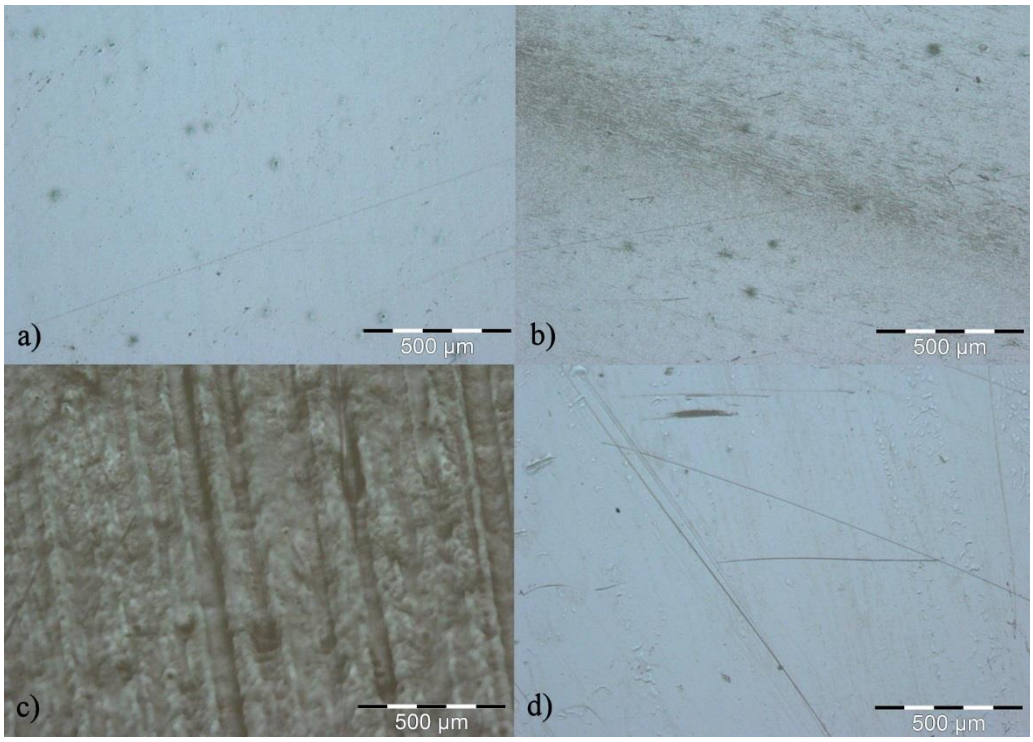

Figure 22. *a) injection-molded surface b) faults in injection-molded surface c) extruded, rough surface d) extruded smooth surface.*

When Figures 22 a) and 22 b) are compared, it may be observed that the difference between smooth surface and faults is quite significant. These faults cover approximately 2-15% of substrate surfaces. On the other hand, surface of extruded substrate in Figure 22 c) is more evenly patterned. Other side of the extruded substrates (Figure 22 d)) is smooth and shiny, and it was decided that rougher side of the substrate would be used to print test samples, since the smoother side was observed to be quite similar to the injection-molded substrate surface.

First, these substrates were compared to surface treated substrates by the measured surface energy values. In Table 15, the measured surface energy values for different substrates obtained in the initial tests are listed. Surface energy values in Table 15 indicate that especially oxygen plasma and flame-pyrolytic silicating had a great impact on the measured surface energy, since surface energies were observed to exceed Dyne-pen range, indicating that surface energy was more than doubled. It was observed that surface profile obtained with plasma treatment was roughened by increasing exposure power, and therefore 75 W exposure power was selected for plasma treatment.

In addition, it was observed that even one-minute and two-minute etching with sulfuric acid did increase substrate surface energy. However, it seemed that surface energy was saturated after five-minute treatment, since no further increment was observed with longer etching times. Furthermore, surface profile appeared to be similar. Therefore, it was decided that five-minute acid etching would be used in test sample fabrication.

On the contrary, etching with KOH did not modify substrate surface energy even with the longer etching times. A higher KOH concentration (30%) was applied to the substrates to see if stronger base solution would improve results, but it was observed, that the higher concentration did not have any effect on the surface energy either. In addition, no alterations could be observed in surface profile. Therefore, it was decided that for further analysis, substrate would be treated with 5-10% KOH concentration.

In addition, it was observed that ethyltriglycol coating did not change surface energy of substrate pretreated with sulfuric acid. When the ethyltriglycol coating is sprayed on the substrate with acid remnants, it is likely that these chemicals react and form new functional groups on the surface. However, it seems that these new bonds are not able to change the surface energy of the surface.

Furthermore, to be able to optimize sample fabrication process before printing, surface energies of acid etched samples and plasma treated samples were measured over time to see if surface energy would decrease. It was observed that surface energies did not change over time, which indicates that these treatments caused a permanent modification of the surface. However, since the surface energies were measured only within the Dyne pen range, it is not certain whether there has been any reduction in the absolute surface energy values obtained with plasma treatment.

Table 15. *Measured surface energy values.*

Surface treatment				
Surface energy (mN/m)				
Reference				
30-32				
Oxygen plasma				
25W/1min.		**50W/1min.**		**75 W/1min.**
≥ 60		≥ 60		≥ 60
Sulfuric acid (98 %) etching				
1 min.	**2 min.**	**5 min.**	**10 min.**	**15 min.**
38	46	56-58	58-60	58-60
KOH (5-10 %) etching				
1 min.	**2 min.**	**5 min.**	**10 min.**	**15 min.**
32-34	32-34	32-34	32-34	32-34
KOH (30 %) etching				
1 min.	**2 min.**	**5 min.**	**10 min.**	**15 min.**
	-	32-34	32-34	-
Flame pyrolytic silicating (NanoFlame)				
≥ 60				
Ethyltriglycol coating *(3 coating layers, curing in 100 ºC/10-20 min.)*				
33-39				
Ethyltriglycol coating & sulfuric acid etching *(5 min. etching,1 coating layer, curing in 100 ºC/10-20 min.)*				
58-60				
Extrusion				
30-32				

After treatment parameter selection, test substrates were fabricated accordingly. The obtained surface profiles for these test substrates are presented in Figure 23. In this Figure, measured R_q-values are presented as a function of measured R_t-values.

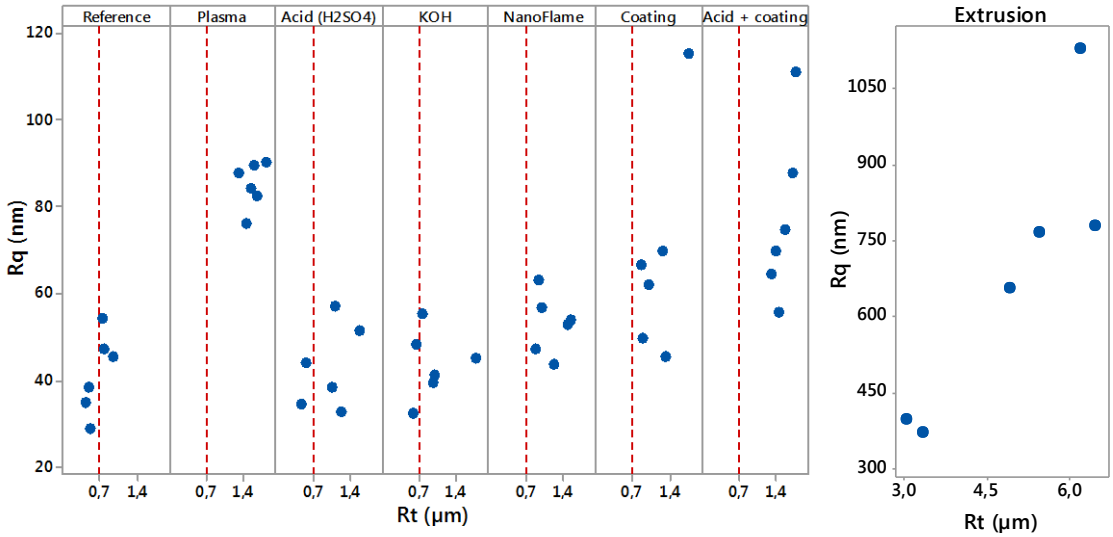

Figure 23. *Measured R_q as a function of R_t. R_t value 0.7µm used as a reference.*

By Figure 23 can be observed that the R_q-value of the injection-molded substrate is below 60 nm and range R_t is below 1 µm. Roughness parameters of extruded substrate are presented on a separate scale, since measured values were significantly larger than other values. Since the extruded substrate is same material as the reference substrate, the extremely rough surface profile is caused by the molding process.

All treatments seem to alter at least one of roughness parameters. Etching with either KOH or sulfuric acid did not seem to cause any significant alterations in RMS-roughness, but minor alteration in height range of surface profile was observed. Obtained values with both Nanoflame and ethyltriglycol were higher, almost 1.5 times higher than the original values. However, there is a significant variation in the measured values of ethyltriglycol coated surface, most likely due to the uneven coating.

The most significant alterations of surface profile were obtained with plasma treatment and the chemical treatment by etching and coating. These roughness values are 2-3 times higher than the original values. Plasma treatment seems to produce less variation, whereas with other treatments, a lot of variation can be observed. This is most likely due to the nature of treatment; plasma parameters may be controlled during treatment and thus the whole substrate is treated equally, whereas other treatments are manual and conditions cannot be controlled as strictly.

In Table 16 are presented the measured surface energy values and calculated roughness parameter means for each test substrate. The results in Table 16 indicate that no direct relation between measured surface energy and surface roughness parameters could be found. Plasma treatment both cleans and etches the substrate surface, which explains the relation between measured values. Since neither of etching treatments did cause signifi-

cant alteration of surface roughness parameters, it is likely that the increased surface energy of the acid etched substrates is due to the acid remnants on the surface, and the substrates have not been etched physically.

Table 16. *Surface energies and surface roughness parameters.*

Treatment	Surface energy (mN/m)	R_q mean (nm)	R_t mean (µm)
Reference	30-32	41,5	0,65
Plasma	≥ 60	85,0	1,58
Sulfuric acid	58-60	43,0	1,02
KOH	32-34	43,6	0,95
Nanoflame	≥ 60	52,9	1,17
Coating	33-39	68,1	1,18
Acid + coating	58-60	77,2	1,53
Extrusion	30-32	684,0	4,92

Similar results can be observed with NanoFlame treatment, where surface energy has been increased due to the silicon oxide on the surface, but surface profile has not been altered significantly. As discussed above, coating with ethyltriglycol did not cause significant alteration of surface energy, but surface was even 1.5 times rougher than in the reference case. Furthermore, with both plasma treatment and the combined chemical treatment, two times higher surface energies and 2-3 times higher surface roughness values were obtained.

6.2 Print quality

In this section, the results obtained by the optical inspection of printed lines are presented. The results of line thickness measurements with the optical profilometer are demonstrated in Figure 24. In this Figure, the main effects of used inks are plotted.

Comparison of measured R_t values presented in Figure 24 reveals that measured thicknesses differ greatly depending on the ink used. Most variation is observed with Novacentrix HPS-021LV ink, whereas HPS-FG32 from same manufacturer led to least variation in thickness. Asahi LS411AW seemed to result in thickest lines. Some variation is observed with SuNChemical CRSN2442 and DuPont 5064H, but it is not as significant as with HPS-021LV. These results are most likely related to the ink viscosity and metal contents. LS411AW viscosity is significantly higher than that of other inks, and it has highest metal contents. Thus, this ink will not spread as easily, and more metal particles remain after curing, resulting to higher layer. Viscosities of HPS-021LV and CRSN2442 are rather low compared to other inks, but they have high metal contents of 70% and 75%.

Low viscosity inks spread easier than high viscosity inks, but more ink is deposited through the screen. Therefore, obtained thickness values are only a bit lower than with LS411AW.

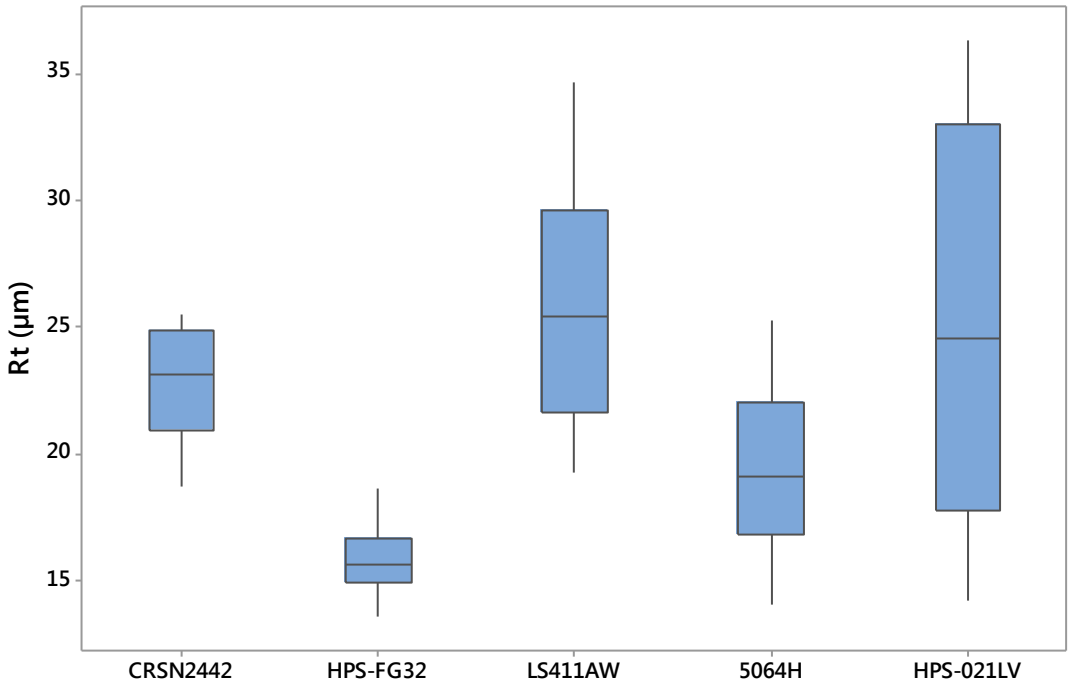

Figure 24. *Measured line thickness values for the printed conductors.*

Other parameters having an impact on these results are ink amount on the screen and ink behavior during printing. Thinnest lines have been printed with HPS-FG32, and are most likely caused by smaller amount of ink on the screen. With CRSN2442 and HPS-021LV, tendency to dry on the screen was observed. With CRSN2442, drying was not that significant, but with HPS-021LV, clogged screen had to be cleaned several times during the printing process. Furthermore, this tendency to dry quickly may lead to ink drying on the substrate between the squeegee movements, which could explain the significant variation in HPS-021LV line thickness values. Undesirable drying tendency of aqueous ink may be reduced by adding solvents to the mixture. In for example [76], organic solvent was added successfully to aqueous screen printing inks to prevent ink drying and screen clogging.

It is also possible that curing parameters have affected results: the optimum curing conditions have not been determined for these samples. Therefore, some samples may have been sintered more effectively than others, and different solvent concentrations remain in the structures after curing.

In addition to obtained line thickness values, RMS roughness R_q was measured to compare the uniformity of the printed lines. Great variation was observed and it seemed that higher line thicknesses led to more porous line surfaces. However, it seemed that printing parameters and ink behavior during printing affected these results. For example, thick lines obtained with LS411AW were smoother than thick lines obtained with ink HPS-021LV. Some examples of this surface roughness variation in a conductor are presented in Figure 25 for LS411AW and in Figure 26 for HPS-021LV.

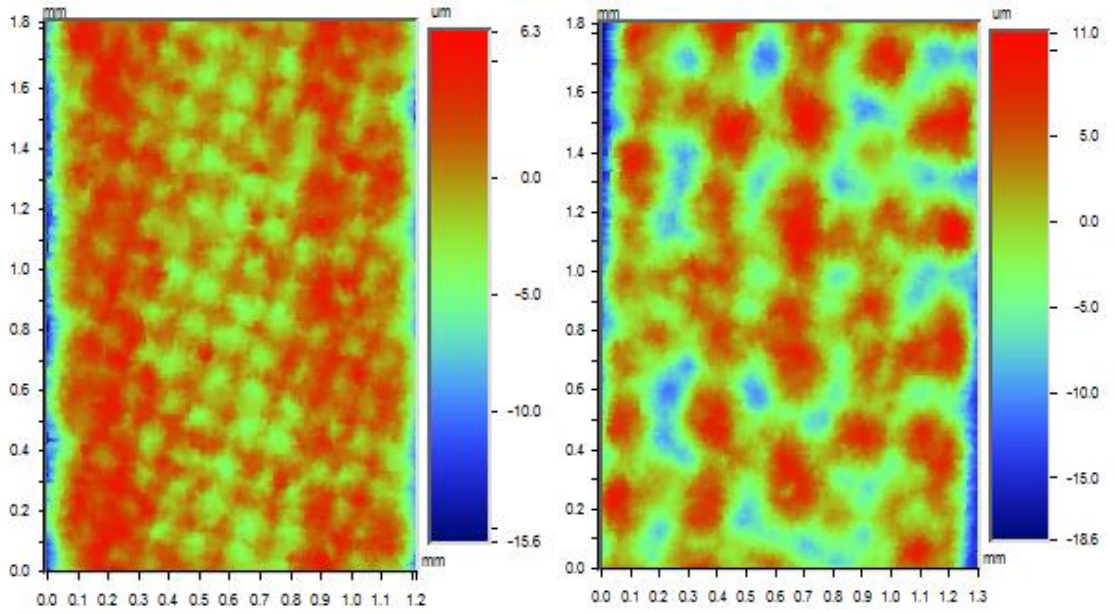

Figure 25. *Profilometer pictures of line profiles with LS411AW. a) Line with average thickness b) thick line.*

Measured R_q and R_t values for the conductors are presented numerically in Figure 27, so that R_q is presented as a function of R_t. It can be seen, that lines with maximum thickness below 25 µm are likely to be more uniform than lines with greater maximum value of line thickness. This result indicates that variation in line thickness is dependent on process parameters, which need further optimization.

As already suggested in equation (4), line thickness has a great impact on the final resistivity of the printed lines. In addition, other line thickness-related parameters should be considered carefully, especially in HF-applications. In for example [77], the effects of different fabrication methods and materials on the quality of passive UHF (Ultra High Frequency) RFID tags was determined. It was concluded, that uniform line structure is essential for the tags to operate.

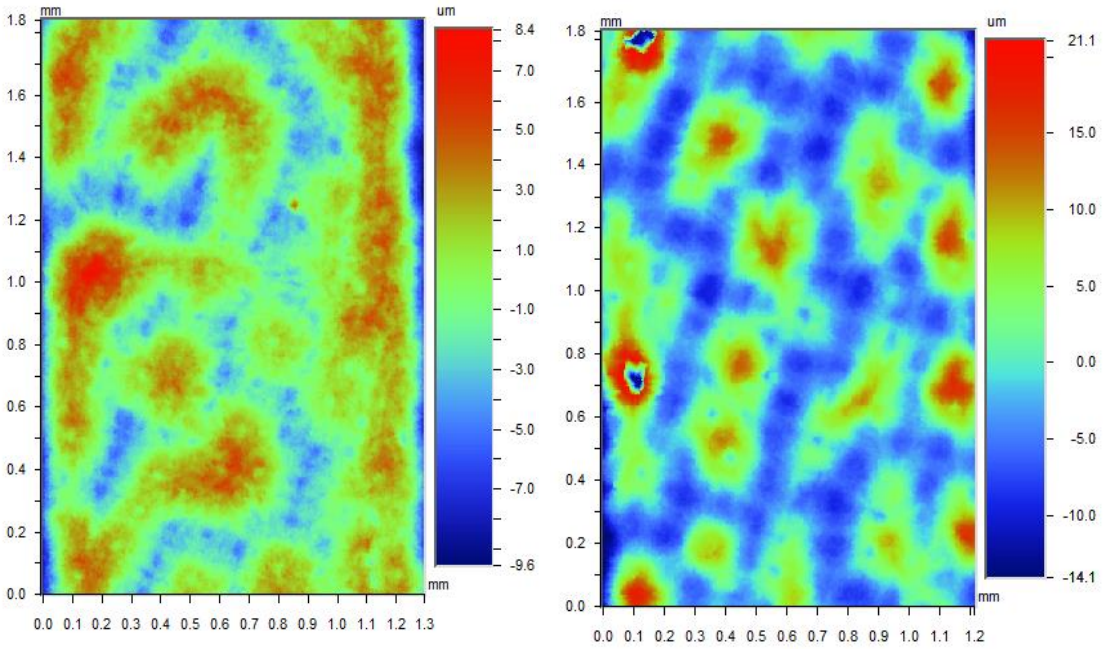

Figure 26. *Profilometer pictures of line profiles with HPS-021LV. a) Line with average thickness b) thick line.*

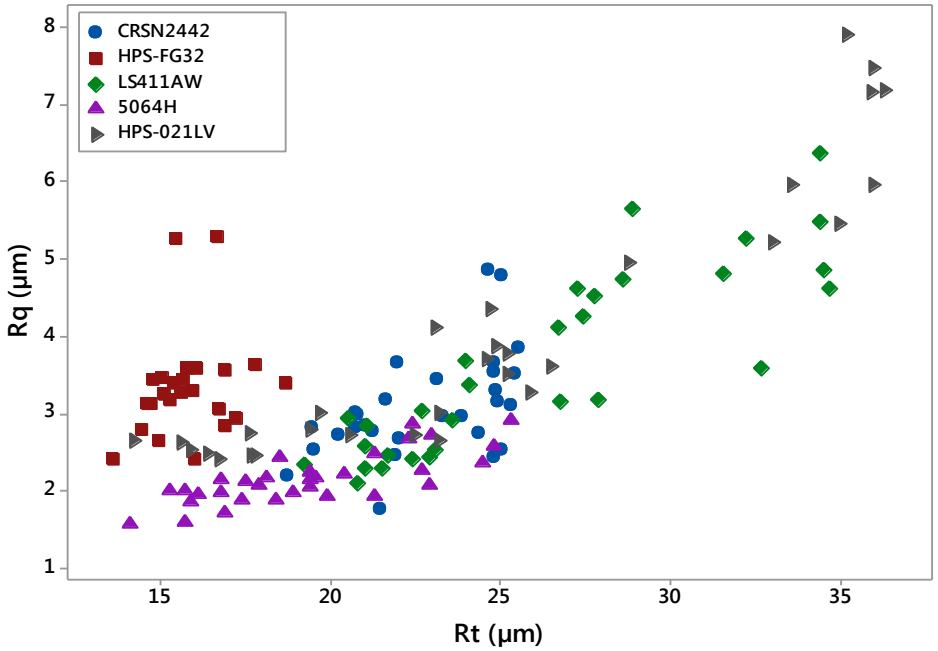

Figure 27. *Rq-values of line thickness as a function of line thickness R_t with inks all inks.*

Another important parameter related to line thickness, especially at high frequencies, is skin effect. Current density is packed near the conductor surface, and below the surface

amplitude is attenuated. By the penetration depth, amplitude is close to zero [77]. Therefore, it is essential to ensure that lines are thick enough, to minimize losses in the conductors due to skin effect.

However, penetration depth inversely proportional to the used frequency: as the operating frequency increases, penetration depth is decreased and maximum line thickness value becomes less significant [78]. However, the uniformity of the printed lines becomes more important at high frequencies, since the signal is likely to be transmitted only in the surface of the conductor, and thus roughness of the conductor surface lengthens signal line, causing more losses. For example, most of the printed lines in this study would be poor quality conductors, if penetration depth would be only 5 µm.

Therefore, optimization of printed line surface roughness is necessary to produce good quality conductors. To avoid additional process steps, smoother lines could be obtained by optimized screen parameters. However, it is not always possible to produce smooth lines by only adjustment of printing parameters and methods for line smoothening afterwards exist. In [57] and [79], printed lines were smoothened by calendaring. Printed structures were heated and pressed to achieve more uniform surfaces. [57] observed that the smoothened line surface enabled significantly better conductivity for LS411AW ink.

In this study, conductor line widths were measured from microscope images to see the effects of substrate wettability. Measurement data for inks CRSN2442, LS411AW, 5064H and HPS-021LV by reference substrate and two treated substrates is presented in Figure 28. Most of the measured line width values were observed to be in the range from 1200 µm to 1400 µm. Due to the rather small difference in line widths, compared to the wet line width of 1.3mm, line lengths were not measured for further analysis.

The measurement of line widths with selected substrate-ink combinations revealed that both the surface roughness and the surface energy of the substrate have an impact on line width. With almost all inks, plasma treatment resulted in widest lines. Furthermore, results of extruded substrate and the substrate treated with both acid and ethyltriglycol appear to be the same. This result supports the conclusion that both surface parameters have an effect on the wetting of the ink-substrate interface, since extruded substrate has the same surface energy as the reference substrate, but is clearly the roughest of the substrates. On the other hand, measured surface roughness of chemically etched and coated substrates was lower, but their surface energy is twice that of the extruded substrate.

The most significant abnormities from this trend are observed with CRSN2442 ink. The effects seem to be the exact opposite of those with other inks. This is in contradiction with the measured surface energies and result is probably caused by printing parameters: CRSN2442 seemed to dry during the printing process. It is possible that some screen openings have been clogged and thus line width is decreased.

SEM was used to inspect the differences between flake topologies of the cured patterns. Obtained SEM images are included in Figure 29. It can be observed that HPS-FG32 and HPS-021LV inks seem to have rather similar flake topology. The shape and size of the silver flakes can be determined from the Figure. Inks seem to include both smaller and bigger flakes. However, ink HPS-FG32 composition seems to be less compact than that of ink HPS-021LV.

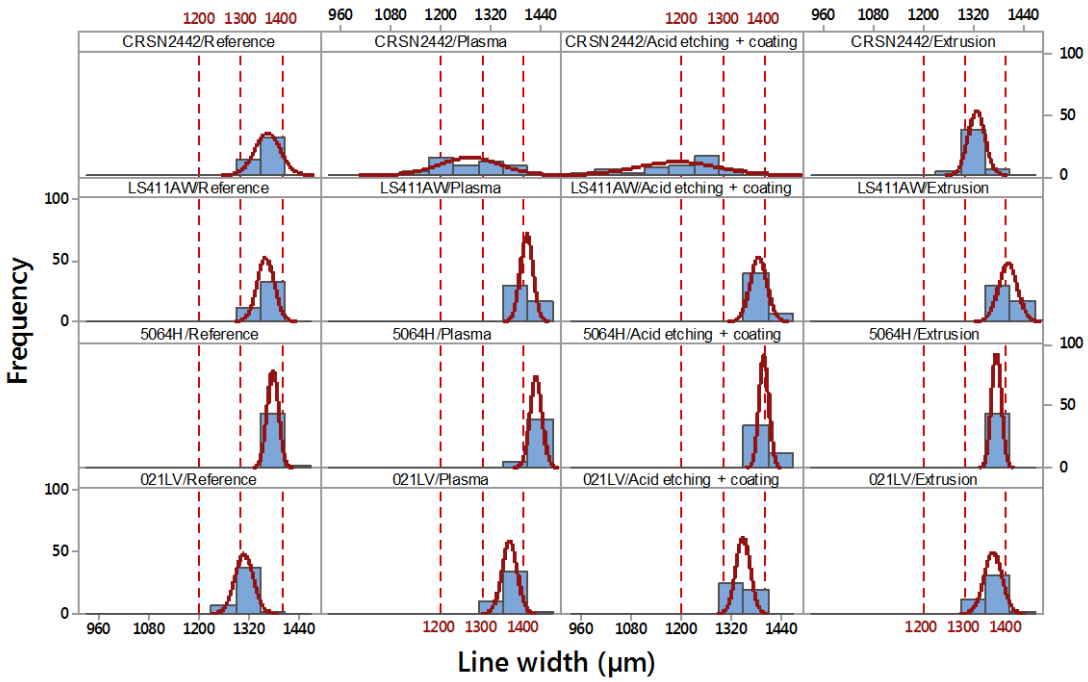

Figure 28. *Measured line widths forCRSN2442, LS411AW, 5064H and HPS-021LV inks on reference, plasma treated, etched & coated and extruded substrates.*

On the other hand, flakes cannot be told apart as easily with other inks. CRSN2442 composition differs from other pastes, as the line surface consists of small flakes. On the other hand, LS411AW line surface seems to consist of both smaller and bigger particles, whereas surface of 5064H consists mostly of bigger particles.

In [56], the relation between flake size and print resolution was studied. It was observed that line width had an impact on thickness, surface roughness and aspect ratio of the printed lines with LS411AW and 5064H. As line width decreased, aspect ratio and uniformity of the printed lines seemed to decrease. This deformation was more significant with 5064H than with LS411AW. This result could be caused by the ink composition: bigger flakes require more space to form a uniform structure, whereas the combination of differently sized flakes could help to achieve compact patterns with better resolution.

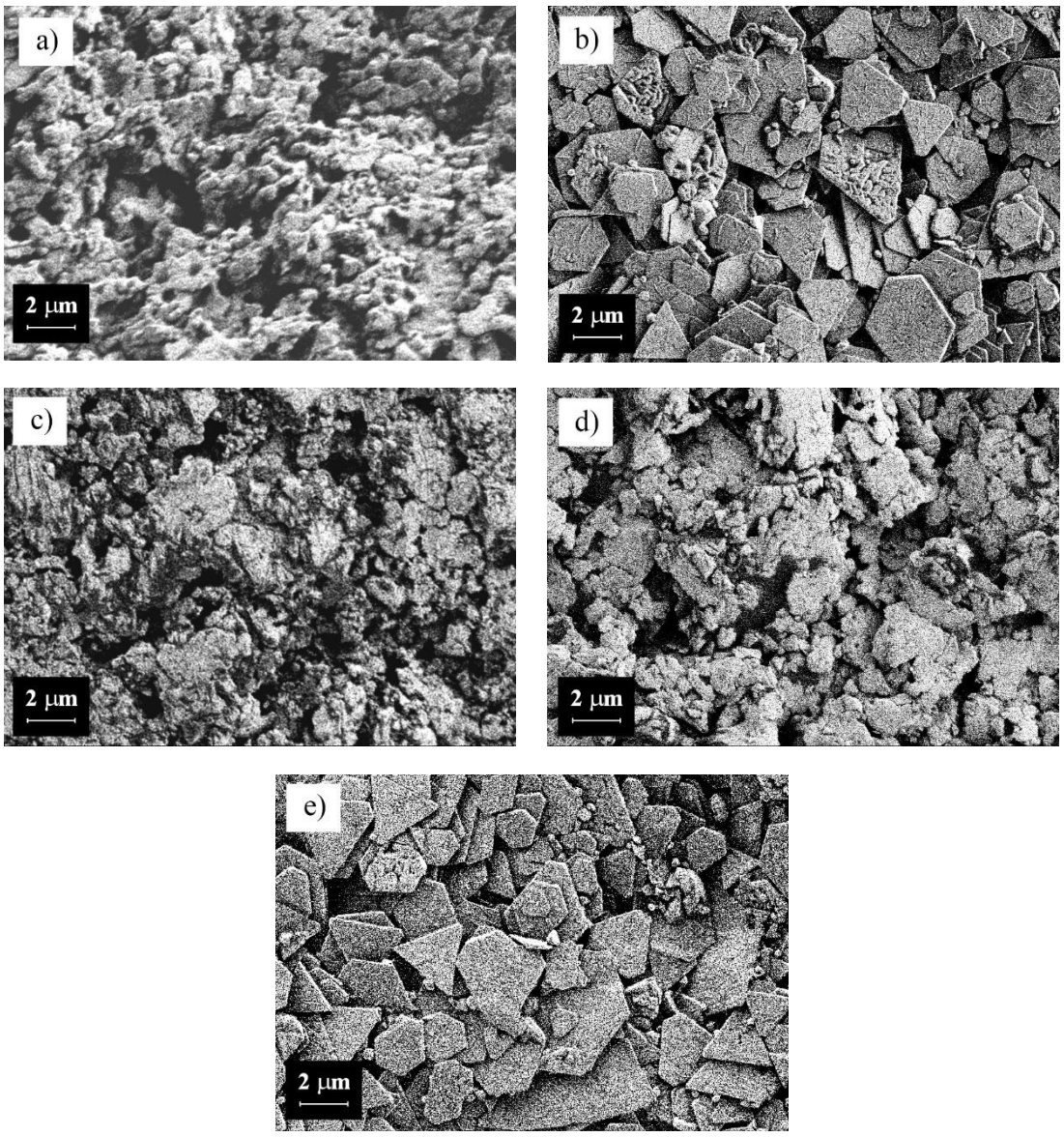

Figure 29. *SEM images of flake topologies with a) CRSN2442 b) HPS-FG32 c) LS411AW d) 5064H and e) HPS-021LV. 15k magnification, EHT 1.00 kV.*

6.3 Conductivity

Sheet resistances of the printed conductors were calculated by equation (6), based on the voltages measured by 10 mA supply current. For the initial calculation of the conductivity values, width and length of the printed lines were assumed to be close to the designed pattern dimensions. The numerical conductivity results are presented in Figure 30. Each column of Figure 30 contains results for one ink and each row contains results for one substrate.

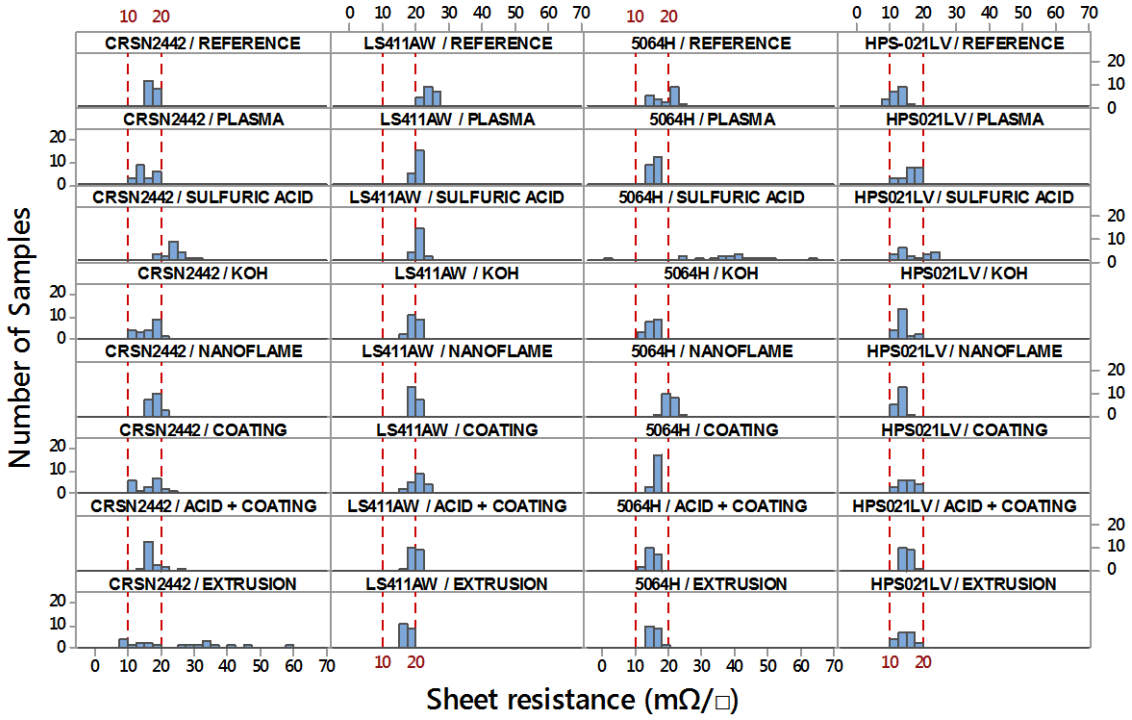

Figure 30. *Measured sheet resistances, 10 mΩ/□ and 20 mΩ/□ as references.*

Figure 30 reveals that most of the measured sheet resistances are between 10 mΩ/□ and 20 mΩ/□. As expected, lowest sheet resistances were measured with Novacentrix HPS-021LV, DuPont 5064H and SunChemical CRSN2442, and their results are rather similar. On the other hand, sheet resistances measured with Asahi LS411AW are a bit higher. Therefore, it may be concluded that obtained sheet resistances were excellent, compared to the manufacturer information presented earlier. Thus, by this main effect, both printing process and curing conditions seem to have been sufficient for these ink-substrate combinations.

However, results obtained with HPS-FG32 were significantly worse with recommended sintering conditions, and it was discarded from this comparative analysis. New samples

were fabricated on three substrates to see the effects of doubled sintering time. The results of this comparison are included in Figure 31. These results indicate that longer sintering time resulted to significantly better sheet resistance values, but as no sheet resistance values below 40 mΩ/□ could be measured, it was concluded that this ink was not able to compete with other inks and should be discarded from further analysis.

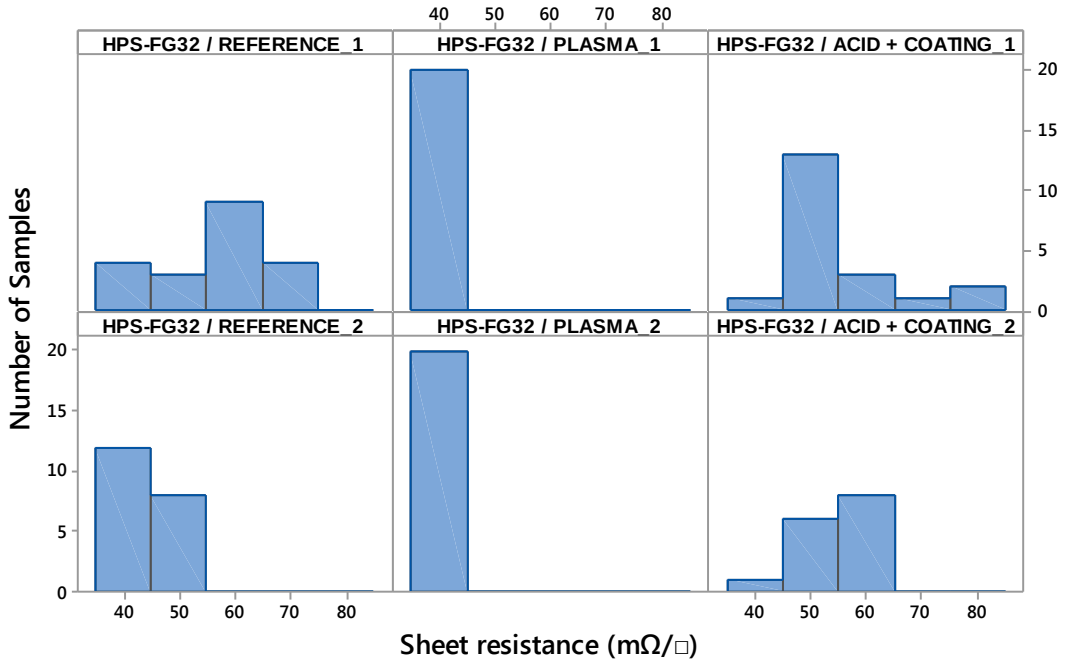

Figure 31. *Measured sheet resistances with HPS-FG32.*

To see the effects of line width on conductivity results, sheet resistances were calculated again with the measured line widths. In Table 17 are presented sheet resistance values of Asahi LS411AW ink with both designed line widths and measured line widths.

Table 17. *Measures sheet resistances of LS411AW ink with ideal line widths and measured line widths.*

Ink-substrate combination	Sheet resistance (mΩ/□) designed line width	Sheet resistance (mΩ/□) measured line width
LS411AW / Reference	24,05	25,16
LS411AW / Plasma	20,48	22,20
LS411AW / Acid +coating	20,03	21,34
LS411AW / Extrusion	17,18	18,51

Table 17 results indicate that 100µm difference in line widths may result to even 2 mΩ (10 %) difference in measured sheet resistances. This difference is quite remarkable, and indicates that process optimization is needed. However, as process parameters for used inks could not be optimized in this study, designed line width values were used to compare measured sheet resistances.

After the initial sheet resistance measurements, a normality test was run for the most successful inks to see whether measurement data was normally distributed or not. Normally distributed data indicates that used ink is reliable, printing process was successful and curing conditions have been sufficient. On the other hand, if anomalies can be observed, it is likely that at least one of these parameters needs further optimization.

The most important normality test parameters include AD (Anderson-Darling) value and P (Probability) -value, which are dependent on the used CL (Confidence Level). If a CL of 95 % is used, a P-value below 0.05 indicates that the likelihood of normal distribution is below 5 %, and therefore data cannot be assumed to be normally distributed. Furthermore, if obtained P-value is at least 0.05, there is at least 5 % likelihood of normal distribution. In addition, obtained AD value should be inspected. The critical value for this parameter is 0.75. If calculated AD value is below 0.75, data may be normally distributed and if not, analysis tools of normally distributed data should be discarded. If both AD value and P-value indicate that data is normally distributed, obtained standard deviation σ is valid for this data. Mean value μ can be used for comparison even though data is not normally distributed. [80-82]

Table 18 contains the normality test results with CL of 95 % for measured sheet resistances. These results indicate that the likelihood of LS411AW sheet resistances to be normally distributed is at least 17 % in all but one of the ink-substrate combinations. On the other hand, it seems that most anomalies occur in 5064H results. To be able to analyze the cause of these anomalies in the data distribution, a normality test was run to those samples, for which P-value was significantly below 0.05. These test results have been included in Appendix A.

Obtained values (Appendix A) indicate that there is a lot of variation between fabricated samples. On the other hand, results reveal the significant drawback of the normality test: even though there is almost no variation in the results and calculated mean is optimal (5064H Extrusion, sample 2), test parameters indicate that distribution would be non-normal, and thus a flaw would have occurred either due to ink or process parameters. Therefore, normality test may be concluded to offer good approximation of process parameters and materials, but more test samples should be fabricated to achieve reliable results.

Table 18. *Normality test of sheet resistances, mΩ/□.*

	CRSN2442					**LS411AW**				
Substrate	μ	σ	N	AD	P	μ	σ	N	AD	P
Reference	17,28	1,13	20	0,321	0,507	24,05	1,73	20	0,379	0,372
Plasma	15,47	2,71	20	0,509	0,175	20,48	0,89	20	0,346	0,223
Sulfuric acid	23,78	3,17	20	0,407	0,317	21,34	1,33	20	0,395	0,340
KOH	16,14	3,25	20	0,507	0,177	19,43	1,74	20	0,636	0,083
NanoFlame	18,35	1,73	20	0,199	0,867	19,96	1,08	20	0,512	0,171
Coating	16,40	4,49	20	0,467	0,225	20,49	2,02	20	0,425	0,286
Acid + coating	17,50	2,68	20	1,346	0,005	20,03	1,58	20	0,327	0,496
Extrusion	25,13	14,3	20	0,690	0,060	17,18	1,24	20	0,230	0,779
	5064H					**HPS-021LV**				
Substrate	μ	σ	N	AD	P	μ	σ	N	AD	P
Reference	18,86	3,21	20	1,188	0,005	12,24	1,82	20	0,469	0,222
Plasma	15,17	1,17	20	0,739	0,045	16,07	2,48	20	0,575	0,119
Sulfuric acid	37,05	13,8	17	0,533	0,148	17,25	4,66	19	0,944	0,013
KOH	13,90	1,70	18	1,267	0,005	14,00	1,94	20	0,680	0,064
NanoFlame	19,96	1,51	20	0,261	0,670	13,00	1,41	20	0,548	0,138
Coating	15,73	1,02	20	0,328	0,492	15,27	2,09	19	0,531	0,152
Acid + coating	14,41	1,45	19	0,156	0,945	15,21	1,41	20	0,694	0,059
Extrusion	14,63	1,81	20	1,385	0,005	14,37	1,95	20	0,303	0,541

After the normality test of anomaly distributed data, two samples of each ink-substrate combination were inspected to find the cause for the differences between samples. Measured sheet resistance values for each conductor of the samples are presented in Appendix B. As each sample consisted of ten conductors printed on same substrate, calculated sheet resistances were plotted by the conductor order to enable more accurate analysis. Conclusions are summarized in Table 19.

Table 19 conclusions are based on the comparison of line thickness parameters, visual inspection of the samples and comparison of curing conditions. Consequently, these results emphasize the complexity of the printing process. With CRSN2442 printed on etched and coated substrate, quality issues were observed in the conductive lines of the second sample, caused by the clogging of the screen. This is most likely related to ink behavior, as CRSN2442 ink was observed to dry rather fast in the process.

Table 19. *Causes for sample set differences, non-normal distributions.*

Ink-substrate combination	Cause for sample set differences
CRSN2442 / Acid + coating	Ink behavior
DuPont 5064H / Reference	Printing parameters
DuPont 5064H / KOH	Printing parameters
DuPont 5064H / Extrusion	Curing conditions
HPS-021LV / Sulfuric acid	Ink behavior

With DuPont ink printed on the reference substrate, it was observed that the samples were similar, but the measured sheet resistances were higher for conductors 6-10 than those of conductors 1-5. The inspection of line thicknesses revealed that conductors 1-5 were a few microns thicker than other conductors, indicating that squeegee alignment has been askew. However, this phenomenon could not be observed with same ink and KOH-treated substrate. Instead, sheet resistances were almost identical in one sample, but values differed between the two samples. This result indicates that either ink amount on the screen or curing conditions have affected results. However, as no significant difference in line thickness was observed and same curing conditions were used for both samples, the relationship between these results cannot be determined. Sample set placement in curing oven may have affected results.

Finally, HPS-021LV printed on acid etched substrate was inspected. It was observed that print quality of first sample was worse than that of the second sample. Line structures of the first sample are significantly more porous, and thus sheet resistance is higher. This difference is most likely due to the fast drying of the aqueous ink, as observed earlier.

If obtained sheet resistances are compared for example to results of [71], it seems that obtained sheet resistances from 10 mΩ/□ to 20 mΩ/□ would be well suited for printed HF applications. However, as observed in [71], HF performance of printed conductors is not directly proportional to the measured sheet resistance values, and therefore, characterization of HF properties is needed to provide good quality conductors for HF applications. This characterization includes for example transmission loss measurements and printing process optimization.

6.4 Adhesion

The results of the ASTM D3359 crosscut test for each ink-substrate combination are presented below in Figure 32.

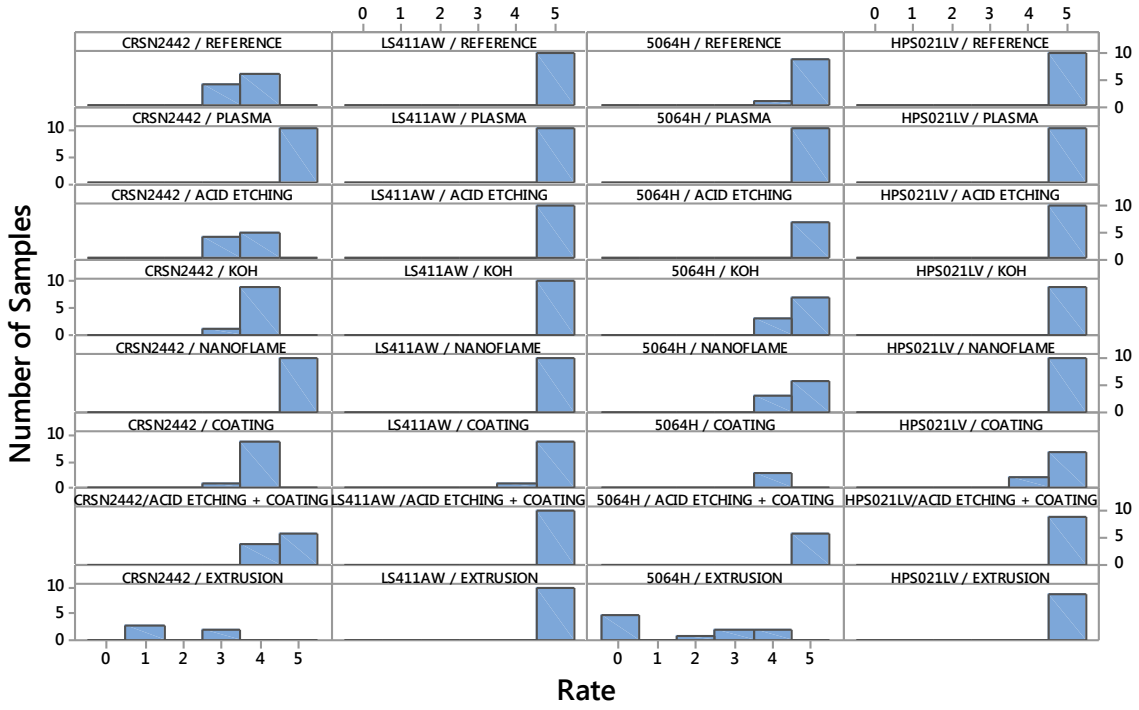

Figure 32. *Adhesion classification results.*

In Figure 32, each row contains information of one ink. Columns from left to right present substrates. As it was observed that all samples from the first set printed with HPS-FG32 ink experienced an ink cohesion failure in the crosscut test. In addition, the remaining silver structure on the substrate was conductive, whereas the top layer removed by tape was not. This result indicates that samples were not cured thoroughly. In [29], similar ink behavior in adhesion tests was observed due to insufficient curing times. Therefore, those results are not included in Figure 32. Since measured sheet resistance of HPS-FG32 ink remained high even with doubled sintering time, the mechanical performance of this ink was not evaluated.

The crosscut test results indicate that plasma, NanoFlame treatment and the combined treatment of acid etching and spray coating improved adhesion significantly, based on

CRSN2442 ink results. With these treatments, level of adhesion was improved significantly from the results obtained with the bare injection-molded substrate. On the other hand, either acid etching only or spray coating without prior etching step did not seem to improve results. Similar result was observed with KOH treatment.

These results indicate that both surface roughness and surface energy of the substrate have an important role in the formation of adhesive bonds between ink and substrate: mechanical interlocking is more likely with rough, hydrophilic surface. In addition, this result indicates that ethyltriglycol is a useful adhesion promoter, but a prior treatment is needed to make substrate more hydrophilic, thus enabling even coating.

In Figure 33, cross-section images obtained with SEM demonstrate the interface between ink and substrate in two cases. In Figure 33a), the interface of CRSN2442 and reference substrate is presented, and in Figure 33b), the interface between CRSN2442 ink and the chemically etched and coated substrate is presented. The comparison of these cross-sections indicates that rougher surface profile may have enhanced ink interlocking on the substrate surface. However, more analysis of interface cross-sections is needed before any conclusions can be made.

On the other hand, it may be observed that flake composition is not entirely compact, especially on the top of ink layer. It is possible that longer sintering times are needed to remove all solvent from the structure. In [29], effects of sintering time and temperature on printed structure performance was studied. It was observed that both conductivity and adhesion of the cured structures are highly dependent on sintering conditions. Sufficient conductivity could be achieved faster than good adhesion. In this study, only datasheet curing conditions were used to be able to compare test samples. However, the effects of sintering conditions on both conductivity and adhesion of these ink-substrate combinations should be studied further.

Adhesion on the extruded surface was even worse than adhesion of the injection-molded substrate with two of the used inks (CRSN2442 and 5064H). However, adhesion of LS411AW and HPS021LV was extremely good on this substrate. This result could be caused by the phenomenon discussed in Subchapter 2.1.3: as the hydrophobic surface profile is made rougher, contact angle is even higher, and thus ink interlocking onto the substrate surface is prevented, because ink cannot form physical contact with the notches on surface. The difference between ink results could be due to the ink composition differences observed in Figure 29 SEM images: ink consisting of multiple flake sizes may be able to interlock on the rough surface better than those inks containing only flakes with approximately same size.

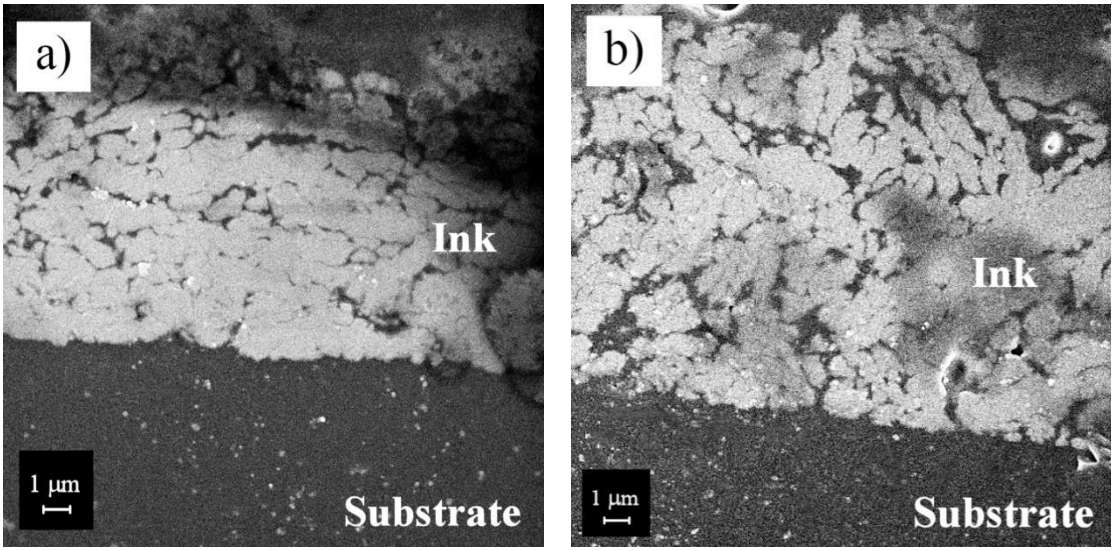

Figure 33. *Cross-section images of a) reference substrate and b) acid etched and spray coated substrate. 9k magnification, EHT 5.0 kV.*

Another important result obtained from this test was the significance of faults observed on the injection-molded surface. Altogether ten silver squares were fabricated for each ink-substrate combination. Closer inspection of Figure 32 reveals that more than one square was discarded from the analysis with most ink-substrate combinations. This was due to the observation that the faults on the injection-molded substrates led to adhesion failures. However, these results are not comparable to the adhesion failures obtained on the smooth substrates and were thus ignored. Furthermore, this result indicates that the molding process influences the adhesion of the ink-substrate interface, and should be considered carefully.

6.5 Reliability

The ink-substrate combinations selected for the accelerated environmental tests are listed in Table 20. First, DuPont 5064H and Novacentrix HPS-021LV were selected based on both the conductivity and adhesion results. Measured sheet resistances of Asahi LS411AW were a bit higher, but as the adhesion of this ink was superior to the others, it was selected to further analysis. Plasma treatment as well as the combined treatment of acid etching and spray coating were selected, based on the performance in the crosscut tests. In addition, NanoFlame treatment was considered as an alternative, but was discarded since combined chemical treatment provided better adhesion results for 5064H. Untreated injection-molded substrates were used as a reference in these tests.

After the accelerated environmental stress tests, adhesion was rated for tested samples. It was also observed that dark marks had been appeared to the silver squares, most likely

due corrosion. In Figures 34-36 are presented the visually observed corrosion marks on silver squares after both tests.

As shown in Figures 34-36, minor corrosion marks could be observed in LS411AW and 5064H samples after 85/85 test. Furthermore, amount of dark marks was increased significantly with both inks after salt mist test. On the other hand, no signs of aging could be observed visually on the surface of HPS-021LV ink layers after either tests.

Table 20. *Selected substrate-ink combinations for the environmental tests.*

Ink	Substrate	Sheet resistance (mΩ/□)	Adhesion classification (mean)
LS411AW	1	24,05	5
	2	20,48	5
	7	20,03	5
5064H	1	18,86	4,9
	2	15,17	5
	7	15,10	5
HPS-021LV	1	12,24	5
	2	16,07	5
	7	15,21	5

However, the results of the crosscut tests indicated that LS411AW and 5064H ink survived these tests better than HPS-021LV. Failure types encountered in these adhesion tests are presented in Figures 37 and 38. By the comparison of these test results, it can be concluded that most of the substrate-ink combinations survived the 85/85 test. As this test simulates the reliability in generic storage conditions, this is a promising result from the aspect of product lifetime. Some delicate cohesion issues were observed with a few samples of HPS-021LV. However, only light shadows of ink could be observed in tapes, and therefore these cohesion failures are not significant.

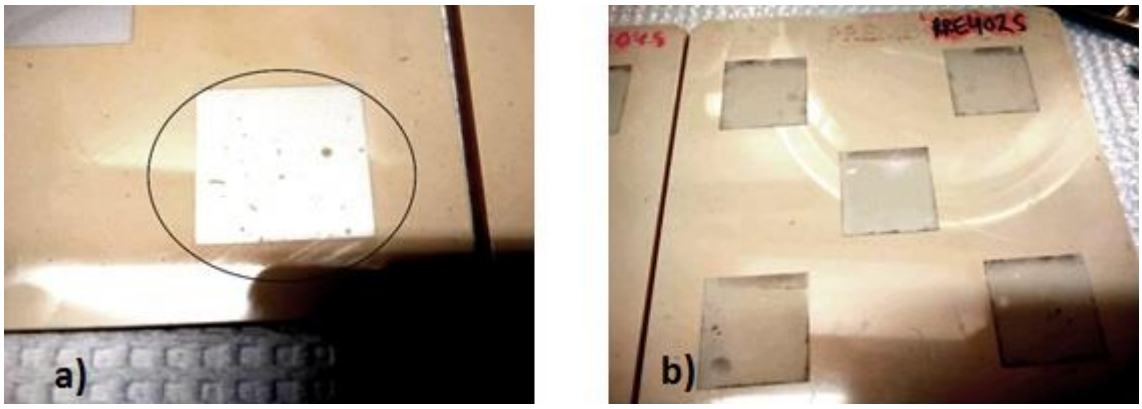

Figure 34. *5064H corrosion n after a) 85/85 test, b) salt mist test.*

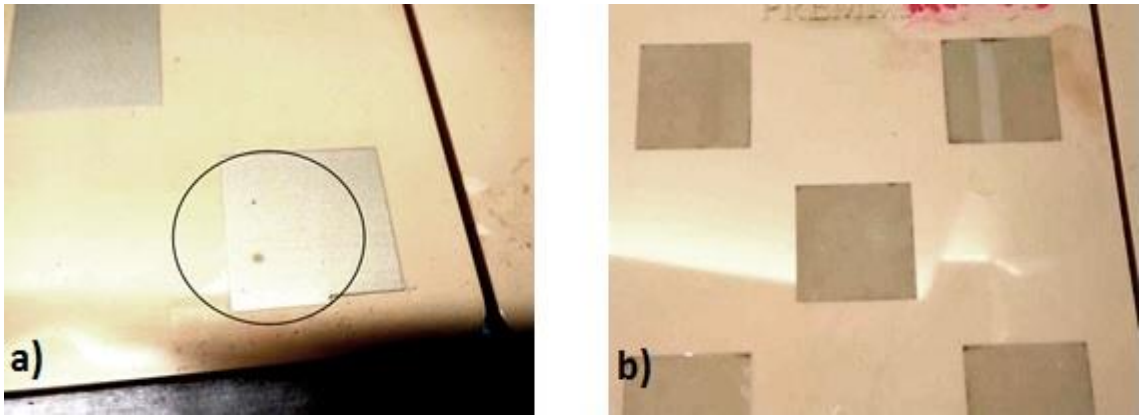

Figure 35. *LS411AW corrosion after a) 85/85 test, b) salt mist test.*

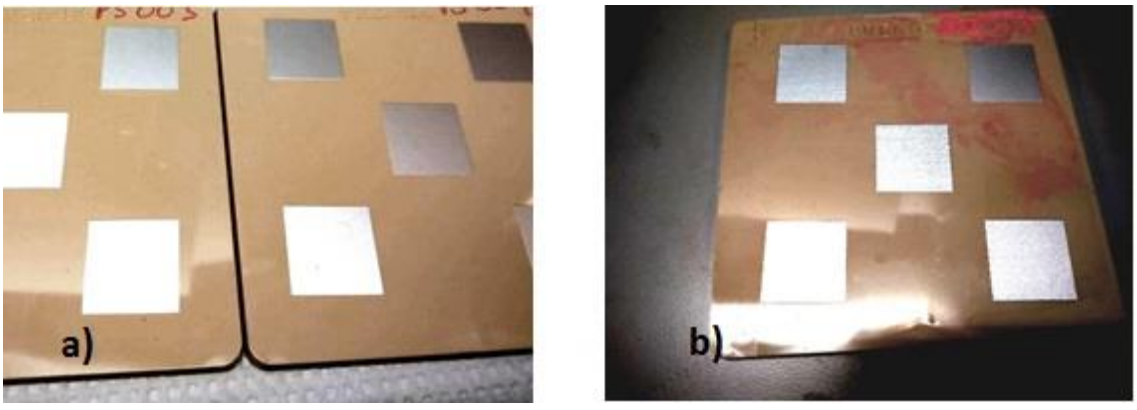

Figure 36. *HPS-021LV corrosion after a) 85/85 test, b) salt mist test.*

On the other hand, the salt mist test had a great impact on the ink-substrate interface behavior. HPS-021LV adhesion was worsened dramatically: all samples failed either by adhesion or ink cohesion. In many test samples, ink was flaking off even prior to tape placement, and thus adhesion had failed completely. In most cases, both ink cohesion and

adhesion failed, so that cohesion failures were experienced in the middle of the squares and the square edges were flaking off. The impact of curing conditions could be excluded, since the removed ink layer remained conductive.

On the other hand, only a few adhesion failures occurred with 5064H ink, whereas ink cohesion failed in most samples. It was observed that failures occurred in those sections of the squares, in which corrosion was also observed visually. However, other layers of the ink squares were not removed, indicating that adhesion of this ink remained excellent despite the salt exposure.

LS411AW seemed to be most resistant to corrosion in both of these tests. Almost 50% of the samples survived salt mist test with the reference substrates, whereas over 50% of the plasma treated substrates and almost 75% of acid etched and coated substrates survived salt mist conditions. Minor cohesion failures were observed in the corners of the squares due to corrosion. These removed layers were significantly thinner than the layers removed with other inks.

Adhesion was classified by ASTM-D3359 standard for those samples, which had remained intact or only the interface adhesion had failed. The results of this classification are presented in Figures 39 and40. By Figure 39 results can be concluded that 85/85 test did not cause adhesion degradation compared to the initial results of Figure 32, despite the few cohesion failures of HPS-021LV.

However, the results presented in Figure 40 indicate that none of the inks could survive the cyclic salt mist test. In this test, the degradation of adhesion level was most significant with aqueous HPS-021LV ink. Its adhesion on the reference substrate was decreased from 5B to 2B-0B. Ink cohesion failure occurred in 5% of the samples. The adhesion level of plasma treated samples could not be rated, since ink cohesion failed in all test samples. In addition, minor adhesion failures were observed in the corners of the test patterns. On the other hand, the adhesion rate of chemically treated samples remained in 4B, whereas ink cohesion failed in approximately 30 % of the samples. These results indicate that the interface adhesion fails before the ink cohesion, and surface treatments would improve results.

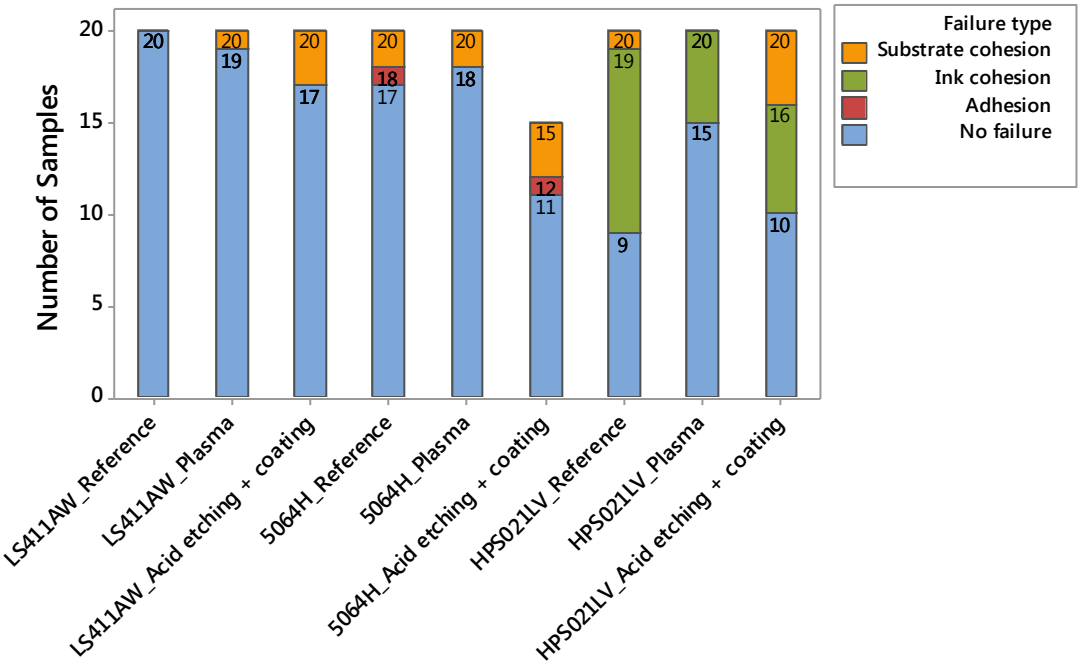

Figure 37. *Occurred failure types after 85/85 test.*

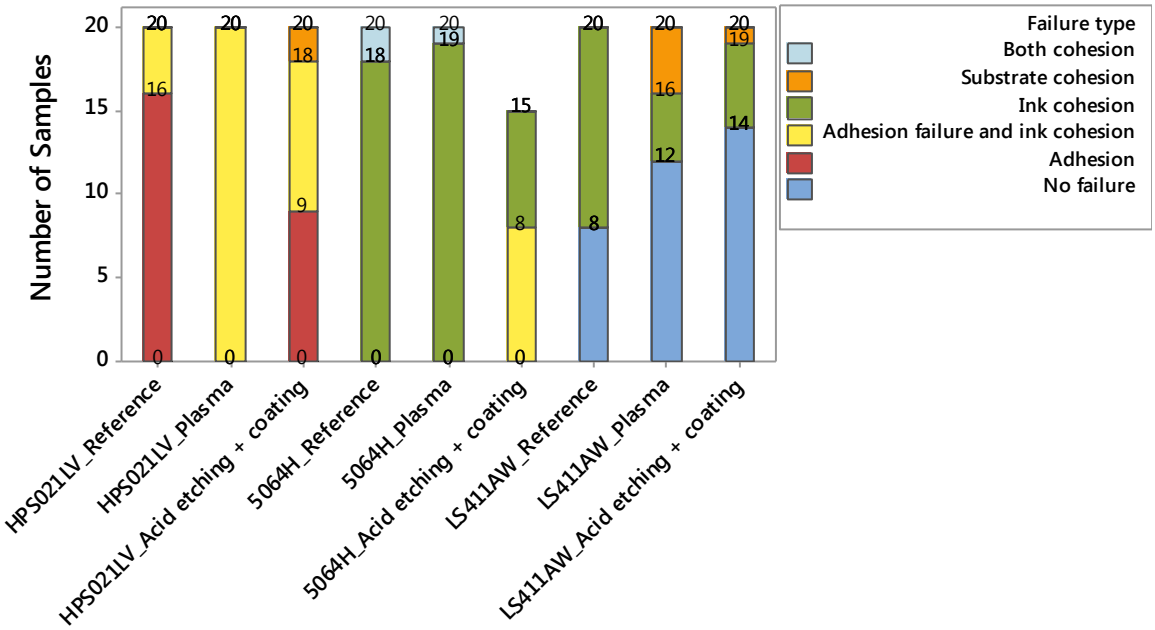

Figure 38. *Occurred failure types after salt mist test.*

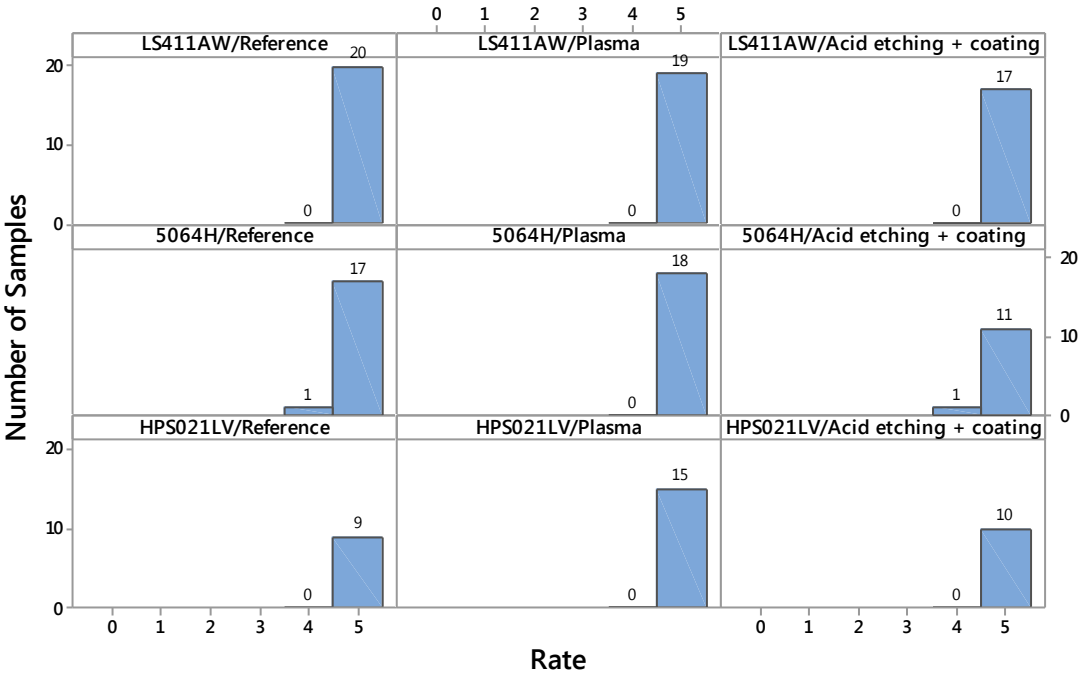

Figure 39. *Adhesion classification results after 85/85 test.*

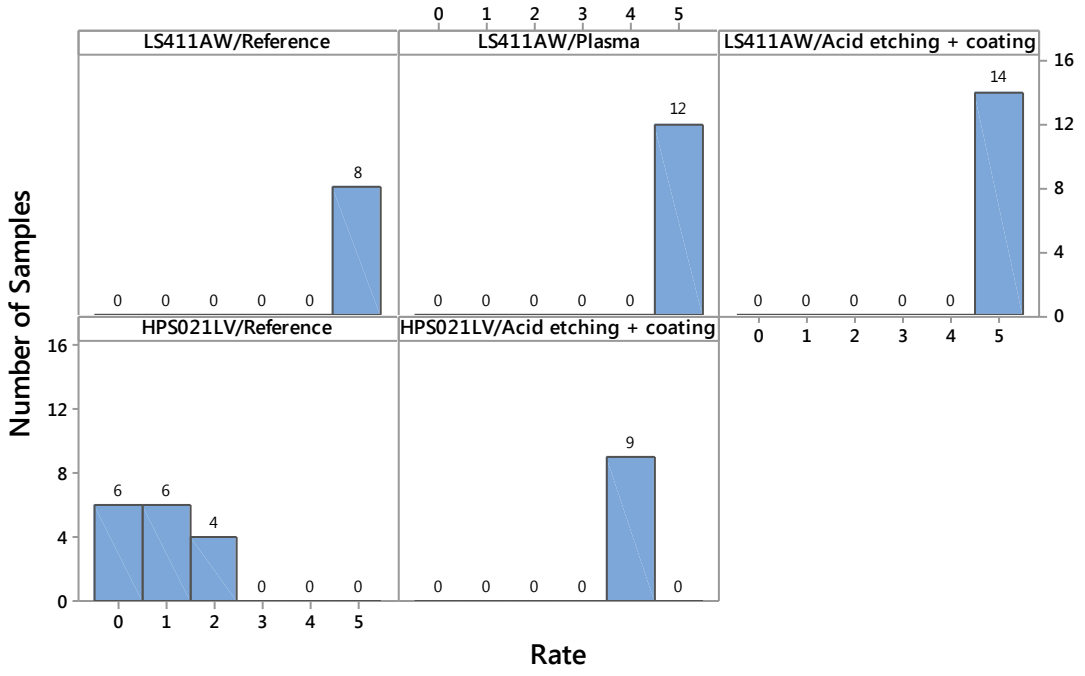

Figure 40. *Adhesion classification results after salt mist test.*

In addition, ink cohesion seems to have failed with other inks, rather than ink adhesion, but since the ink removal has occurred only in the corroded parts, it may be concluded that ink adhesion has remained very good with most of the samples. The difference of the corrosion mechanism between the interface and ink layers may be related to the difference between ink compositions inspected with SEM. As the cured lines printed with 5064H and LS411AW are more porously structured, the corrosive compounds may penetrate the ink more easily, compared to the compact structure obtained with HPS-021LV, and thus ink cohesion fails before the interface adhesion. In [84] was observed, that silver tends to react with sodium chloride in humid environment, where relative humidity is greater than 75 %, forming silver chloride.

This observation is supported by the SEM images taken from top of the 5064H silver layer, where visually observed aging was most significant. The obtained SEM images are presented in Figure 41. Figure 41 a) is taken from the middle of silver square and Figure 41 b) is taken from the dark edge of square. New, differently shaped particles have emerged on the ink surface where aging was observed (Figure 41 a)). Comparison of these results to the results obtained in [84] indicates that these particles are most likely silver chloride, which has been formed in the salty and humid conditions, and possible remnants of sodium chloride.

On the other hand, these particles could not be detected in the middle of the squares (Figure 41 a)). In addition, it was observed that the silver flake structure is more compact in the middle of the square. Thus, the attachment of the rather large sodium chloride crystals to the ink surface may have been prevented, and therefore silver chloride particles have not been formed.

Furthermore, the level of adhesion degradation in salt mist test was highly dependable on the both ink and substrate. It seems that plasma treated substrate was the most successful choice in the 85/85 test, whereas chemically treated substrate led to best results in the salt mist test. However, both treatments improved the durability of the samples significantly.

In [71] was observed that salt mist test caused significant degradation of adhesion, but that adhesion degradation was less significant, when suitable protective coating was applied. Thus, applying protective coating enabled better results than the bare interface. In conclusion, especially in outdoor applications, the importance of protective coating is emphasized when a long lifetime of a device is desired. With protective coating, corrosion of ink-substrate interface is reduced.

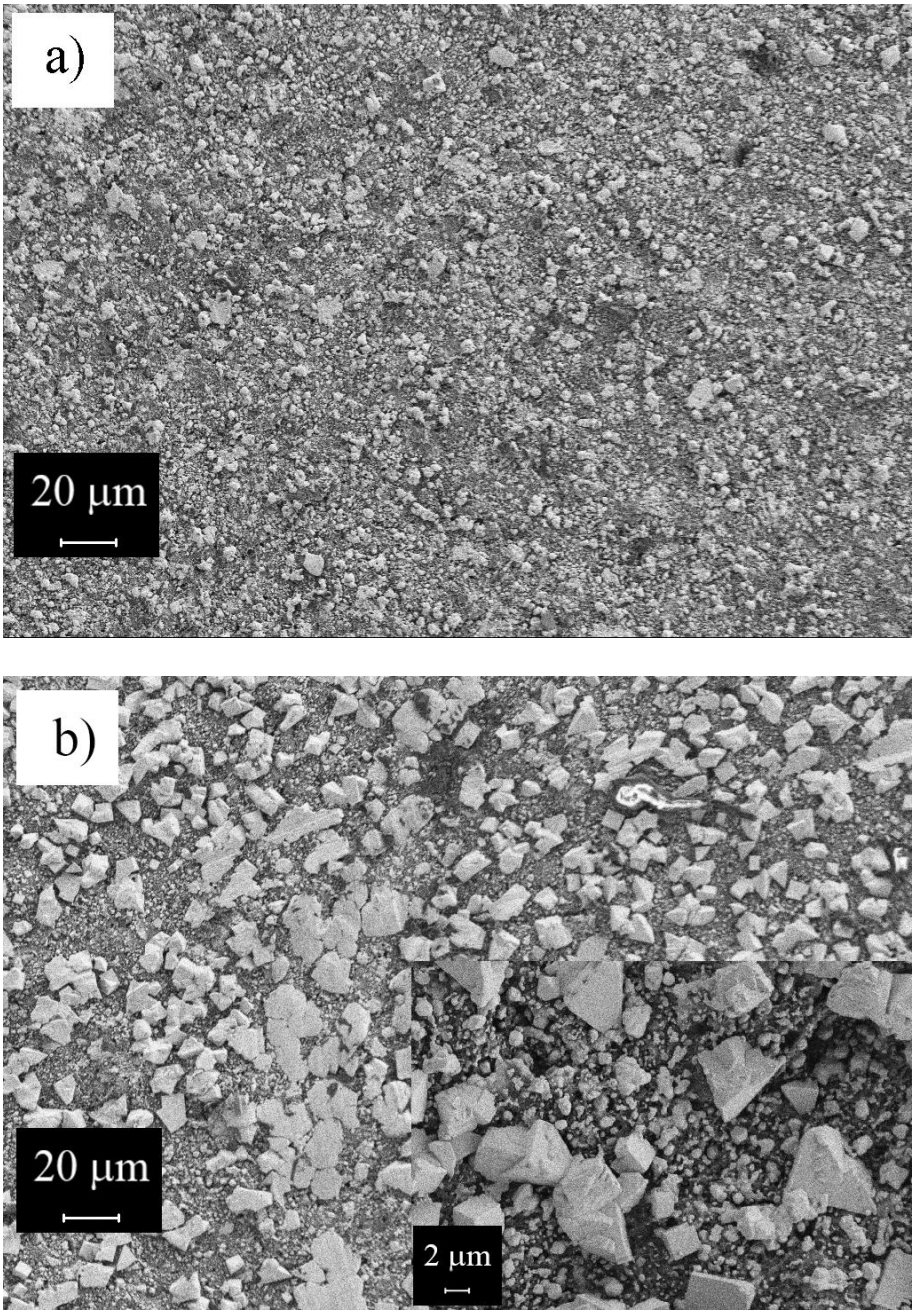

Figure 41. *SEM images obtained from a) middle of the square b) square edge. 917X magnification, EHT 3.00 kV.*

7. CONCLUSIONS

In this thesis, performance of silver inks screen printed on a PPE based, low surface energy substrate was evaluated. The objective was to find such substrate-ink combinations, which would provide both good electrical and mechanical performance of printed structures. PPE is attractive substrate material for HF applications for its low dissipation factor and permittivity. In addition, injection-molding technology enables usage of creative multidimensional substrates.

For the performance study, five commercially available, screen printable silver inks were selected based on both literature survey and manufacturer recommendations. The benefit of using commercial inks is that their composition is well developed for a large variation of applications. The criteria for ink selection included high silver contents to enable good conductivity. Good conductivity is crucial in especially HF applications. Inks with different viscosities were selected so that effects on ink behavior and final results could be compared.

PPE substrate surface is rather smooth and its surface energy is low. On the other hand, high surface energy and rough surface are typically needed to improve wetting and to promote adhesion of substrate-ink interfaces. Therefore, different surface treatments were used to modify substrate surface. These treatments included oxygen plasma treatment, etching with both sulfuric acid and KOH, flame-pyrolytic silicating and coating with ethyltriglycol. Most of these treatments have been used successfully in literature, and ethyltriglycol coating was chosen based on ink manufacturer recommendation. A PPE based substrate fabricated by extrusion was chosen as one test substrate to inspect the effects of molding process.

Test patterns were screen printed with all inks on each substrate surface. Conductivity of printed conductors was evaluated by sheet resistance measurements and adhesion was evaluated with crosscut test. Based on the results obtained in these tests, ink-substrate combinations with best performance were selected for accelerated environmental tests. In this thesis, environmental reliability tests included exposure to elevated temperature in humid conditions and cyclic salt mist test. These tests were used to simulate effects of aging in storage conditions and reliability in salty and humid atmosphere, respectively.

Promising results were obtained in sheet resistance measurements. Low sheet resistances between 10 mΩ/□ and 25 mΩ/□ were measured with all inks expect one, for which sheet resistances below 40 mΩ/□ could not be measured, and it was discarded from further analysis. Lowest values are well suited for HF applications. However, as a lot of variation

in line thicknesses was observed and many conductors were rather porous, process optimization and transmission line characterization is needed before these inks can be utilized in HF applications.

In addition to the measured sheet resistances, adhesion of the printed structures was evaluated by the ASTM-D3359 crosscut test. It was observed that one of the used inks performed poorly on reference substrate (5-15% ink removal), but results could be improved with surface treatments. On the other hand, three of the used inks performed extremely well in the adhesion tests: ink removal below 5 % could be obtained even with the reference substrate. In these tests, oxygen plasma, flame pyrolytic silicating and combined chemical treatment by etching and coating provided best results. This result indicates that mechanical interlocking and strong chemical bonds are needed to provide good adhesion. It was also observed that PPE surface faults caused by molding affect adhesion negatively.

All of the samples fabricated for reliability tests survived well in elevated temperature and humid conditions. This is a promising result considering product lifetime in neutral environment. However, salty and humid environment caused significant degradation in both ink cohesion and interface adhesion. Furthermore, aging effects were highly dependent on both ink selection and substrate surface treatment. This result emphasizes the importance of protective coating in printed electronics applications.

Based on performance test results, such substrate-ink combinations were found, which could be utilized in printed electronics applications. The most effective surface modification methods include plasma treatment, flame-pyrolytic silicating and combined chemical treatment with etchind and coating. Plasma treatment and flame-pyrolytic silicating enable short treatment times, and especially plasma is both user-friendly and environmentally safe treatment. In addition, the combined chemical etching and coating provided enhanced adhesion and reliability, but the processing time is significantly longer and not as environmentally friendly as for example plasma treatment. Therefore, plasma treatment is recommended as an adhesion promoting method for these PPE based substrates.

In addition to suitable surface treatments, promising printing inks were found. Since this was a benchmark study on this subject, more research is needed to optimize printing process, before explicit conclusions of ink performance can be given. In addition, effects of curing conditions should be studied further. In this study, only datasheet curing conditions were used. Despite the excellent sheet resistance values obtained, as electrical performance at high frequencies is not directly proportional to the measured sheet resistance values, future research should be focused on high frequency features of these substrate-ink interfaces. In addition to conductivity properties, the effect of surface treatments on substrate dielectric properties should be inspected as well. Furthermore, as it was observed that exposure to salty and humid environment caused significant performance degradation, importance of protection is emphasized. To achieve reliable printed structures

that could be utilized in harsh outdoor applications, such as for example marine environment, environmental protection solutions, such as printed barrier layers, should be studied.

REFERENCES

[1] K. Suganuma, Introduction, in: Suganuma (ed.), Introduction to Printed Electronics, 74 ed., Springer New Yprk, New York, 2014, pp. 1-22.

[2] Lehtimäki S. Printed Supercapacitors for Energy Harvesting Applications. Tampere University of Technology, 2017. 46 p. (Tampere University of Technology. Publication).

[3] The Internet of Things, Optomec, web page. Available (accessed 4/18): https://www.optomec.com/printed-electronics/aerosol-jet-core-applications/internet-of-things/.

[4] K. Suganuma, Printing Technology, in: Suganuma (ed.), Introduction to Printed Electronics, 74 ed., Springer New Yprk, New York, 2014, pp. 23-48.

[5] D. Novaković, N. Kašiković, G. Vladić, M. Pál, 15 - Screen Printing, in: J. Izdebska, S. Thomas (ed.), Printing on Polymers, William Andrew Publishing, 2016, pp. 247-261.

[6] K. Kim, K. Jung, S. Jung, Design and fabrication of screen-printed silver circuits for stretchable electronics, Microelectronic Engineering, Vol. 120, 2014, pp. 216-220.

[7] Tiina Vuorinen et al., Printed, skin-mounted hybrid system for ECG measurements, in: 2016 6th Electronic System-Integration Technology Conference (ESTC), IEEE, 2016, pp. 1-6.

[8] Z. Żołek-Tryznowska, 6 - Rheology of Printing Inks, in: J. Izdebska, S. Thomas (ed.), Printing on Polymers, William Andrew Publishing, 2016, pp. 87-99.

[9] A. Pekarovicova, V. Husovska, 3 - Printing Ink Formulations, in: J. Izdebska, S. Thomas (ed.), Printing on Polymers, William Andrew Publishing, 2016, pp. 41-55.

[10] Z. Żołek-Tryznowska, 6 - Rheology of Printing Inks, in: J. Izdebska, S. Thomas (ed.), Printing on Polymers, William Andrew Publishing, 2016, pp. 87-99.

[11] P. De Gennes, F. Brochard-Wyart, D. Quéré, Capillarity: Deformable interfaces, in: Capillarity and Wetting Phenomena: Drops, Bubbles, Pearls, Waves, Springer Science and Business Media, Inc., New York, USA, 2004, pp. 2-3.

[12] Viscosity, Surface Tension, Specific Density and Molecular Weight of Selected Liquids, Diversified Enterprises, web page. Available (accessed 02/07): https://www.accudynetest.com/visc_table.html.

[13] K. Grundke, Characterization of Polymer Surfaces by Wetting and Electrokinetic Measurements – Contact Angle, Interfacial Tension, Zeta Potential, in: M. Stamm (ed.), Polymer surfaces and interfaces, Springer Berlin Heidelberg, Heidelberg, 2008, pp. 103-138.

[14] M.J. Joyce, Flexographic Printing of Conductive Silver Inks onto PDMS: Surface Treatment and Novel Processes for Creating Printed Electronics Devices, Ph.D., 2016, Available: http://scholarworks.wmich.edu/dissertations/1615.

[15] D. Savastano, Choosing the Right Substrates for Flexible and Printed electronics, Printed Electronics NOW, 2014, pp. 8.4.2017. http://www.printedelectronicsnow.com/issues/2014-11-02/view_features/choosing-the-right-substrates-for-flexible-printed-electronics.

[16] Critical Surface Tension, Surface Free Energy, Contact Angles with Water, and Hansen Solubility Parameters for Various Polymers, Diversified Enterprises, web page. Available (accessed 02/06): https://www.accudynetest.com/polytable_01.html.

[17] E. Sipilä, Novel Manufacturing Methods and Materials for UHF RFID Tags in Identification and Sensing Applications, Doctor of Science in Technology, 2016, .

[18] T. Björninen, J. Virkki, L. Sydänheimo, L. Ukkonen, Manufacturing of antennas for passive UHF RFID tags by direct write dispensing of copper and silver inks on textiles, Electromagnetics in Advanced Applications (ICEAA), 2015 International Conference on, pp. 589-592.

[19] J. Lee, Chapter 1.2 - Surface Tension and Contact Angle, in: S. Seetharaman (ed.), Treatise on Process Metallurgy, Elsevier, Boston, 2014, pp. 11-18.

[20] P. De Gennes, F. Brochard-Wyart, D. Quéré, Capillarity: Deformable interfaces, in: Capillarity and Wetting Phenomena: Drops, Bubbles, Pearls, Waves, Springer Science and Business Media, Inc., New York, USA, 2004, pp. 20.

[21] P. De Gennes, F. Brochard-Wyart, D. Quéré, Special Interfaces, in: Capillarity and Wetting Phenomena: Drops, Bubbles, Pearls, Waves, Springer Science and Business Media, Inc., New York, USA, 2004, pp. 221.

[22] S. Ebnesajjad, C.F. Ebnesajjad, Introduction to Surface Preparation, in: Surface treatment of materials for adhesive bonding, 2 ed., William Andrew Publishing, Oxford, 2013, pp. 3-6.

[23] S. Ebnesajjad, Chapter 5 - Theories of Adhesion, in: Surface Treatment of Materials for Adhesive Bonding, 2 ed., William Andrew Publishing, Oxford, 2014, pp. 77-91.

[24] Izdebska, J. & Thomas, S. (ed.). 2016. Printing on Polymers. William Andrew Publishing.

[25] M. Kiiski, Evaluation of Novel Substrate Materials in Inkjet Printed Electronics, M.Sc., 2008.

[26] C.W. Foster, R.O. Kadara, C.E. Banks, Fundamentals of Screen-Printing Electrochemical Architectures, in: Screen-Printing Electrochemical Architectures, Springer International Publishing, Cham, 2016, pp. 13-23.

[27] D. Tobjörk, H. Aarnio, P. Pulkkinen, R. Bollström, A. Määttänen, P. Ihalainen, T. Mäkelä, J. Peltonen, M. Toivakka, H. Tenhu, R. Österbacka, IR-sintering of ink-jet printed metal-nanoparticles on paper, Thin Solid Films, Vol. 520, No. 7, 2012, pp. 2949-2955.

[28] E. Halonen, T. Viiru, K. Östman, A.L. Cabezas, M. Mäntysalo, Oven Sintering Process Optimization for Inkjet-Printed Ag Nanoparticle Ink, IEEE Transactions on Components, Packaging and Manufacturing Technology, Vol. 3, No. 2, 2013, pp. 350-356.

[29] J. Niittynen, R. Abbel, M. Mäntysalo, J. Perelaer, U.S. Schubert, D. Lupo, Alternative sintering methods compared to conventional thermal sintering for inkjet printed silver nanoparticle ink, Thin Solid Films, Vol. 556, 2014, pp. 452-459.

[30] W. Lowrie, Earths agethermal and electrical properties, in: Fundamentals of Geophysics, 2 ed., Cambridge University Press, 2007, pp. 254.

[31] S. Franssila, Micrometrology and Materials Characterization, in: Introduction to Microfabrication, 2 ed., Wiley, 2010.

[32] E. Halonen, E. Heinonen, M. Mäntysalo, The Effect of Laser Sintering Process Parameters on Cu Nanoparticle Ink in Romm Conditions, Optics and Photonics Journal, Vol. 3, 2013, pp. 40-44.

[33] G. Polino, R. Abbel, S. Shanmugam, Y. Galagan, A Benchmark Study of Commercially Available Copper Nanoparticle Inks for Applications in Organic Electronic Devices, Organic electronics, Vol. 34, 2016, pp. 130-138.

[34] A. Kamyshny, S. Magdassi, Conductive Nanomaterials for Printed Electronics, Small, Vol. 10, No. 17, 2014, pp. 3515-3535.

[35] R. Serway, J. Jewett, 27. Current and resistance, in: Physics for Scientists and Engineers, 7 ed., Cengage Learning, 2007, .

[36] U. Zorll, Adhesion Testing, in: A.A. Tracton (ed.), Coatings Technology: Fundamentals, Testing, and Processing Techniques, CRC Press, 2006, pp. 6-1-6-13.

[37] ISO 4624:2016, Paints and Varnishes - Pull-off test for adhesion, 3rd ed., ISO - International Organization for Standardization, 2016.

[38] R.K. Ulrich, Reliability Considerations, in: R.K. Ulrich, W.D. Brown (ed.), Advanced Electronic Packaging, 2 ed., John Wiley & Sons, Inc., 2006, pp. 651-690.

[39] J. Coonrod, Understanding When To Use FR-4 Or High Frequency Laminates, OnBoarg Technology, 2011, pp. 26-30.

[40] Preperm$_{(R)}$ L260 Technical Datasheet, Premix Oy.

[41] Injection Molding Concepts, in: D.M. Bryce (ed.), Plastic Injection Molding: Manufacturing Startup and Management, 4 ed., Society of Manufacturing Engineers, 1999, pp. 1-2.

[42] J. A. Paulsen, M. Renn, K. Christenson, R. Plourde, Printing conformal electronics on 3D structures with Aerosol Jet technology, 2012 Future of Instrumentation International Workshop (FIIW) Proceedings, pp. 1-4.

[43] T. Leneke, S. Hirsch, B. Schmidt, A multilayer process for the connection of fine-pitch-devices on molded interconnect devices (MIDs), Circuit World, Vol. 35, No. 2, 2009, pp. 23-29.

[44] Fundamentals of the Extrusion Process, in: Sidney Levy, James F. Carley (ed.), Plastics Extrusion Technology Handbook, Industrial Press Inc., 1989, pp. 1.

[45] CRSN2442 Conductive Silver Ink, Technical Data Sheet, SunChemical.

[46] Metalon HPS-FG32 Silver Screen Ink, Datasheet, Novacentrix.

[47] Asahi LS-411AW Silver Conductive Paste, Datasheet, Asahi Chemical Research Laboratory CO., LTD.

[48] DuPont 5064H, Technical Data Sheet, DuPont.

[49] Metalon HPS-021LV Silver Screen Ink, Datasheet, Novacentrix, .

[50] K.L. Kaiser, Skin Depth, Wire Impedance, and Nonideal Resistors, in: Electromagnetic Compatibility Handbook, CRC Press, 2004, pp. 5-8.

[51] E. Sipila, Experimental Study on Brush-Painted Passive RFID-Based Humidity Sensors Embedded into Plywood Structures, 2016, pp. 8.

[52] M. Fighera, P.D. Van der Wal, H. Shea, Comparison of Six Different Ag Inks for Coulometric Removal of Chloride Ions from Seawater: Towards an Integrated Microfluidic Platform for Desalination, ECS Trans., Vol. 75, No. 41, 2017, pp. 1-12.

[53] T. Muck, Printed UHF RFID antenna on coated cardboard, Advances in Printing and Media Technology, September, IARIGAI, Darmstadt, Germany, pp. 83-90.

[54] U. Kavcic, UHF RFID Tags with Printed Antennas on Recycled Papers and Cardboards, Materials and Technology, Vol. 48, No. 2, 2014, pp. 261-267.

[55] T. Happonen, T. Ritvonen, P. Korhonen, J. Häkkinen, T. Fabritius, Bending reliability of printed conductors deposited on plastic foil with various silver pastes, The International Journal of Advanced Manufacturing Technology, Vol. 82, No. 9, 2016, pp. 1663-1673.

[56] E. Jansson, J. Hast, J. Petäjä, J. Honkala, J. Häkkinen, O. Huttunen, Improving Conductivity of Rotary Screen Printed Microparticle Silver Conductors Using a Roll-to-Roll Calendering Process, Journal of Print and Media Technology Research, Vol. 4, No. 1, 2015, pp. 19-26.

[57] J. V. Voutilainen, T. Happonen, J. Häkkinen, Reliability of silkscreen printed planar capacitors and inductors under accelerated thermal cycling and humidity bias life testing, 2012 4th Electronic System-Integration Technology Conference, pp. 1-6.

[58] E.V. Agina, A.S. Sizov, M.Y. Yablokov, O.V. Borshchev, A.A. Bessonov, M.N. Kirikova, M.J.A. Bailey, S.A. Ponomarenko, Polymer Surface Engineering for Efficient Printing of Highly Conductive Metal Nanoparticle Inks, ACS Applied Materials & Interfaces, Vol. 7, No. 22, 2015, pp. 11755-11764.

[59] T. Laine-Ma, P. Ruuskanen, S. Kortet, M. Karttunen, Electroless copper plating and surface characterization of thermoplastic PPO based printed circuit boards, Circuit World, Vol. 35, No. 4, 2009, pp. 22-30.

[60] M.O.H. Cioffi, H. Voorwald, R.P. Mota, Surface energy increase of oxygen-plasma-treated PET, Materials Characterization, Vol. 50, No. 2, 2003, pp. 209-215.

[61] A. Vesel, M. Mozetič, 7 - Low-Pressure Plasma-Assisted Polymer Surface Modifications, in: J. Izdebska, S. Thomas (ed.), Printing on Polymers, William Andrew Publishing, 2016, pp. 101-121.

[62] T. Laine-Ma, P. Ruuskanen, S. Pasanen, M. Karttunen, Pad printing of polymeric silver ink conductors on thermoplastic foils, Circuit World, Vol. 42, No. 4, 2016, pp. 170-177.

[63] R. Morent, Study of the ageing behaviour of polymer films treated with a dielectric barrier discharge in air, helium and argon at medium pressure, Surface & Coatings Technology, Vol. 201, 2007, pp. 7847-7854.

[64] A. Vesel, I. Junkar, U. Cvelbar, J. Kovac, M. Mozetic, Surface modification of polyester by oxygen- and nitrogen-plasma treatment, Surface and Interface Analysis, Vol. 40, No. 11, 2008, pp. 1444-1453.

[65] Cleaning with low-pressure plasma, Diener Electronic GmbH, web page. Available (accessed 02/28): https://www.plasma.com/en/plasmatechnik/low-pressure-plasma/cleaning/.

[66] Polytec PT, NanoFlame Surface Pretreatment, web page. Available (accessed 12/15): http://www.polytec-pt.com/int/products/oberflaechenvorbehandlung/nanoflame-vorbehandlungsgeraete/.

[67] V. Pekkanen, M. Mäntysalo, K. Kaija, P. Mansikkamäki, E. Kunnari, K. Laine, J. Niittynen, S. Koskinen, E. Halonen, U. Caglar, Utilizing inkjet printing to fabricate electrical interconnections in a system-in-package, Microelectronic Engineering, Vol. 87, No. 11, 2010, pp. 2382-2390.

[68] E. Ranucci, Ã Sandgren, N. Andronova, A. Albertsson, Improved polyimide/metal adhesion by chemical modification approaches, Journal of Applied Polymer Science, Vol. 82, No. 8, 2001, pp. 1971-1985.

[69] High modulus polyester monofilament mesh for technical screen printing applications, NBC Meshtec Inc., web page. Available (accessed 02/28): http://www.nbc-jp.com/eng/product/2016Alpha_l_ux_ex_spec.pdf.

[70] U. Caglar, P. Mansikkamaki, Temperature-Dependent Reliability of Inkjet-Printed Silver Structure in Constant Humidity Environment, NIP24: 24th International Conference on Digital Printing technologies, 7.9-12.9., Pittsburgh, USA, pp. 387-390.

[71] E. Halonen, Environmental protection of Inkjet-printed Ag conductors, Microelectronic Engineering, Vol. 88, No. 9, 2011, pp. 2970-2976.

[72] JEDEC STANDARD, JESD22-A101C Steady State Temperature Humidity Bias Life Test, JEDEC Solid State Technology Association, USA, 2009.

[73] IEC 60068 2-52, International Electrotechnical Commission, 1996.

[74] E.S. Gadelmawla, M.M. Koura, T.M.A. Maksoud, I.M. Elewa, H.H. Soliman, Roughness parameters, Journal of Materials Processing Technology, Vol. 123, No. 1, 2002, pp. 133-145.

[75] ASTM D3359-09e2, Standard Test Methods for Measuring Adhesion by Tape Test, ASTM International, Pennsylvania, 2009.

[76] R. Faddoul, N. Reverdy-Bruas, A. Blayo, Formulation and screen printing of water based conductive flake silver pastes onto green ceramic tapes for electronic applications, Materials Science and Engineering: B, Vol. 177, No. 13, 2012, pp. 1053-1066.

[77] T. Björninen, S. Merilampi, L. Ukkonen, L. Sydänheimo, P. Ruuskanen, The Effect of Fabrication Method on Passive UHF RFID Tag Performance, International Journal of Antennas and Propagation, Vol. 2009, 2009, pp. 8.

[78] H. Yang, Electromagnetics, in: K.W. Chen (ed.), The Electrical Engineering Handbook, Academic Press, 2004, pp. 518.

[79] L. Leppanen, Bendability of Flip-Chip Attachment on Screen Printed Interconnections, Master of Science (Tech.), 2016, Available: http://URN.fi/URN:NBN:fi:tty-201604043773.

[80] Normal Test Plot, SkyMark, web page. Available (accessed 4/1): http://www.skymark.com/resources/tools/normal_test_plot.asp.

[81] The Standard Deviation, University of Leicester, web page. Available (accessed 4/1): http://libweb.surrey.ac.uk/library/skills/Number%20Skills%20Leicester/page_17.htm.

[82] J. Frost, How to Identify the Distribution of Your Data by using Minitab, web page. Available (accessed 4/1): http://blog.minitab.com/blog/adventures-in-statistics-2/how-to-identify-the-distribution-of-your-data-using-minitab.

[83] U. Caglar, P. Mansikkamaki, Investigation of mechanical performance of silver inkjet-printed structures, Journal of Materials Science and Engineering, Vol. 2, No. 10, 2008, pp. 35-42.

[84] H. Lin, G.S. Frankel, Accelerated Atmospheric Corrosion Testing of Ag, CORROSION, Vol. 69, No. 11, 2013, pp. 1060-1072.

APPENDIX A: COMPARISON BETWEEN SHEET RESISTANCE DISTRIBUTION ANOMALIES

Normality test of sample sets, 95 % CL

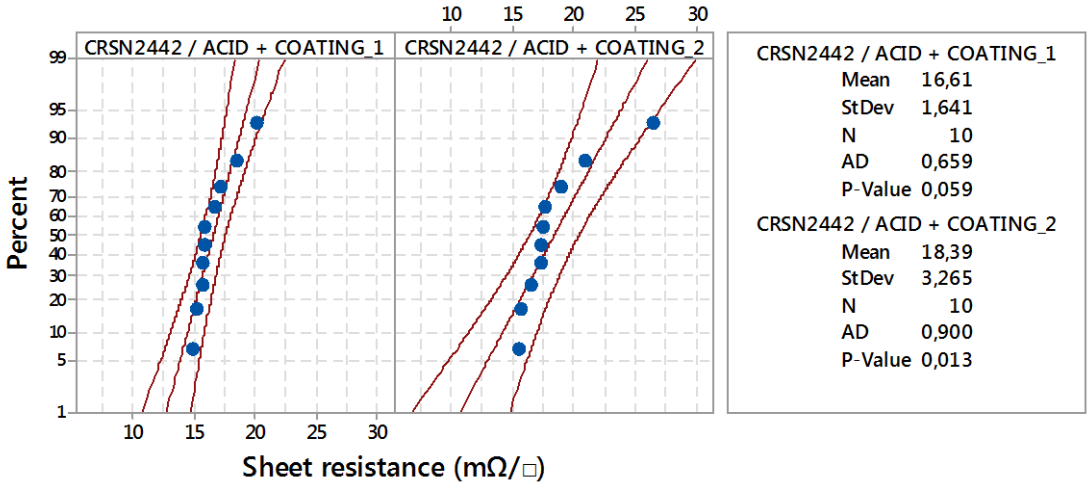

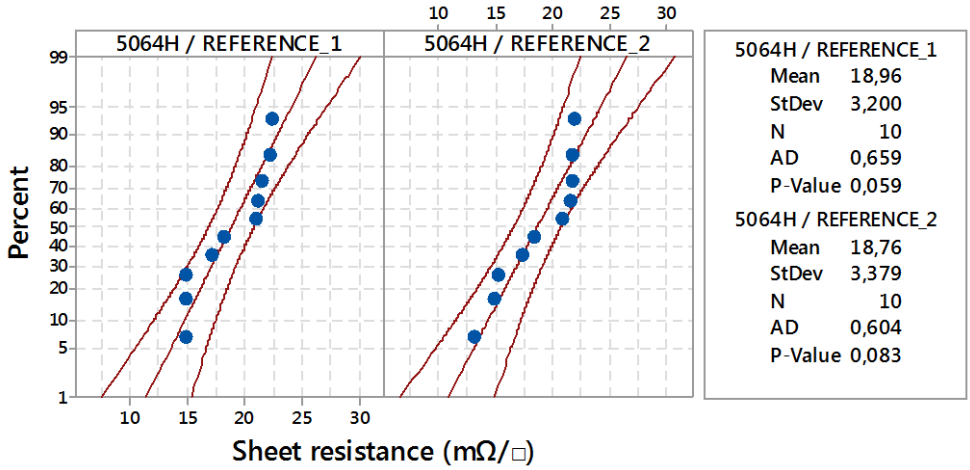

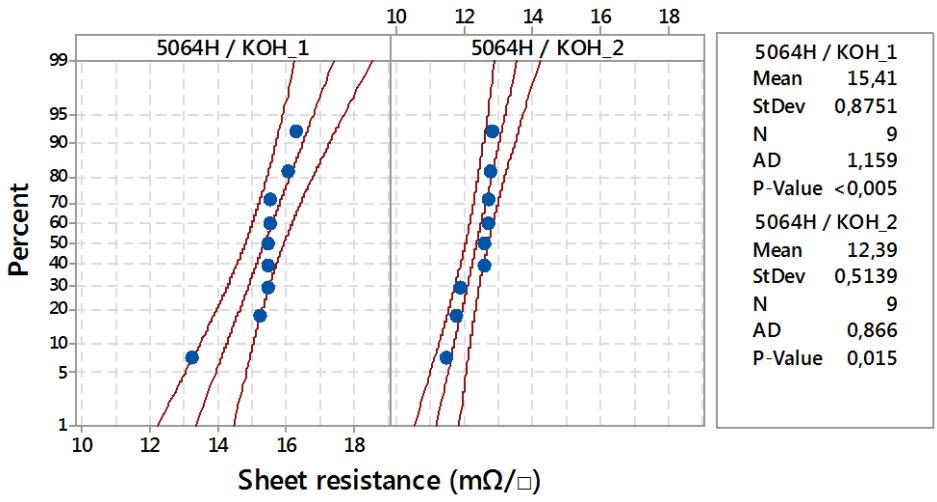

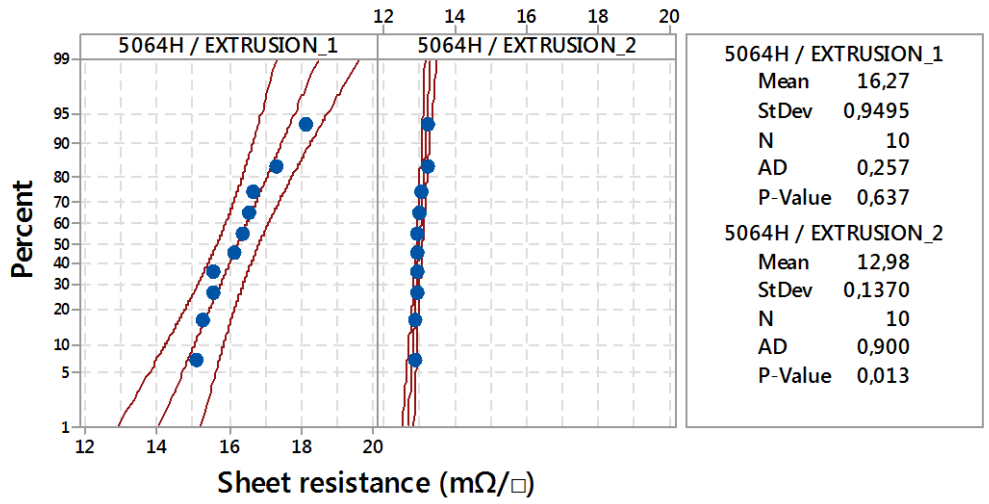
5064H / EXTRUSION_1
5064H / EXTRUSION_2
Percent
Sheet resistance (mΩ/□)
5064H / EXTRUSION_1
Mean 16,27
StDev 0,9495
N 10
AD 0,257
P-Value 0,637
5064H / EXTRUSION_2
Mean 12,98
StDev 0,1370
N 10
AD 0,900
P-Value 0,013

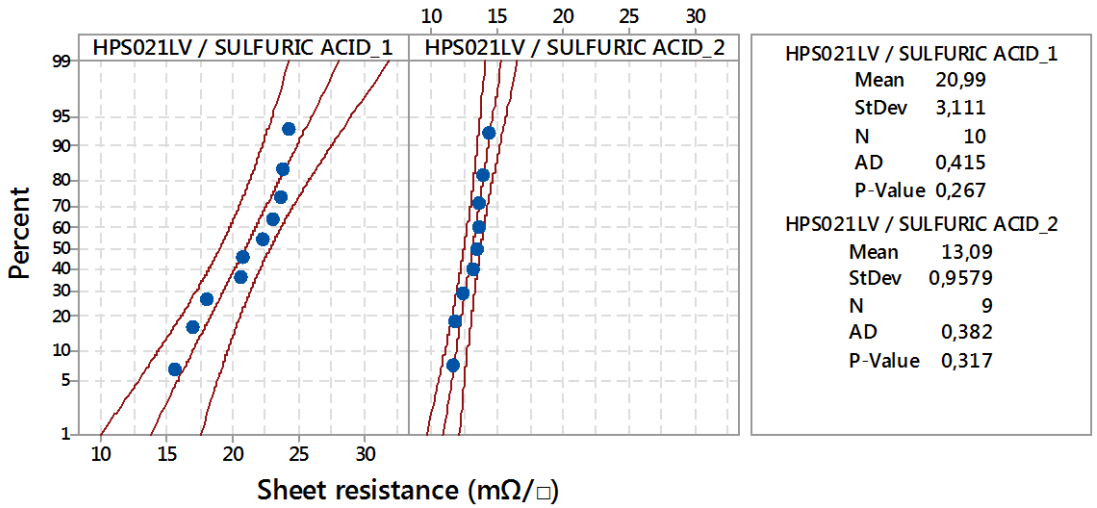
HPS021LV / SULFURIC ACID_1
HPS021LV / SULFURIC ACID_2
Percent
Sheet resistance (mΩ/□)
HPS021LV / SULFURIC ACID_1
Mean 20,99
StDev 3,111
N 10
AD 0,415
P-Value 0,267
HPS021LV / SULFURIC ACID_2
Mean 13,09
StDev 0,9579
N 9
AD 0,382
P-Value 0,317

APPENDIX B: CONDUCTOR SHEET RESISTANCES FOR ABNORMALLY DISTRIBUTED POPULATIONS

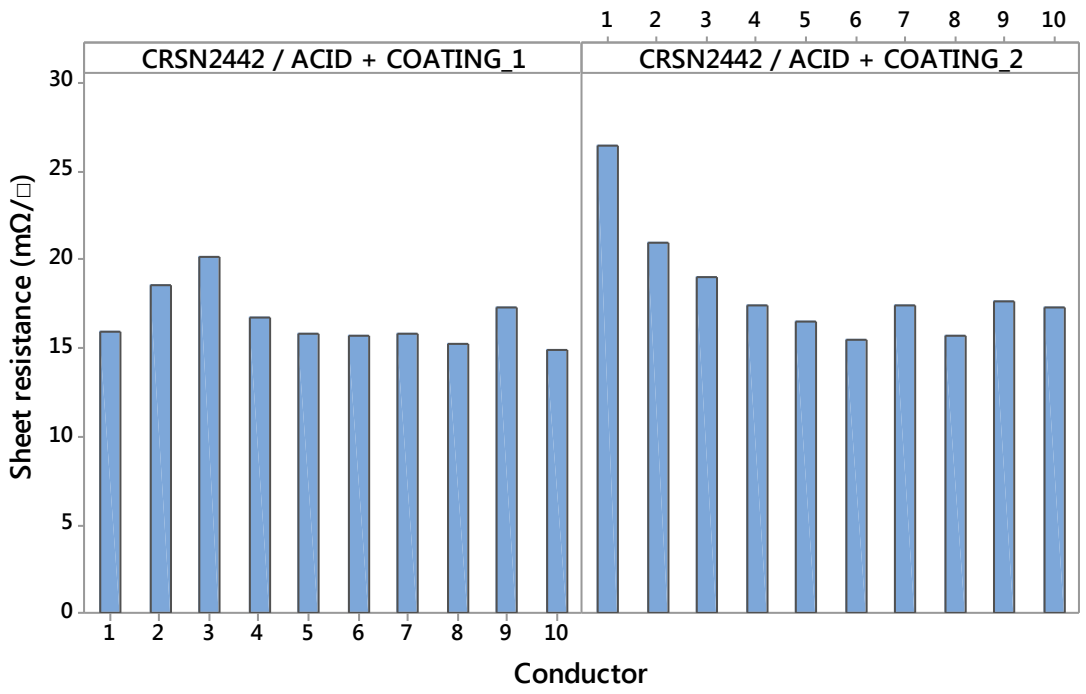

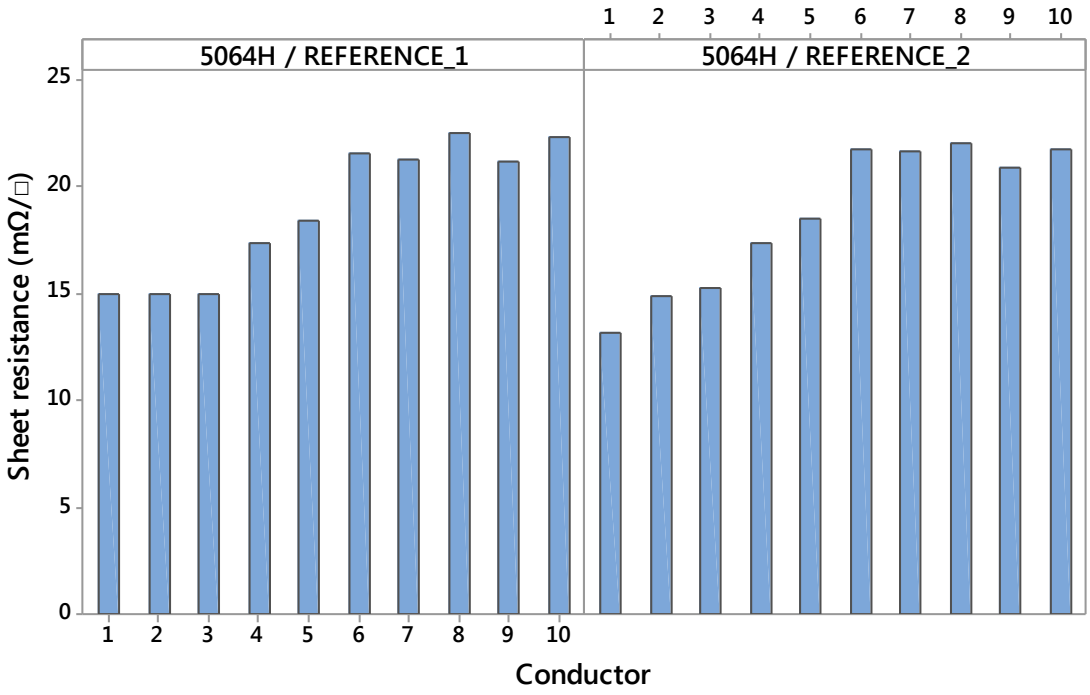

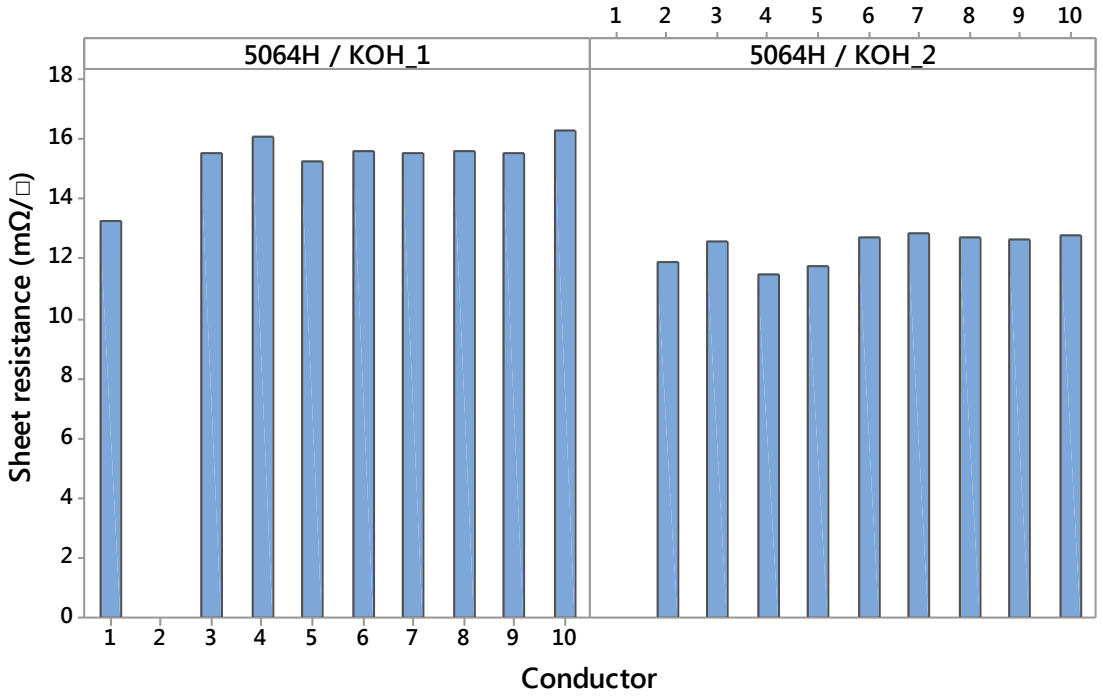
5064H / KOH_1
5064H / KOH_2
Sheet resistance (mΩ/□)
Conductor
0
2
4
6
8
10
12
14
16
18
1
2
3
4
5
6
7
8
9
10

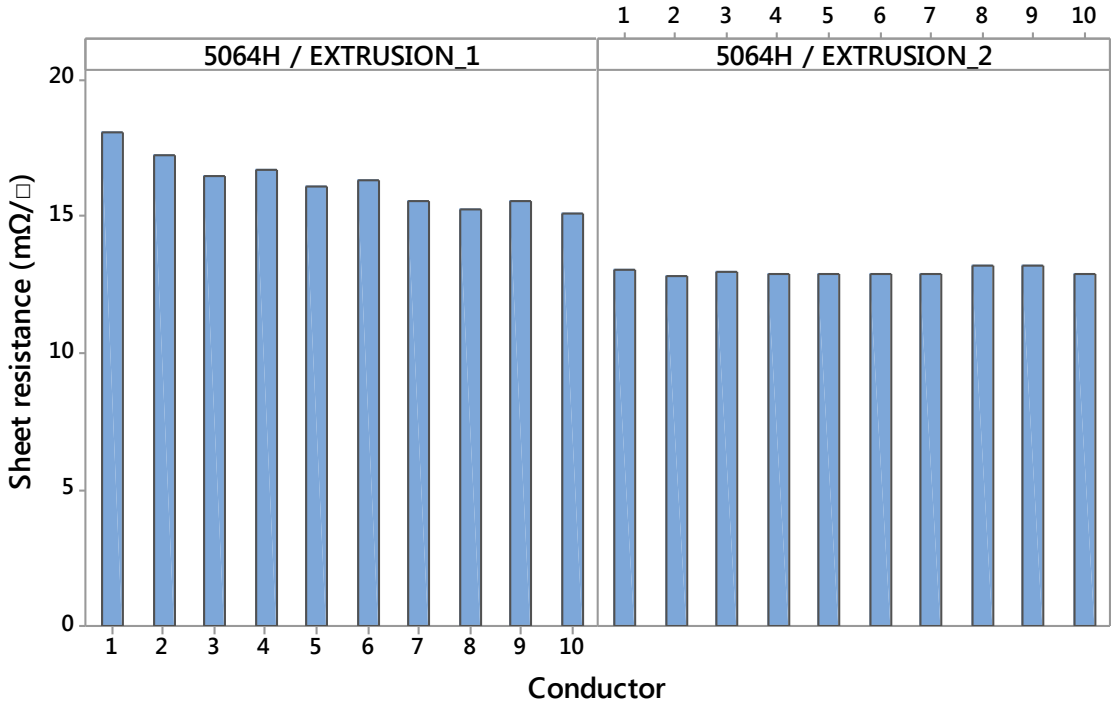
5064H / EXTRUSION_1
5064H / EXTRUSION_2
Sheet resistance (mΩ/□)
Conductor
0
5
10
15
20
1
2
3
4
5
6
7
8
9
10

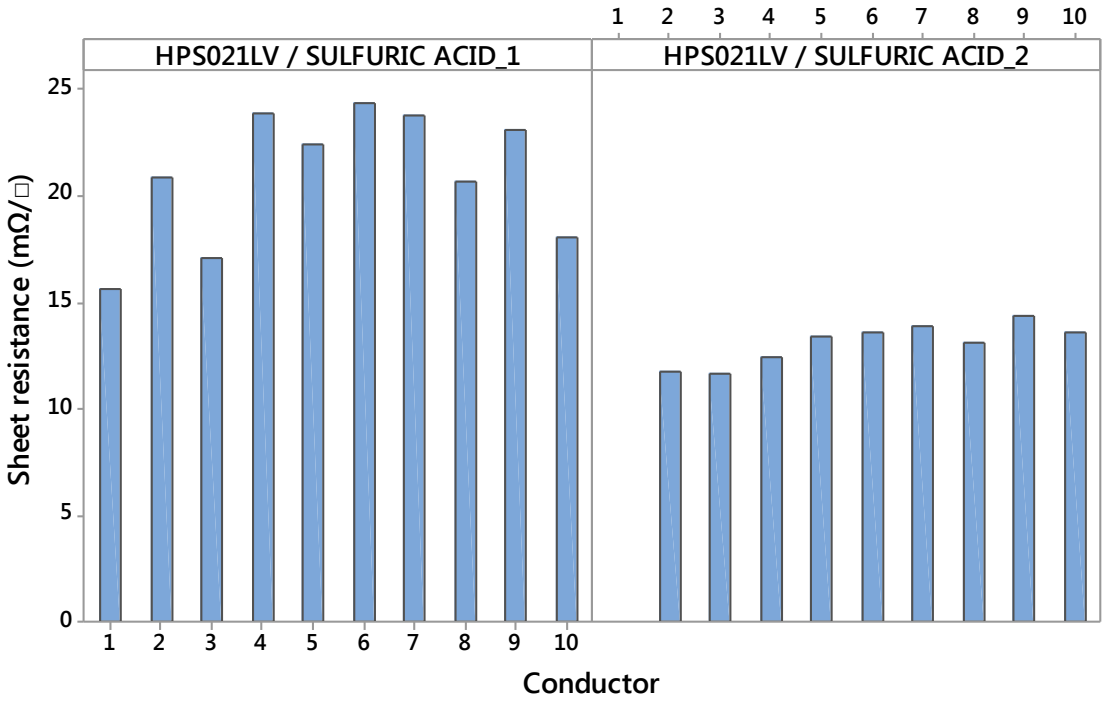
HPS021LV / SULFURIC ACID_1
HPS021LV / SULFURIC ACID_2
Sheet resistance (mΩ/□)
Conductor
0
5
10
15
20
25
1
2
3
4
5
6
7
8
9
10